A THEORETICAL ANALYSIS OF INTERACTING AND NON-INTERACTING DARK ENERGY

Thesis Submitted for the Award of the Degree of

DOCTOR OF PHILOSOPHY

in

Physics

By

Jaskirat Kaur

Registration Number: 12208562

Supervised By

Dr. Shankar Dayal Pathak (23439)

Department of Physics (Associate Professor)

Lovely Professional University

LOVELY PROFESSIONAL UNIVERSITY, PUNJAB

2025

DECLARATION

I, hereby declared that the presented work in the thesis entitled "**A Theoretical Analysis of Interacting and Non-Interacting Dark Energy**" in fulfilment of degree of **Doctor of Philosophy (Ph. D.)** is outcome of research work carried out by me under the supervision of Dr. Shankar Dayal Pathak, working as Associate Professor, in the Department of Physics, School of Chemical Engineering and Physical Sciences of Lovely Professional University, Punjab, India. In keeping with general practice of reporting scientific observations, due acknowledgements have been made whenever work described here has been based on findings of other investigator. This work has not been submitted in part or full to any other University or Institute for the award of any degree.

(Signature of Scholar)

Name of the scholar: **Jaskirat Kaur**

Registration No.: **12208562**

Department/school:

Department of Physics, School of Chemical Engineering and Physical Sciences

Lovely Professional University,

Punjab, India

CERTIFICATE

This is to certify that the work reported in the Ph. D. thesis entitled "**A Theoretical Analysis of Interacting and Non-Interacting Dark Energy"** submitted in fulfillment of the requirement for the award of degree of **Doctor of Philosophy (Ph.D.)** in the Department of Physics, School of Chemical Engineering and Physical Sciences, is a research work carried out Jaskirat Kaur, Registration Number: 12208562, is Bonafide record of his/her original work carried out under my supervision and that no part of thesis has been submitted for any other degree, diploma or equivalent course.

(Signature of Supervisor)

Name of supervisor: Dr. Shankar Dayal Pathak

Designation: Associate Professor

Department/school: Department of Physics, School of Chemical Engineering and Physical Sciences

University: Lovely Professional University, Punjab, India

Dedicated to Mom, Dad, Amitoj and Noor

Abstract

The accelerated expansion of the universe, supported by various astrophysical observations, has posed profound questions about the nature of its dominant energy components, namely dark energy (DE) and dark matter (DM). Although both remain elusive in their physical origin, it is widely believed that they play crucial yet distinct roles in cosmic evolution. This thesis, titled **"A Theoretical Analysis of Interacting and Non-Interacting Dark Energy"**, aims to explore the dynamics of these components in both coupled and uncoupled scenarios to deepen our understanding of the universe's accelerating phase.

The first part of the work investigates models of interacting quintessence, wherein a canonical scalar field representing dark energy is allowed to exchange energy with the dark matter sector. Various forms of the interaction term are considered and their implications on the background cosmology are studied. Special attention is paid to the behavior of dark energy near the inflection point of the scale factor evolution, a regime where the nature of cosmic acceleration undergoes qualitative changes. Analytical and numerical techniques are employed to understand how the interaction affects the stability and dynamics of the universe across different epochs. Observational constraints on the coupling parameter are also examined using model-independent diagnostics to ensure consistency with current data.

The second part focuses on the case of a minimally coupled tachyon field, a non-canonical scalar field derived from string theory, which is considered a candidate for dark energy in the absence of direct coupling to dark matter. This framework allows the isolated behavior of dark energy to be analyzed, providing a comparative foundation to assess the influence of interaction terms studied in the quintessence model. The evolution of the equation of state, energy density and pressure is derived analytically, and the model's compatibility with late-time acceleration is discussed in detail.

Finally, the thesis explores the theoretical possibility that the interaction between dark energy and dark matter might signify a new kind of fundamental interaction— one

beyond the four known forces of nature. By systematically analyzing the coupling dynamics and evaluating their compatibility with observational data, an effective theory of this "fifth interaction" is proposed. The results suggest that, under certain parameter conditions, the DE-DM interaction could offer a unified framework that explains both the dark sectors in a consistent manner.

This study thus provides a theoretical foundation for both interacting and non-interacting dark energy models, offers insights into the dynamics near the cosmic inflection point, and opens new avenues for understanding the universe through the lens of fundamental interactions.

Acknowledgements

"Somewhere, something incredible is waiting to be known."
— Carl Sagan

The completion of this thesis is the result of a long journey filled with curiosity, efforts and growth. Along the way, I faced challenges that tested my strength, moments of success that expanded my knowledge and many opportunities to reflect and grow as a researcher. As I reach this important point, I feel deep gratitude for the many people whose support, encouragement and guidance have brightened my path. Their faith in me has been a steady source of strength, helping me navigate the challenges of this research journey.

Above all, I would like to express my deepest gratitude to my **parents and siblings** for their unwavering support, constant encouragement and unconditional love throughout every stage of my academic journey. Their faith in me even during the most challenging times has been my greatest strength. This achievement would not have been possible without their patience and belief in my dreams. Their silent sacrifices and constant encouragement have been the bedrock of my strength.

I would like to express my deepest gratitude to my supervisor, **Dr. Shankar Dayal Pathak** whose invaluable guidance, unwavering support and encouragement to explore new ideas have been instrumental throughout this research journey. His insightful feedback and thoughtful suggestions have greatly enhanced the quality of this work. His mentorship has profoundly shaped my scientific thinking, research skills and approach to problem-solving for which I am sincerely thankful. Furthermore, **Dr. Shankar Dayal Pathak's** guidance in the writing phase of this thesis was invaluable in navigating the complexities of academic discourse. His insights helped ensure the clarity, coherence and scholarly depth.

I sincerely thank **Prof. Dr. Maxim Khlopov, Dr. Vikash Kumar Ojha, Dr. Manabendra Sharma and Dr. Maxim Krasnov** for their valuable guidance, thoughtful discussions and insightful feedback throughout this research journey. I am also grateful to the **IUCAA's** Visiting Programme for providing me with the opportunity to access their excellent library resources and engage with researchers and facility actively working in the fields of cosmology, astrophysics and astronomy.

I am sincerely thankful to the faculty and staff of the Department of Physics. Special thanks to the Head of School **Prof. Dr. Kailash Chandra Juglan** and the panel members **Dr. Mukesh Kumar (HOD), Dr. Oriza Kamboj** and **Dr. A. K.**

Srivastava for their critical insights, invaluable feedback and insightful thoughts at various stages of this work.

My heartfelt thanks goes to my fellow researchers **Sahit Kumar and Gaurav Bhandari** for their encouragement at each stage, valuable discussions and emotional support throughout this journey, their camaraderie has made this path more meaningful and special thanks to them for the shared frustrations and the laughter that helped lighten even the most demanding days. A special thanks to Manisha and Upasna for their friendship, encouragement and unwavering support, their companionship has made this journey memorable. I also want to acknowledge my Ph.D friends Alex, Simran ma'am, Mashahid, Amit sir, Sachit sir, Hemanshi and Shalini for the support.

I would like to thank the administrative staff for their support in coordinating various aspects of my academic journey. Finally, I dedicate this thesis to all those who have supported me in ways both big and small, known and unknown. Thank you all for being part of this incredible journey. This thesis is as much a product of collective support as it is of individual effort. To all who have played a part, however big or small, I offer my heartfelt thanks.

Jaskirat Kaur

Contents

List of Tables

List of Figures

Chapter 1

Introduction

The study of the structure and evolution of the universe has been a center of focus in modern theoretical and observational cosmology. One of the prominent discoveries in cosmology is the accelerated expansion of the universe; at present our universe is not only expanding, but this expansion rate is also accelerating, which is confirmed by Type Ia supernovae observation [1, 2] and High-z Supernovae [3]. This discovery fundamentally challenged the classical view of cosmic evolution and implied the existence of some unknown energy component which could be responsible for this acceleration at the present epoch. In order to explain this phenomenon, the concept of "Dark Energy"(DE) was introduced as an exotic form of energy with negative pressure that counteracts the gravitational attraction of matter while a pressureless, non-relativistic component that interacts extremely weakly with standard matter particles is referred to as "dark matter". In 1933, Zwicky, through a comparison of the observed stellar mass with the velocity dispersion of galaxies in the Coma cluster, provided the first evidence for the existence of dark matter in the universe [4]. In contrast to DE, dark matter may cluster due to gravitational instability, forming local structures throughout the universe. Indeed, it is known from observation that dark matter has been essential for the development of large-scale structures like galaxies and clusters of galaxies. In the current cosmos, dark matter makes up around 25% of the energy portion, while DE contributes to 70% of the energy content in the universe and approximately around 4% is the baryonic matter while around 0.005% is the radiation. We know at large scales the gravitational force is the dominating force in our universe which has an attractive nature. Unlike baryonic matter and radiation which contributes to the attractive gravitational effects shaping

our cosmic structure; DE, on the other hand, exhibits repulsive gravitational properties leading to accelerated the expansion of space-time, despite the observational evidence, the exact nature and origin of DE are still unknown. *Is DE a manifestation of "Cosmological constant"; as initially suggested by Einstein or is it the result of a dynamical scalar field(s) which can evolve over time? or alternatively, could it indicate the modification in General Relativity itself?* These questions continue to derive extensive research in theoretical and observational cosmology. Recent advancements from the Dark Energy Spectroscopic Instrument (DESI) [5] have significantly enhanced the understanding of DE and indicated the dynamical nature of DE but future data is needed to clearly clarify it.

1.1 Historical Context and Theoretical Foundation:

Dark energy is one of the most intriguing and puzzling concepts in modern cosmology, and its story begins over a century ago. In 1917, Albert Einstein introduced the cosmological constant, denoted by the Greek letter Λ, into his field equations of General Relativity. At the time, the prevailing belief was that the universe was static and unchanging and Λ was his way of balancing the gravitational pull of matter to prevent the universe from collapsing under its own weight. However, this idea was soon challenged; when Edwin Hubble in 1929 [6] discovered that the universe is actually expanding.

For much of the 20^{th} century, cosmologists worked under the assumption that the universe's expansion, while ongoing, was slowing down due to the gravitational attraction of matter. It wasn't until the late 1990s that this view was turned upside down. Observations of distant Type Ia supernovae by two independent teams [1–3] revealed something unexpected—the expansion of the universe is not slowing down but speeding up. This shocking discovery hinted at the existence of a mysterious force or energy causing this acceleration, which came to be known as *Dark Energy*. As more data poured in from measurements of the cosmic microwave background (CMB), galaxy surveys and large-scale structure (which we will discuss in upcoming section) cosmologists realized that DE makes up about 70% of the total energy content of the universe. Meanwhile, DM accounts for roughly 25%, and the ordinary matter that makes up stars, planets etc. comprises less than 5%. Radiation, once dominant in the early universe, now contributes only a minuscule amount. Despite being the majority component of the universe today,

DE remains a profound mystery. Some scientists believe it might be a constant energy embedded in space itself, while others suggest it could be the effect of a slowly evolving field, or even a signal that our understanding of gravity needs revision. What's clear is that DE plays a crucial role in shaping the fate of the cosmos and unlocking its nature could lead to a revolutionary shift in our understanding of the universe; its origins and fate.

1.1.1 Theoretical Foundation:

The cosmological model is based on Einstein's tensor field equations, which explain the geometry of space-time and provide information on the energy-momentum components in the current universe:

$$R_{\mu\nu} - \frac{1}{2}Rg_{\mu\nu} = \frac{8\pi G}{c^4}T_{\mu\nu} \tag{1.1}$$

here Greek indices runs from 0 to 3 representing space-time co-ordinates and Latin indices runs from 1 to 3 representing only space co-ordinates, $R_{\mu\nu}$ is the Ricci tensor, R is the Ricci scalar which can be obtained by contracting Ricci tensor, $g_{\mu\nu}$ is the metric tensor, $T_{\mu\nu}$ is the energy-momentum tensor and G is the Gravitational constant. GR connects space-time energy-momentum and gravitation and could reduce to ODE's (ordinary differential equations) forming a rich class of models to study the non-linear field equation dynamics. In his later work on static universe theory, Einstein created a static solution to his field equations by inserting a constant term into the left-hand side. This constant is termed as "Cosmological constant (Λ)" and the field equation (1.1) changes to:

$$R_{\mu\nu} - \frac{1}{2}Rg_{\mu\nu} + \Lambda g_{\mu\nu} = \frac{8\pi G}{c^4}T_{\mu\nu} \tag{1.2}$$

But later, when Hubble in 1929 [6] came up with the discovery of the expanding universe, Einstein dropped the idea of the cosmological constant. Later, though, the cosmological constant Λ was brought up again as a possible option for DE to explain why the universe is expanding faster than ever.

Another fundamental base of standard cosmology is the "Cosmological Principle," which states that at a large scale our universe is isotropic and homogeneous. Thus, the line element representing such a universe is given by:

$$ds^2 = g_{\mu\nu}dx^\mu dx^\nu = -c^2dt^2 + a^2(t)\left[dr^2 + \zeta^2(r)\left(d\theta^2 + sin^2\theta d\Phi^2\right)\right] \tag{1.3}$$

here $g_{\mu\nu}$ represent the metric tensor, $a(t)$ represents the scale factor, t is the cosmic time and (r, θ, Φ) are the spherical co-ordinates with:

$$\zeta(r) = \begin{cases} \frac{1}{K} sin\sqrt{K}r & K > 0 \text{ (Closed curvature)} \\ r & K = 0 \text{ (Flat space-time)} \\ \frac{1}{|K|} sinh\sqrt{|K|}r & K < 0 \text{ (Open curvature)} \end{cases} \tag{1.4}$$

With K as the curvature, generally in cosmology three values of K are considered, i.e., $(1, 0, -1)$ representing closed, flat and open universes, respectively. Here in this thesis, all calculations are carried out for flat curvature i.e. $K = 0$. As we know, at different epochs different matter-energy and field components were dominating, which can be classified into relativistic matter, i.e., during early times radiation and relic neutrinos were the dominating components; then non-relativistic components like baryonic and dark matter components came into the picture, which helped in the large-scale structure formations; then, at the late-time epoch, DE was the dominating component, which is responsible for the accelerating universe.

1.1.1.1 Friedmann-Lemaître-Robertson-Walker (FLRW) Model:

Friedmann developed a set of equations that govern the expansion of the universe, taking into account the Robertson-Walker metric Eq.(1.3), which characterizes the homogeneous and isotropic universe [7, 8]. Friedmann equations for all above-mentioned components (radiation, DE and matter) in the units of $c = 1$ are:

$$H^2 = \left(\frac{\dot{a}(t)}{a(t)}\right)^2 = \frac{8\pi G}{3} \sum_n \rho_n - \frac{K}{a^2} \tag{1.5}$$

for the case of flat universe the above equation can be rewritten as:

$$H^2 = \left(\frac{\dot{a}}{a}\right)^2 = \frac{8\pi G}{3} \sum_n \rho_n \tag{1.6}$$

and

$$\frac{\ddot{a}(t)}{a(t)} = -\frac{4\pi G}{3} \left(\sum_n \rho_n + 3 \sum_n p_n\right) \tag{1.7}$$

here summation of ρ_n over n represents the sum of all energy densities of each component like radiation(r), DE(de) or matter(m), similarly sum of p_n represents the total pressure

of all components, H is the Hubble parameter, a is the scale factor which depends on cosmic time t and $(\dot{})$ represents the derivative with respect to cosmic time (t). So, the first Friedmann Eq.(1.6) contain first order derivative of scale factor which represents the expansion rate whereas 2nd Eq.(1.7) contains second order derivative representing the acceleration so, one can determine the cosmic evolution by specifying the properties of individual components in above mentioned equations.In fact if we see the second Friedmann Eq.(1.7) to represent the accelerating universe the bracketed term needs to be negative i.e. $(\rho_n + 3p_n) < 0$ and from this condition equation of state (EoS) can be obtained as:

$$w_n = \frac{p_n}{\rho_n} < -\frac{1}{3} \tag{1.8}$$

which implies, in order to obtain an accelerating universe EoS parameter w_n needs to be less than $-1/3$. Other from of these equations is in the terms of density parameters which makes it easier to handle the model parameters, these dimensionless energy density parameters like Ω_r for radiation, Ω_m for matter and Ω_{de} for DE are given as:

$$\Omega_r = \frac{\rho_r}{\rho_c} = \frac{8\pi G}{3H^2}\rho_r \tag{1.9}$$

$$\Omega_m = \frac{\rho_m}{\rho_c} = \frac{8\pi G}{3H^2}\rho_m \tag{1.10}$$

$$\Omega_{de} = \frac{\rho_{de}}{\rho_c} = \frac{8\pi G}{3H^2}\rho_{de} \tag{1.11}$$

and on adding energy density parameter of component we get:

$$\Omega_r + \Omega_m + \Omega_{de} = 1 \tag{1.12}$$

These equations highlights how different energy components contributes to the total energy density of the universe. Further to ensure the conservation of energy momentum, the covariant derivative of energy momentum tensor needs to be zero i.e. $\nabla^\mu T_{\mu\nu} = 0$ which yields the following energy conservation equation in terms of energy density as:

$$\dot{\rho}_n + 3H(\rho_n + p_n) = 0 \tag{1.13}$$

The scaling solution of this energy conservation equation describes how the energy density of the different components can evolve as the universe expands:

$$\rho_n = \rho_n^0 \left(\frac{a}{a_0}\right)^{-3(1+w_n)} \tag{1.14}$$

For different components like radiation, matter and DE the above scaling solution reads:

$$\rho_r \propto a^{-4} \tag{1.15a}$$

$$\rho_m \propto a^{-3} \tag{1.15b}$$

$$\rho_{de} \propto a^{-3(1+w_{de})} \tag{1.15c}$$

where EoS parameter for radiation is $w_r = 1/3$, for matter component $w_m = 0$ and w_{de} can take the different values depending on the different form of DE scalar field models. One can broadly say that there are two primary approaches to develop a theory to explain this accelerated expansion.

- The first one is the "Modified Theory of Gravity" in which there is modification in the gravity sector of Eintein's Field equations.
- Second is the "Modified Matter Models" in which matter part in the Einstein field equation is modified via the introduction of additional component like DE.

In this thesis our main focus is the analysis of DE Models of two kinds interacting and non-interacting which we will discuss in details in next chapters.
Since the behavior of these models is closely linked to the expansion history of the universe, it is essential, first to understand how cosmic distances are defined and measured. In cosmology, distance isn't a simple, single concept—because the universe is expanding, the way we define and measure distance depends on what we're trying to observe or calculate. So, in the next section, let's learn about the major cosmic distances.

1.2 Cosmic Distances:

As our universe is itself dynamic in nature(i.e. accelerating), understanding distances in cosmology is a little more complicated than in classical physics. The separation between two distant galaxies evolves as the fabric of spacetime stretches, making the very concept of "distance" dependent on time also along with co-ordinates. To account for this, several distinct definitions of distance are used, each tailored to a specific observational or theoretical purpose. In this section, we explore the various distance measures used in cosmology and their interrelationships. For more details readers can go through [9].

1.2.1 Comoving Distance $D_c(z)$:

The comoving distance is perhaps the most fundamental of the cosmological distance measures. It represents the separation between two points in the universe, measured along a path at constant cosmic time. This distance remains fixed for objects that are moving only with the Hubble flow meaning they are not subject to local gravitational interactions. Mathematically, the comoving distance to an object at redshift z is given by:

$$D_C(z) = c \int_0^z \frac{dz'}{H(z')} \tag{1.16}$$

where c is the speed of light, and $H(z)$ is the Hubble parameter, describing the expansion rate of the universe as a function of redshift. This measure is particularly useful in theoretical models and large-scale simulations, as it offers a static "coordinate" system that remains unaffected by the expansion of spacetime. We will be using comoving co-ordinates throughout the thesis.

1.2.2 Proper Distance $D_p(z)$:

The proper distance refers to the actual, physical separation between two points in the universe, measured at a specific moment in cosmic time. Proper distance is related to comoving distance as follows:

$$D_p(z) = a(t) \cdot D_c(z) \tag{1.17}$$

here $a(t)$ is the scale-factor and the important point about proper distance is its value changes with time; In other words, galaxies that are comoving (moving only because the universe is expanding) will have a growing proper distance between them simply because space itself is getting stretched. Unlike some other cosmological distances, the proper distance isn't something we can measure directly with telescopes. We can't place a physical ruler across the universe or pause cosmic expansion. What we can observe are redshifts, apparent brightness and angular sizes, and from these we infer other types of distances, like luminosity distance and angular diameter distance. Despite this, proper distance is still incredibly useful especially when we're thinking about the size of the observable universe, or when we want to model how far light has traveled over cosmic time. It helps give a clearer picture of the structure and scale of the universe at different moments in its history.

1.2.3 Luminosity Distance $D_L(Z)$:

Luminosity distance is measured using "light," i.e. it measures how far an object appears based on how dim it looks, assuming we know the actual brightness. For example, if we observe a Type Ia supernova which is a stellar explosion known to have a consistent intrinsic brightness, we can estimate how far it is based on its observed flux. So, it is the ratio of luminosity L and 4π times bolomeric flux S of an steller object:

$$D_L(z) = \sqrt{\frac{L}{4\pi S}} \tag{1.18}$$

The apparent brightness of an object would follow a simple inverse-square law for the case if universe is static, i.e. the farther the object is, the dimmer it appears to be. However, our universe is not static rather it is expanding. So, this cosmic expansion will affect the movement of light across the expanding universe:

- The wavelength of the light "redshift" i.e. wavelength of light stretches as it travels through space.
- Due to time dilation, the arrival rate of photons is reduced .
- The light spreads over a larger area because space itself is expanding.

All these effects needs to be included while measuring luminosity distance. Thus, another way to express luminosity distance is given by:

$$D_L(z) = (1 + z) \cdot D_C(z) \tag{1.19}$$

where:

- z is the redshift of the object,
- $D_C(z)$ is the comoving distance.

This formulation allows astronomers to account for the expansion of the universe when interpreting the observed brightness of distant objects such as supernovae or quasars. Unlike proper or comoving distance, which are more theoretical or coordinate-based, luminosity distance is directly connected to what we observe. Luminosity distance therefore plays a crucial role in observational cosmology, enabling us to probe the large-scale geometry and dynamics of the universe.

1.2.4 Angular Diameter Distance $D_A(z)$:

Another important observational distance is $D_A(z)$, which connects an object's physical size to the angle it occupies in the sky. This is based on simple geometry. In flat, static space, the relation would be:

$$D = \frac{l}{\theta} \tag{1.20}$$

where l is the actual size of an object, D is the distance to the object and θ is the observed angular size in radians. So, in terms of angular diameter distance this formula takes the form:

$$D_A = \frac{l}{\theta} \tag{1.21}$$

But! our universe is expanding! So, just like luminosity distance cosmic expansion will also affects the angular diameter distance. For objects very far away, the angular diameter distance actually starts to decrease with redshift after a certain point. This means that very distant galaxies can appear larger on the sky than closer ones of the same size! This seemingly strange effect happens because the light was emitted when

the universe was smaller, so the object took up a larger angle in the past than it would now. So, the angular diameter is reated to comoving distance as:

$$D_A(z) = \frac{D_C(z)}{(1+z)} \tag{1.22}$$

or using Eq.(1.19), we get:

$$D_A(z) = \frac{D_L(z)}{(1+z)^2} \tag{1.23}$$

This distance is crucial when studying standard rulers—objects or patterns in the universe whose physical size we already know. A famous example is the baryon acoustic oscillation (BAO) scale, which acts like a cosmic ruler embedded in the distribution of galaxies. By measuring how large this ruler appears at different redshifts, we can infer how space has expanded over time.

1.3 Observational Evidence of Dark Energy (DE):

Multiple independent astrophysical and cosmological observations support the presence of DM and DE through their gravitational effects on visible matter, radiation and Large scale structure of the universe. The existence of DE is strongly supported by a variety of independent astronomical observations. These observations point towards a component of the universe that exerts negative pressure, causing the expansion of the universe to accelerate. Key evidence comes from Type Ia Supernovae, cosmic microwave background measurements, baryon acoustic oscillations, and large-scale structure surveys. Together, they build a consistent and compelling case for a universe dominated by DE at the present epoch. This section explore some of the observations supporting the presence of DE:

1.3.1 Type Ia Supernovae (Standard Candles):

One of the most significant breakthroughs in observational cosmology came in the late 1990s, when astronomers studying distant Type Ia supernovae made an unexpected discovery. Type Ia supernovae are among the most important tools for measuring cosmic distances due to their consistent peak luminosity, earning them the title of “standard candles.” In the late 1990s, two independent research teams; the High-Z Supernova

Search Team [3] and the Supernova Cosmology Project [2] provided the first compelling evidence for the accelerated expansion of the universe. The High-Z team analyzed both spectral and photometric data for 16 distant and 34 nearby supernovae, concluding with high statistical confidence (greater than 99.5%) that the deceleration parameter q_0 is negative, with an estimated value of $q_0 = -1 \pm 0.4$. Meanwhile, the Supernova Cosmology Project examined 42 supernovae in the redshift range $0.18 \leq z \leq 0.83$ and also found strong support for a non-zero, positive cosmological constant. Their analysis yields a joint probability distribution of $\Omega_m - \Omega_\Lambda$ plane; $0.8\Omega_m + 0.6\Omega_\Lambda \approx -0.2 \pm 0.1$, implying a clearly negative q_0 (see [2]) . In other words, these supernovae appeared dimmer than expected in a decelerating universe, indicating that the expansion is actually speeding up!. These findings, based on the brightness-redshift relation of supernovae, provided the first direct evidence for the existence of DE and revolutionized our understanding of the universe's expansion history. Most strikingly, the measured luminosity distances of 16 high-redshift supernovae indicate they are about $10-15\%$ farther away than would be anticipated in a universe dominated solely by matter with no cosmological constant. This deviation points toward an accelerating expansion, implying the presence of a repulsive force. This analysis lends strong support to cosmological models that include a positive cosmological constant Λ, favoring a universe that will continue expanding indefinitely. For more details readers can refer to [10, 11].

1.3.2 Cosmic Microwave Background (CMB):

Missions like WMAP [12] and Planck [13] provides the precise measurement of the early universe and its parameters through the study of Cosmic Microwave Background (CMB) spectrum. CMB provides the faint afterglow of the Big Bang and has temperature fluctuation information. CMB serves as a powerful and independent tool for understanding the large-scale properties of the universe, including the presence of DE. By examining the tiny fluctuations in temperature across the CMB, precise information about the geometry of space is obtained. In particular, the angular position of the first acoustic peak in the CMB power spectrum originating from sound waves in the early universe around redshift $z \approx 1100$ is extremely sensitive to the overall spatial curvature. Observational data show that this peak aligns with a nearly flat universe, suggesting that the total energy density is very close to the critical value required for flatness. However, measurements of the actual matter content—including both visible matter and dark matter fall

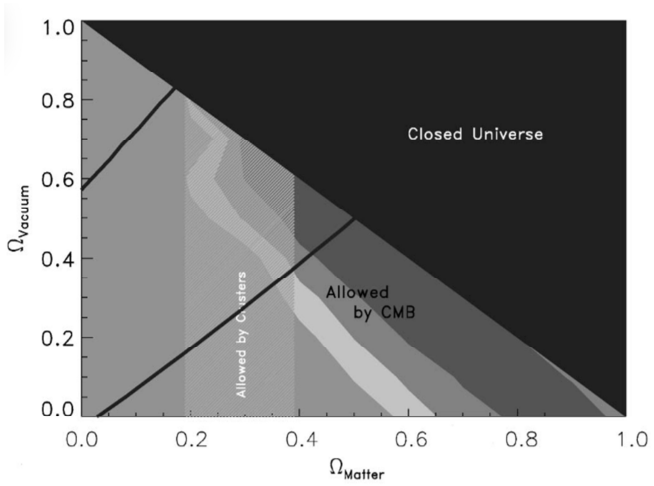

FIGURE 1.1: This figure shows the likelihood contour plot in the $\Omega_m - \Omega_\Lambda$ (matter density–vacuum energy density) plane. It combines results from three major cosmological observations: Cosmic Microwave Background (CMB), galaxy clusters, and Type Ia supernovae. The different shades correspond to likelihood contours for $\Delta\chi^2 = 1, 4, 9$which roughly represent confidence intervals $(68\%, 95\%,$ and $99\%)$. The striped vertical band labeled "Allowed by Clusters" shows the range of Ω_m values (matter density) derived from galaxy cluster baryon fraction measurements, which lies in the range $0.2 < \Omega_m < 0.4$. This plot is taken from [14]

short of this critical density. In fact, the total matter density parameter Ω_m appears to be less than 0.4. To maintain a flat geometry as indicated by the CMB, there must be an additional form of energy contributing roughly $\Omega_\Lambda \approx 0.6 - 0.7$ (see [14]). This missing piece, which does not behave like ordinary matter or radiation, is what we refer to as DE. The simplest explanation for it is a cosmological constant Λ, a term originally introduced by Einstein as mentioned in Section (1.1.1).

1.3.3 Baryon Acostic Osscilations (BAO):

Baryon Acoustic Oscillations (BAOs) provide a robust method for exploring the expansion history of the universe and have emerged as strong evidence supporting the existence of DE. These oscillations originated as sound waves in the photon-baryon plasma of the early universe and left a characteristic scale, the sound horizon $r_s(z_{\text{drag}})$, observable in the large-scale structure of galaxies. This scale functions as a standard ruler in cosmology. By measuring its angular size across the sky and its extent along the line of sight, cosmologists construct a spherically averaged distance measure known

as the volume-averaged distance in natural units (c=1), defined as:

$$D_V(z) = \left[(1+z)^2 D_A^2(z) \cdot \frac{z}{H(z)}\right]^{1/3}, \tag{1.24}$$

where $H(z)$ is the Hubble parameter. This measure incorporates both transverse and radial components of the BAO signal. Observations from galaxy surveys such as the Sloan Digital Sky Survey (SDSS) and the 2dF Galaxy Redshift Survey (2dF GRS) have determined $D_V(z)$ and the relative distance ratio $d_z = r_s(z_{\text{drag}})/D_V(z)$ at different redshifts. These results consistently align with cosmological models that include DE, disfavoring those dominated solely by matter [15–17].

Moreover, statistical analyses show that BAO data alone can constrain the relationship between the matter density parameter Ω_m and the DE EoS w_{de}, though the two parameters exhibit a strong degeneracy. An approximate relation capturing this dependence is given by:

$$\Omega_m \approx 0.282 + 0.0935(1 + w_{\text{de}}) + 0.015(1 + w_{\text{de}})^2. \tag{1.25}$$

This relation intersects with other independent constraints, including supernova observations, near $\Omega_m \approx 0.275$ and $w_{\text{de}} \approx -1.06$, values compatible with a cosmological constant. When BAO measurements are combined with Type Ia supernovae data or Cosmic Microwave Background (CMB) results, the precision on both parameters significantly improves. For instance, joint analyses yield constraints such as $\Omega_m = 0.29 \pm 0.02$ and $w_{\text{de}} = -0.97 \pm 0.11$. In summary, BAO observations especially when integrated with complementary cosmological probes offer strong and independent support for the presence of DE in the universe.

1.3.4 Dark Energy Spectroscopic Instrument (DESI):

The first data release (DR1) from the Dark Energy Spectroscopic Instrument (DESI) in 2024 [5] has significantly enhanced our understanding of the late-time acceleration of the universe and the nature of DE. Analysis of the data under the widely used Chevallier–Polarski–Linder (CPL) parameterization of the DE EoS:

$$w(z) = w_0 + w_a \frac{z}{1+z},$$

shows a preference for dynamical DE over the standard ΛCDM model at more than 2σ confidence level [5]. In this framework, the parameters w_0 and w_a respectively describe the present-day value and the redshift evolution of the DE EoS. These observations align with other recent studies that also favor a dynamical nature of DE under the CPL framework [18, 19]. However, not all investigations converge on CPL being the optimal model some analyses report that alternative parameterizations may better capture the behavior of DE across cosmic time [20]. Beyond CPL, the DESI 2024 dataset has also been used to test and constrain a broad range of dynamical DE models, many of which outperform ΛCDM in terms of goodness-of-fit [21–23]. When evaluated using model selection techniques such as Bayesian evidence and information criteria, these evolving models often show greater consistency with the observed large-scale structure and distance measurements.

In evolving DE cosmologies, the Hubble expansion rate becomes:

$$H(z)^2 = H_0^2 \left[\Omega_m (1+z)^3 + \Omega_r (1+z)^4 + \Omega_{de} \exp\left(3 \int_0^z \frac{1+w(z')}{1+z'} \, dz' \right) \right] \tag{1.26}$$

which directly incorporates the redshift evolution of $w(z)$. DESI's precise BAO measurements across redshifts help constrain this expansion history, offering improved insights into cosmic acceleration.

Overall, DESI 2024 results reinforce the view that DE may be dynamic rather than static, challenging the long-held assumption of a constant Λ, and opening new avenues for understanding the physics behind the accelerating universe.

1.4 Dark Energy Models:

As discussed earlier, DE derive the observed accelerated expansion of the universe. In order to describe its behaviour several models are proposed. These models can be broadly categorized into Non-Interacting and Interacting DE Models, depending on whether DE exchanges energy with other components or not. Below are some of the DE models which are proposed to explain the present expansion:

1.4.1 Cosmological Constant:

The very first and the simplest model to explain DE is the cosmological constant, Λ [24] which represents a constant energy density that fills space uniformly. Einstein initially added Λ in his field equations to allow for static universe. The field equations Eq.(1.2) with Λ are give as:

$$R_{\mu\nu} - \frac{1}{2}Rg_{\mu\nu} + \Lambda g_{\mu\nu} = \frac{8\pi G}{c^4}T_{\mu\nu} \tag{1.27}$$

here the term $\Lambda g_{\mu\nu}$ effectively acts like an additional source of energy-momentum with constant density and negative pressure. We can think of Λ as a form of fluid with constant energy density ρ_Λ and pressure p_Λ which are given as:

$$\rho_\Lambda = \frac{\Lambda}{8\pi G} \tag{1.28a}$$

and

$$p_\Lambda = -\rho_\Lambda \tag{1.28b}$$

This negative pressure causes a repulsive gravitational effect, leading to accelerated expansion. This leads to a constant EoS parameter:

$$w_\Lambda = \frac{p_\Lambda}{\rho_\Lambda} = -1 \tag{1.29}$$

Now, as the evolution of the scale factor $a(t)$ is governed by the Friedmann equations. So, including the cosmological constant, the first and second Friedmann equations, Eq.(1.6) and (1.7) for flat universe becomes:

$$H^2 = \left(\frac{\dot{a}}{a}\right)^2 = \frac{8\pi G}{3}\rho + \frac{\Lambda}{3} \tag{1.30}$$

$$\frac{\ddot{a}}{a} = -\frac{4\pi G}{3}(\rho + 3p) + \frac{\Lambda}{3} \tag{1.31}$$

In a universe dominated entirely by the cosmological constant, the scale factor evolves as [25, 26]

$$a(t) \propto e^{Ht}, \qquad H = \sqrt{\frac{\Lambda}{3}} \tag{1.32}$$

This describes an exponentially expanding de Sitter universe, which is consistent with current observations of the late-time universe. Despite its observational success, the cosmological constant faces two significant theoretical problems:

- **Fine-Tuning Problem:** Quantum field theories predict a vacuum energy density that is many orders of magnitude larger than the observed value of Λ [27]. Since even the vacuum state possesses energy due to zero-point fluctuations, a naive estimate of the vacuum energy density obtained by summing the zero-point energies up to a momentum cutoff Λ_c gives:

$$\rho_{\text{vac}} \sim \frac{\Lambda_c^4}{16\pi^2} \tag{1.33}$$

If we take the cutoff to be at the Planck scale, $\Lambda_c \sim M_{\text{Pl}} \sim 10^{19}\,\text{GeV}$, then:

$$\rho_{\text{vac}} \sim 10^{76}\,\text{GeV}^4 \tag{1.34}$$

In contrast, observational bounds (from the current acceleration of the universe) suggest:

$$\rho_\Lambda^{\text{obs}} \sim 10^{-47}\,\text{GeV}^4 \tag{1.35}$$

This represents a discrepancy of more than 120 orders of magnitude:

$$\frac{\rho_{\text{vac}}^{\text{theory}}}{\rho_\Lambda^{\text{obs}}} \sim 10^{123} \tag{1.36}$$

This is the essence of the cosmological constant problem: why is the vacuum energy so small compared to theoretical expectations, and why is it not exactly zero? To reconcile the tiny observed value with the huge theoretical expectation, an extraordinary fine-tuning is required. The bare cosmological constant Λ in Einstein's equations must cancel the quantum contributions with extreme precision:

$$|\Lambda + 8\pi G\rho_{\text{vac}}| \lesssim 10^{-47}\,\text{GeV}^4 \tag{1.37}$$

This cancellation must be accurate to at least 123 decimal places, which seems highly unnatural without some underlying symmetry or mechanism.

- **Cosmological Coincidence Problem:** In addition to the fine-tuning, another intriguing puzzle arises when considering the timing of its dominance: the so-called **coincidence problem**. This problem questions why the energy densities of matter and DE are of the same order of magnitude precisely at the present epoch, even though they evolve very differently over cosmic time. In an expanding universe described by FLRW metric, the energy densities of different components scale differently with the scale factor $a(t)$. For a flat universe with pressureless matter (dust) and a cosmological constant Λ, using Eq. (1.15b) and (1.15a) the energy densities evolve as:

$$\rho_m(a) = \rho_m^0 a^{-3} \tag{1.38}$$

$$\rho_\Lambda(a) = \rho_\Lambda^0 = \text{constant} \tag{1.39}$$

As the universe expands, $a(t)$ increases, and the matter energy density ρ_m rapidly decreases, while ρ_Λ remains constant. In the early universe ($a \ll 1$), matter dominates; in the far future ($a \gg 1$), DE dominates. However, *today*, we find:

$$\frac{\rho_m^0}{\rho_\Lambda^0} \sim \mathcal{O}(1)$$

This near equality appears to occur at a very special moment in the universe's history, suggesting a fine-tuned coincidence. Why is it that we happen to live during the very brief period in cosmic history when $\rho_m \sim \rho_\Lambda$? Given that the two quantities evolve so differently, one would expect them to differ by many orders of magnitude unless there is some mechanism synchronizing their evolution. Several ideas have been proposed to address the coincidence problem:

1. **Interacting Dark Energy Models**: These models allow energy exchange between DE and dark matter, making their ratio evolve more slowly and naturally remain near unity for longer.
2. **Tracker or Attractor Solutions**: Scalar field models (e.g., quintessence) can have attractor behaviors where DE dynamically adjusts itself to be comparable with matter over extended periods.
3. **Anthropic Principle**: In a multiverse scenario, only those universes where the densities coincide at the right time allow for observers. Hence, it is not

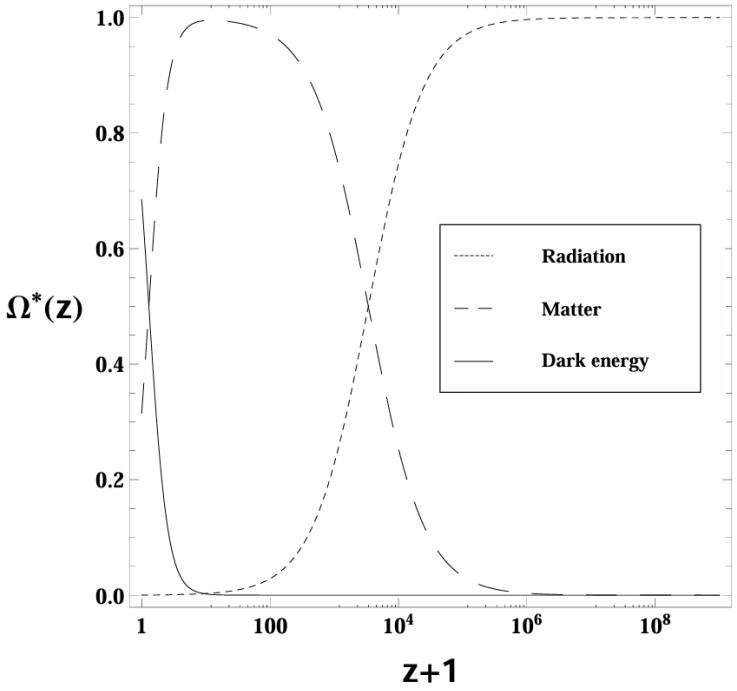

FIGURE 1.2: Plot shows how the energy densities Ω of radiation, matter and DE evolve with respect to redshift z. Plot is from [28]

surprising that we observe such a coincidence.

4. **Phantom Cosmologies**: In phantom models with a finite lifetime, the period of comparable dark matter and DE densities occupies a larger fraction of cosmic time, making the coincidence less severe.

The coincidence problem adds another layer of mystery to the DE puzzle. Unlike the fine-tuning problem, which asks *why* Λ is small, the coincidence problem asks *why now*. Both problems suggest that the standard cosmological constant model, though observationally successful, may be incomplete without new physics to explain these striking features.

Nevertheless, the cosmological constant remains the most straightforward explanation for DE and a cornerstone of the standard model of cosmology, known as the ΛCDM model.

1.4.2 Non-Interacting Dark Energy Models:

Non-interacting DE models are some of the simplest and most studied frameworks in cosmology, which assume that DE evolves "independently" from other components of

the universe, such as DM and radiation, without exchanging energy or momentum with them. In these models, each component follows its own conservation law and evolves according to its own dynamics, governed by the overall expansion. In the standard ΛCDM, as we know the universe is described by the FLRW metric Eq.(3.1) and the dynamics are governed by the Friedmann equations Eq. (1.6) and (1.7). So, assuming there is no interaction between DE and matter, the energy conservation equations or continuity equation Eq. (1.13) for each component are separately satisfied:

$$\dot{\rho}_m + 3H\rho_m(1 + w_m) = \dot{\rho}_m + 3H\rho_m = 0, \tag{1.40}$$

$$\dot{\rho}_r + 3H\rho_r(1 + w_r) = \dot{\rho}_r + 4H\rho_r = 0, \tag{1.41}$$

$$\dot{\rho}_{de} + 3H(1 + w_{de})\rho_{de} = 0, \tag{1.42}$$

where:

- ρ_m is the energy density of matter and $w_m = 0$,
- ρ_r is the energy density of radiation and $w_r = 1/3$,
- ρ_{de} is the energy density of DE,
- $H = \dot{a}/a$ is the Hubble parameter,
- $w_{de} = p_{de}/\rho_{de}$ is the EoS parameter for DE.

Here, we can see that the DE component evolves independently based only on its own properties, especially its EoS w_{de}.

The simplest non-interacting DE model is the Cosmological Constant(DE) + Cold Dark Matter , denoted by ΛCDM, which has a constant energy density and a fixed EoS, i.e., EoS doesn't vary with cosmic time t:

$$w_\Lambda = -1, \tag{1.43}$$

leading to:

$$\dot{\rho}_{de} = \dot{\rho}_\Lambda = 0. \tag{1.44}$$

This means that the energy density of the cosmological constant remains unchanged as the universe expands. Despite its success in explaining the current accelerated expansion,

the cosmological constant faces the famous fine-tuning and coincidence problems, as discussed earlier.

A scalar field ϕ associates a single value to every point of spacetime, depending only on the x^μ spacetime coordinates. Now for a spatially flat and homogeneous universe the action combining GR and Scalar field can be written as:

$$\mathcal{S} = \int \sqrt{-g}\left(\frac{\mathcal{R}}{2\kappa^2} + \mathcal{L}_\phi\right) d^4x + \mathcal{S}_m \tag{1.45}$$

here $\mathcal{R}$ is the Ricci scalar, $g = |g_{\mu\nu}|$ is the determinant if metric tensor, ϕ is the associated scalar field, $\kappa^2 = 8\pi G$ with G as the gravitational constant, $\mathcal{S}_m$ is action associated with the matter component of the universe and $\mathcal{L}_\phi$ is the Lagrangian density associated with the particular model of scalar field and it governs the dynamics which typically contains the kinetic term and potential term. Using this action and the Lagrangian density associated with the particular model all equations required to describe the dynamics of the particular model can be obtained. The energy density and pressure can be obtained easily from the energy momentum tensor whose equation is:

$$T^{\mu\nu} = \frac{\partial \mathcal{L}_\phi}{\partial(\partial_\mu \phi)}\partial^\mu \phi - g^{\mu\nu}\mathcal{L}_\phi \tag{1.46}$$

The configuration space of the system consists of the metric and the scalar field. And the dynamics is obtained by varying the action w.r.t. these degrees of freedom to yield the Einstein equation and the Klein-Gordon equation. Before moving towards our proposed model let's discuss the dynamics of three classes of scalar field independently:

1.4.3 Quintessence

Many authors propose [29–35] Quintessence as one of the candidates for DE, which describes DE as a slowly evolving scalar field ϕ rolling down a potential $V(\phi)$. Unlike cosmological constants this canonical scalar field is time-dependent with dynamic or varying EoS [32–35]. Now for the case of this quintessence scalar field model, the Lagrangian density is given by:

$$\mathcal{L}_\phi = -\frac{1}{2}g^{\mu\nu}\partial_\mu\phi\partial_\nu\phi - V(\phi) \tag{1.47}$$

The first component reflects the kinetic term, whereas $V(\phi)$ indicates the potential associated with quintessence. Thus, the action for this scalar field model may be stated as follows:

$$\mathcal{S}_{quin} = \int \sqrt{-g}\left(\frac{\mathcal{R}}{2\kappa^2} - \frac{1}{2}g^{\mu\nu}\partial_\mu\phi\partial_\nu\phi - V(\phi)\right)d^4x + \mathcal{S}_m \tag{1.48}$$

Now for this model in FLRW background, the contribution of energy density and pressure are given by:

$$\rho_\phi = \frac{1}{2}\dot{\phi}^2 + V(\phi) \tag{1.49}$$

and

$$p_\phi = \frac{1}{2}\dot{\phi}^2 - V(\phi) \tag{1.50}$$

In flat universe the variation of action Eq.(1.48) with respect to ϕ provides required the evolution equation or equation of motion for this quintessence scalar field as:

$$\ddot{\phi} + 3H\dot{\phi} + V'(\phi) = 0 \tag{1.51}$$

where $H = \frac{\dot{a}}{a}$ is the Hubble parameter, $V'(\phi) = \frac{dV}{d\phi}$. One can also obtain this evolution equation from the continuity equation and the dynamical EoS which evolves over time is found to be:

$$w_\phi \equiv \frac{p_\phi}{\rho_\phi} = \frac{\dot{\phi}^2 - 2V(\phi)}{\dot{\phi}^2 + 2V(\phi)} \tag{1.52}$$

For the scalar field to evolve slowly the potential needs to be shallow enough so that ϕ can roll down the potential slowly to provide required accelerated expansion i.e. if $V(\phi) >> \dot{\phi}^2$ then the EoS evolve as $w \longrightarrow -1$ which could mimic ΛCDM and can be a good candidate to explain the present accelerated expansion of the universe.

1.4.4 Phantom

One of the modifications of quintessence model is "Phantom" or "Ghost" scalar field model [36–39] which has a negative kinetic component that leads to the EoS $w < -1$ which is consistent with some interpretations of current cosmological data from CMB and BAO, however, this model face some limitations like instabilities, energy condition violation and "Big Rip", but we can't deny the fact that it fits quite well with

observations [38, 39]. Now the Lagrangian density for the case of phantom is given by:

$$\mathcal{L}_\phi = \frac{1}{2} g^{\mu\nu} \partial_\mu \phi \partial_\nu \phi - V(\phi) \tag{1.53}$$

Therefore, the action for phantom model can be written as:

$$\mathcal{S}_{phan} = \int \sqrt{-g} \left(\frac{\mathcal{R}}{2\kappa^2} + \frac{1}{2} g^{\mu\nu} \partial_\mu \phi \partial_\nu \phi - V(\phi) \right) d^4x + \mathcal{S}_m \tag{1.54}$$

Similarly, changing the action with respect to the scalar field yields the equation of motion:

$$\ddot{\phi} + 3H\dot{\phi} - V'(\phi) = 0 \tag{1.55}$$

n homogeneous and isotropic spacetime, Eq.(1.46) yields the energy density and pressure for the Phantom field as:

$$\rho_\phi = -\frac{1}{2}\dot{\phi}^2 + V(\phi) \tag{1.56}$$

and

$$p_\phi = -\frac{1}{2}\dot{\phi}^2 - V(\phi) \tag{1.57}$$

As seen in the preceding equation, total energy density remains positive if and only if the potential term dominates the kinetic term, but pressure always remains negative, which is one of the major aspects explaining the universe's rapid expansion. Now using above two equations Eq.(1.56) and (1.57) the EoS can be obtained as follows:

$$w_\phi \equiv \frac{p_\phi}{\rho_\phi} = \frac{\dot{\phi}^2 + 2V(\phi)}{\dot{\phi}^2 - 2V(\phi)} \tag{1.58}$$

here again from the above equation, we can see that for $\rho_\phi > 0 \implies w_\phi < -1$ leading the accelerated expansion of the universe. Thus, phantom scalar field has the ability to explain the accelerated expansion but it can also lead to a big rip tearing apart the cosmos.

1.4.5 Tachyon

Another form of scalar field DE model is "Tachyon" [40–47] which arises from string theory and is considered as one of the candidates for DE and inflation. Lagrangian

density for the case of Tachyon scalar field is given by:

$$\mathcal{L}_\phi = -V(\phi)\sqrt{1-\partial_\mu\phi\partial^\mu\phi} \tag{1.59a}$$

Therefore, the action of tachyonic scalar field model can be written as:

$$\mathcal{S}_{tachyon} = \int \sqrt{-g}\left(\frac{\mathcal{R}}{2\kappa^2} - V(\phi)\sqrt{1-\partial_\mu\phi\partial^\mu\phi}\right) d^4x + \mathcal{S}_m \tag{1.59b}$$

Now, the energy density and pressure for the tachyon scalar field can be obtained by using Eq.(1.46) as:

$$\rho_\phi = \frac{V(\phi)}{\sqrt{1-\dot{\phi}^2}} \tag{1.59c}$$

and

$$p_\phi = -V(\phi)\sqrt{1-\dot{\phi}^2} \tag{1.59d}$$

Varying the tachyonic action in relation to the scalar field ϕ again makes it easy to get the evolution equation or equation of motion for the tachyon scalar field model, which is:

$$\frac{\ddot{\phi}}{(1-\dot{\phi}^2)} + 3H\dot{\phi} + \frac{1}{V}\frac{dV}{d\phi} = 0 \tag{1.59e}$$

For a flat and homogeneous universe, the EoS parameter w_ϕ is given as:

$$w_\phi \equiv \frac{p_\phi}{\rho_\phi} = \dot{\phi}^2 - 1 \tag{1.60}$$

again this tachyonic EoS is time varying as $\dot{\phi}^2$ represents the time derivative of scalar field ϕ. here if $\dot{\phi}^2 << 1$ this tachyonic model mimics cosmological constant behaving like DE, as for this case $w_\phi \longrightarrow -1$ but if $\dot{\phi}^2 \longrightarrow 1$ EoS transition's to pressure-less fluid or dust with $w_\phi \sim 0$ behaving like dark matter, but in this case this model face some instability issues. Acceleration occurs when $\dot{\phi}^2 < \frac{2}{3}$, corresponding to $w_\phi < -\frac{1}{3}$. Tachyon fields can behave like dust at early times and like DE at late times, making them attractive candidates for a unifying picture of cosmic evolution.

Non-interacting DE models are elegant in their simplicity as:

- they, to some extent, matches the observations of cosmic acceleration quite well.

- they avoid the complexities introduced by interaction terms, but can't explain for dark sector interacts.
- they allow theoretical flexibility through different types of scalar fields.

However, they are some problems related to these non-interacting models like:

- they often require fine-tuning of initial conditions.
- they do not naturally explain why the densities of DM and DE are comparable today (the coincidence problem).
- some, like phantom models, predict future singularities with potentially catastrophic consequences.

Nonetheless, non-interacting models continue to serve as a baseline for understanding DE and exploring new physics beyond the standard cosmological model, treating DM and DE as two independent components that evolve separately, each obeying its own conservation law. Their only link is through their contribution to the overall dynamics of the universe via gravity. However, with the growing precision of cosmological observations and the persistent theoretical puzzles, this separation appears overly simplistic. As, non-interacting models still don't alleviate the coincidence and fine-tuning problem. In order to link the evolutionary phases of DE and matter components interacting DE models came into picture which are discussed in more details in our next section.

1.4.6 Interacting Dark Energy Models:

One major motivation for considering ***Interacting DE Models*** is the attempt to address the *coincidence problem* [28]. Currently, the energy densities of DE and DM are of the same order of magnitude, despite having evolved differently throughout cosmic history. Without interaction, this apparent synchrony would seem extremely unlikely. By allowing an exchange of energy between DE and matter components, it becomes possible to link their evolutionary phases, naturally explaining why their densities are comparable today.

From a theoretical perspective, it is common in high-energy physics for fields to interact. Thus, it would seem unnatural for a DE scalar field ϕ to remain entirely isolated from

other sectors, particularly matter [48]. Interactions between dark sectors could arise from fundamental physics or effective field theories, leading to a dynamic interplay that affects the cosmic expansion and structure formation.

Observationally, interacting models offer the possibility of detecting subtle deviations from the predictions of the ΛCDM model. For instance, small modifications in the Hubble expansion rate or in the growth of large-scale structures could hint at energy exchange between dark sectors [49]. Higher-order corrections to the Hubble law, such as cubic terms probed through supernovae type Ia data, might serve as indirect evidence for such interactions [50]. Another advantage of introducing interactions lies in the existence of *scaling solutions* [48]. In these scenarios, the ratio between the DE density and the DM density remains approximately constant over significant periods of time. Such solutions could naturally drive the universe toward an accelerated expansion phase without the need for extreme fine-tuning of initial conditions. So, interacting DE models are motivated by both theoretical expectations and observational possibilities. They offer a richer framework for explaining cosmic acceleration and may address deep-rooted problems like the coincidence problem and open pathways for new observational tests that could shed light on the nature of the dark sector. This transfer of energy between the two components of the dark sector is taken into consideration by several writers [51–57] who are driven to solve the cosmic coincidence issue and fine-tuning. As a result, conservation of energy is conserved globally but broken locally. The energy-momentum tensor $T^{(m)}_{\mu\nu}$ and $T^{(de)}_{\mu\nu}$ may thus be expressed as follows: [58]

$$\nabla^{\mu} T^{(m)}_{\mu\nu} = Q_{\nu} \tag{1.61a}$$

and

$$\nabla^{\mu} T^{(de)}_{\mu\nu} = -Q_{\nu} \tag{1.61b}$$

Thus, the separate non-zero conservation equations for matter and DE can be written as:

$$\dot{\rho}_m + 3H(1 + w_m)\rho_m = Q, \tag{1.62}$$

$$\dot{\rho}_{de} + 3H(1 + w_{de})\rho_{de} = -Q, \tag{1.63}$$

where:

- ρ_m and ρ_{de} are the energy densities of matter and DE respectively,
- w_m and w_{de} is the EoS parameter of matter and DE,
- Q is the interaction or coupling term governing the energy transfer between the components under consideration.

The form of Q can vary depending on the model. Some common choices include

$$Q = \beta H \rho_m, \quad \text{(proportional to matter density)}, \tag{1.64}$$

$$Q = \beta H \rho_{de}, \quad \text{(proportional to DE density)}, \tag{1.65}$$

$$Q = \beta H (\rho_m + \rho_{de}), \quad \text{(proportional to the sum)}. \tag{1.66}$$

Here, β is considered to be a coupling constant, which helps in determining the strength of coupling.

When $Q > 0$, energy flows from DE to matter, and when $Q < 0$, the transfer is in the opposite direction. The sign and magnitude of Q significantly affect the cosmological evolution and can leave observable imprints on the Large Scale Structures (LSS) of the universe.

Coupled Quintessence Scalar Field model: While standard quintessence models assume that the scalar field responsible for DE evolves independently, a more general and natural possibility is that it interacts directly with other components of the universe, particularly matter. This idea leads to the concept of **coupled quintessence** [48], where the scalar field and dark matter exchange energy and momentum as the universe evolves, modifying their evolution as compared to standard uncoupled models with zero coupling. The idea of such a coupling is natural from the perspective of high-energy physics. In theories like string theory or scalar-tensor gravity, scalar fields typically interact with other fields unless forbidden by a symmetry. Therefore, considering a coupling between DE and DM is theoretically motivated. In coupled quintessence, the standard energy-momentum conservation equations are modified similar to the one mentioned in Eq. (1.61a) and (1.61b) :

$$\nabla^\mu T^{(m)}_{\mu\nu} = Q_\nu \tag{1.67a}$$

and

$$\nabla^\mu T^{(de)}_{\mu\nu} = -Q_\nu \tag{1.67b}$$

and these equations reduce to:

$$\dot{\rho}_m + 3H\rho_m = Q, \tag{1.68}$$

$$\dot{\rho}_\phi + 3H(\rho_\phi + p_\phi) = Q, \tag{1.69}$$

where:

- ρ_m is the energy density of DM,
- ρ_ϕ and p_ϕ are the energy densities of scalar field and pressure,
- H is the Hubble parameter.

In coupled quintessence, the total energy remains conserved, but individual components do not conserve energy independently. Instead, energy flows between matter and the scalar field depending on the sign and size of the coupling and the scalar field's dynamics is governed by:

$$\ddot{\phi} + 3H\dot{\phi} + \frac{dV}{d\phi} = \frac{Q}{\dot{\phi}} \tag{1.70}$$

Here, the source term $Q/\dot{\phi}$ represents the effect of the coupling parameter.

Coupled quintessence models offer several important advantages:

- They could provide a potential solution to the **coincidence problem** by allowing matter (DM) and DE densities to evolve together.
- They modify the growth of cosmic structures, leading to distinct observational signatures in the large-scale structure and the cosmic microwave background.
- They naturally lead to attractor [91] behaviors such as the **field-matter-dominated era** (fMDE), where the field energy density remains a fixed fraction of the matter energy density for some period.

While coupled quintessence models offer an interesting alternative to explain cosmic acceleration and address the coincidence problem, they also face several notable challenges:

- **Constraints from Local Gravity Tests:** Coupling between DE and DM introduces a fifth force that can modify gravitational behavior. Precision measurements

Interaction Term Q	**References**
$\beta\rho\dot{\phi}$	[48, 59–68]
$\beta H\rho$	[60, 66, 69]
$\beta\rho\dot{\phi}\phi/a^4$	[70]
$\beta\dot{\phi}^2$	[71, 72]
$\beta H\dot{\phi}^2$	[71]
$\beta\rho$	[66]
$\beta\rho^2/H$	[69]
$\beta\rho\dot{\phi}^2/H$	[69]
$\alpha\rho_\phi^2+\beta\rho^2+\gamma\rho\rho_\phi$	[73]
$\beta\rho f(\phi)\dot{\phi}$	[74–77]
$\eta(\dot{\rho}_i+3H\beta\rho_i)$ with $\eta=-(1+\dot{H}/H^2)$ and $\rho_i=\rho,\rho_\phi,\rho+\rho_\phi$	[78]
$\beta H(\rho_\phi-\rho)$	[79]
$\alpha\dot{\rho}_\phi+\beta\dot{\rho}$	[80]
$\alpha(\rho+\rho_\phi)\dot{\phi}$	[81]
$\eta H^\lambda\rho_m^\alpha\rho_{de}^\beta$	[82]
$H(\alpha\rho_m+\beta\rho_{de})$	[83–85]
$\alpha\rho_m+\beta\rho_{de}$	[84]
$\beta H\rho_{de}^\alpha\rho_m^{1-\alpha}$	[86]
$3H(\lambda+\alpha\rho_m+\beta\rho_{de})$	[87]
$\lambda\rho_m$	[88]
$3H\eta(\rho_m+\rho_{de})^\lambda\rho_m^\alpha\rho_{de}^\beta$	[89]
$\lambda\rho_m\rho_{de}/H$	[90]

TABLE 1.1: Table shows different forms of interaction terms Q proposed in interacting DE models. Here ρ represents the DM density, ρ_ϕ represents the DE (quintessence) scalar field energy density, and H is the Hubble parameter. Table is taken from [58]

within the solar system and laboratory experiments severely constrain such deviations, forcing the coupling strength to be extremely small [48, 92]. This limits the cosmological impact of the coupling.

- **Instabilities and Negative Effective Masses:** Certain choices of coupling

functions or coupling strengths can lead to instabilities in the perturbations. In particular, a negative effective mass can cause uncontrolled growth of fluctuations, spoiling the formation of large-scale structures [93, 94].

- **Fine-Tuning of the Coupling:** Although coupled quintessence models aim to reduce fine-tuning, they often require careful adjustment of the coupling parameter. The coupling must be strong enough to affect cosmic evolution but weak enough to satisfy local gravity constraints, reintroducing fine-tuning issues [48, 95]
- **Impact on Structure Formation:** Coupled quintessence alters the growth rate of cosmic structures. If the coupling is not carefully calibrated, the resulting matter power spectrum may not match observational data from galaxy surveys and weak lensing experiments [95, 96].

While coupled quintessence models involving canonical scalar fields are widely studied, the idea can be extended to other types of scalar fields as well. One can consider models where the DE sector is described by an interacting tachyon field or a phantom field, each bringing distinct dynamics to cosmic evolution. Tachyon fields, which originate from string theory, have a non-standard kinetic term and naturally interpolate between dust-like behavior and DE domination. Phantom fields, on the other hand, possess a negative kinetic energy term and can lead to scenarios of super-acceleration, potentially culminating in a Big Rip singularity.

Beyond these individual cases, there is growing interest in constructing unified models where both DE and DM emerge from a single scalar field framework. In such approaches, the Lagrangian itself is designed to describe a field that behaves like dark matter during the early universe and smoothly transitions to DE behavior at late times. This unification offers an elegant way to explain the apparent balance between dark matter and DE today, without introducing separate and unrelated components.

A particularly important aspect motivating the analysis carried out in this thesis is the behavior of scalar fields near an ***inflection point*** in their potential. The inflection point represents a critical moment where the dynamics of the field change significantly, potentially triggering "slow roll". Studying the behavior of the field near the inflection point provides deep insights into the onset of late-time cosmic acceleration and helps in developing model-independent diagnostics of DE, by carefully analyzing the field

evolution around the inflection point, we can understand how different types of couplings and field properties influence the cosmic expansion.

We will explore these possibilities in more detail in Chapter 6, where models capable of unifying DM and DE through a generalized Lagrangian formulation are presented. Such models aim to explain the late-time acceleration of the universe in a more fundamental and unified manner.

1.5 Thesis structure

The present thesis focuses on exploring the interaction between DE and matter (DM) through scalar field model. To begin with, the behavior of coupled canonical scalar fields near an inflection point was investigated, highlighting how coupling modifies the cosmic expansion history and offering model-independent diagnostics for DE evolution. The analysis was then extended to minimally coupled tachyonic fields, where the distinct dynamical features of tachyon models near inflection points were carefully studied. Based on these results, a generalized Lagrangian framework was developed, aiming to unify different DE scalar fields (quintessence, phantom & tachyon) and DM within a single theoretical framework. This generalized model could also allow for the interpretation of the interaction as a potential fifth fundamental force, and consistent coupling parameters were obtained in agreement with observational constraints. The overall work provides new insights into the role of interacting scalar field in cosmic acceleration and opens new directions for future studies in unified dark sector models.

Chapter (1) This chapter sets the stage for the thesis by providing a broad overview of the current understanding of cosmic acceleration and the challenges associated with explaining it. The motivation for studying DE and its interaction with matter is outlined. Observational evidence for the accelerated expansion of the universe is discussed, along with the problems of the cosmological constant and the coincidence problem along with an overview of different Non-Interacting and Interacting DE models.

Chapter (2) This chapter presents a detailed review of existing work on DE models, both interacting and non-interacting. It covers scalar field theories, quintessence, tachyon models, and their extensions. Particular emphasis is placed on previous attempts to

model the interaction between DE and DM. Based on the gaps and open questions found in the literature, along with the motivation.

Chapter (3) In this chapter is dedicated to analyze the behavior of DE field near inflection points within the framework of coupled canonical scalar field particularly quintessence field and we will study the impact of the coupling on the evolution of the field and the cosmological dynamics. After that we will study how inflection point effects the universe's expansion, and we will later compare the results with observations like Spectral index and slow roll parameters.

Chapter (4) is dedicated to study non minimally coupled tachyon scalar field near inflection point. In this chapter we will consider more general case, instead of choosing potential, we will study different cases of scale factor and from each form of scale factor we will derive a potential and will analyze the behavior of field for each case. Following this, we will do a dynamical system analysis of our developed model.

In the next chapter (5), we delve into a more general model by introducing a generalized scalar field Lagrangian with the aim of unifying DE and DM within a single theoretical framework. The possibility of interpreting the interaction in between dark sector as a fifth fundamental interaction is discussed. Consistent coupling parameters are derived by ensuring agreement with cosmological observations. The chapter highlights how a generalized Lagrangian approach can provide a deeper understanding of the nature of DE interactions.

In the final chapter (7),This final chapter summarizes the major findings of the thesis, emphasizing the significance of investigating interactions between DE and dark matter, especially near inflection points. It reflects on how the generalized models developed contribute to the broader picture of cosmological dynamics. Potential future directions for research are suggested, including observational strategies to further test the existence of a fifth force and refining the coupling parameters with next-generation cosmological surveys.

Chapter 2

Literature Review

The story of DE begins with a discovery that shook the foundations of modern cosmology. In 1998, two independent research teams the ***High-z Supernova Search Team*** [1, 2] and the ***Supernova Cosmology Project*** [3] were investigating distant Type Ia supernovae to measure the deceleration of the universe's expansion. To their surprise, they found the exact opposite! the expansion of the universe was not slowing down, but speeding up. These dimmer than expected supernovae pointed to a startling conclusion that some unknown force was counteracting gravity on cosmic scales. Even other observations like ***CMBR (Cosmic Microwave Background Radiation)*** [97] and ***BAO (Baryonic Acoustic Oscillations)*** [98, 99] indicate the existence of DE.

Huterer and Turner in 1999 [100] investigated how distance measurements from Type Ia supernovae could be used to reconstruct the nature of DE. They proposed a method to derive the scalar field potential directly from observational data, aiming to distinguish a cosmological constant from dynamical DE. Their analysis, supported by Monte Carlo simulations, showed that while reconstruction is theoretically feasible, it demands extremely high-quality data and careful control of observational errors. They concluded that although the method offers a promising approach, significant challenges remain in extracting reliable information from realistic, noisy datasets.

In 2000 [34] ***Varun Sahni and Alexei Starobinsky*** examined both observational and theoretical evidence supporting a small, positive cosmological constant (Λ). They showed that data from Type Ia supernovae, CMB anisotropies, gravitational lensing, and galaxy clustering favor a flat universe with $\Omega_m \approx 0.3$ and $\Omega_\Lambda \approx 0.7$. The authors

analyzed FLRW models with $\Lambda \neq 0$, highlighting various cosmic behaviors and discussed the unresolved cosmological constant problem, where theoretical predictions vastly exceed observed values. Possible solutions such as scalar fields, decaying Λ, and anthropic reasoning were also explored. Their work remains pivotal in understanding DE and the universe's accelerated expansion.

In 2000 ***Chiba et al.*** (2000)[35] proposed a novel DE model in which the dynamics of the scalar field are governed entirely by non-canonical kinetic terms, without requiring a potential. This kinetically driven quintessence framework supports a constant equation of state $w \in (-1, 0)$ and features late-time attractor solutions, allowing the scalar field to evolve toward these solutions from a broad range of initial conditions. The authors further extended their analysis to include phantom energy models with $w < -1$, demonstrating that such models can remain stable under perturbations when the kinetic structure is appropriately chosen. Through both analytical phase space exploration and numerical simulations, they confirmed the attractor nature of the solutions in both quintessential and phantom regimes. Although reconstructing the kinetic Lagrangian from observational data is more challenging than in canonical models, this approach provides a viable alternative to explain cosmic acceleration and may have implications for theories involving violations of the weak energy condition.

In the same year ***Luca Amendola*** (2000)[48] proposed a coupled quintessence model in which a scalar field with an exponential potential is linearly coupled to matter, leading to significant modifications in both the cosmic background evolution and the behavior of perturbations. A key feature of this model is the emergence of a transitional phase called the field-matter-dominated era, characterized by a nearly constant energy contribution from the scalar field during the matter-dominated epoch. The study presents a detailed phase-space analysis, identifying critical points and their stability, and concludes that only one attractor solution can produce accelerated expansion consistent with observational data. By adapting the CMBFAST code, Amendola demonstrated how such coupling affects the cosmic microwave background (CMB) spectrum, resulting in shifts in acoustic peak positions and a suppression of the matter fluctuation amplitude, notably the σ_8 parameter. The observational constraints suggest that the dimensionless coupling constant must satisfy $|\beta| < 0.1$ to agree with current cosmological measurements. Additionally, the model is shown to be mathematically equivalent to certain

Brans-Dicke theories with power-law potentials, highlighting its relevance to broader scalar-tensor frameworks.

Hebecker and Wetterich (2001)[101] present a class of quintessence models that aim to explain the observed acceleration of the universe without introducing unnatural parameters or fine-tuned initial conditions. Their approach involves a scalar field with an exponential potential and a non-canonical kinetic term, allowing a broad range of cosmological behaviors. The study highlights two viable scenarios: one where the kinetic term undergoes a sudden increase (leaping kinetic term), and another where the scalar field evolves slowly before triggering acceleration (runaway quintessence). Both models align with current observations and avoid the small numerical constants required in many other DE models. In contrast, standard models using power-law potentials typically require fine-tuning, making them less natural. The paper also touches on the coincidence problem, suggesting that the onset of cosmic acceleration may be tied to physical transitions such as matter domination, rather than requiring unexplained tuning. Overall, their framework provides a theoretically motivated and observationally consistent alternative to models relying on a cosmological constant.

In 2003 ***J.S Bagla, H.K Jassal and T.Padmanabhan*** [102] explored the possibility of explaining DE using a homogeneous Tachyonic scalar field inspired by string theory. Their work examined two potential forms for the tachyon field: the inverse square potential $V(\phi) \propto \phi^{-2}$ and the exponential potential $V(\phi) \propto e^{-\phi/\phi_0}$. The authors demonstrated that both potentials can result in late-time cosmic acceleration consistent with observational data from Type Ia supernovae. Although the models require tuning of initial conditions, the degree of fine-tuning is similar to that needed in the standard ΛCDM and quintessence frameworks. A distinctive feature of tachyon-based cosmologies is that the energy density of the tachyon field remains comparable to that of non-relativistic matter during the matter-dominated era, which is unlike typical models where DE becomes negligible at early times. Notably, in the case of the exponential potential, the universe passes through a transient accelerated expansion before returning to a decelerated phase, thereby avoiding a future event horizon. The study also investigated implications for structure formation, showing that in many cases, the continued presence of tachyon energy at high redshifts leads to slower growth of density perturbations, potentially conflicting with constraints from cosmic microwave background observations unless model parameters are carefully selected.

Abramo and Finelli (2003)[41] explored the cosmological implications of a tachyonic scalar field governed by an inverse power-law potential $V(\varphi) \propto \varphi^{-n}$. Their analysis revealed that the universe's late-time dynamics depend critically on the value of n: for $n > 2$, the tachyon behaves like dust; for $n = 2$, it yields a power-law expansion; and for $0 < n < 2$, it leads to an accelerating universe. They demonstrated the stability of these solutions and showed that while tachyon field fluctuations can grow in the dust regime, metric perturbations remain constant on large scales. In a background dominated by a perfect fluid, the tachyon can track the dominant component and later transition to drive acceleration, highlighting its potential as a viable DE candidate. This work tries to provide a unified framework connecting early matter-like behavior and late-time cosmic acceleration through tachyon dynamics.

The paper by ***Peebles and Ratra*** (2003)[26] offers a comprehensive review of the cosmological constant and DE, focusing on both theoretical insights and observational developments. It discusses the evolution of ideas from Einstein's introduction of Λ to its modern interpretation as DE, driven by data from Type Ia supernovae, CMB anisotropies, and large-scale structure. The authors emphasize that while the evidence for DE is strong, it is not yet entirely conclusive due to possible systematic uncertainties. They explore alternative models like scalar fields (quintessence) that allow for dynamic DE and may help resolve the fine-tuning and coincidence problems. The paper highlights the unresolved discrepancy between the observed and predicted vacuum energy, calling it one of the major unsolved issues in physics. Ultimately, it underscores the need for deeper theoretical advances, possibly from quantum gravity, to fully understand the nature of DE.

Aguirregabiria and Lazkoz in 2004[103] investigated the dynamics of a spatially flat FRW universe containing a tachyon field with an inverse square potential, $V(T) \propto T^{-2}$, coupled with a barotropic fluid. By reformulating the evolution equations into a two-dimensional autonomous system, they conducted a phase-space analysis and identified several fixed points, including tachyon-dominated and tracking attractors. The tracking solution, characterized by both components redshifting at the same rate, emerges under the condition $\gamma < 1$ and reduces sensitivity to initial conditions, addressing fine-tuning issues. However, observational constraints from nucleosynthesis impose strict bounds on the model parameters, particularly on the coupling constant. While the results support

the cosmological relevance of tachyon fields, limitations arise when trying to match standard epochs like radiation and matter domination.

M. Sami and A. Toporensky in 2004[39] explored the cosmological implications of phantom fields—scalar fields with negative kinetic energy—as a candidate for DE. They examined how different potential functions, particularly those unbounded from above, influence the future evolution of the universe. Their analysis revealed that the steepness of the phantom potential plays a crucial role in determining the cosmic fate. For instance, potentials growing as power laws with exponents $\alpha \leq 4$ lead to a gradual increase in energy density with the equation of state approaching $w = -1$ over infinite time. However, steeper potentials ($\alpha > 4$) and exponential forms result in a "Big Rip" where the energy density diverges in finite time. Even more abrupt singularities arise for potentials steeper than exponential, causing $w \to -\infty$ at a finite scale factor. The study highlights that while some phantom models can lead to asymptotic de Sitter behavior, others predict catastrophic outcomes, all depending on the underlying potential's structure.

Copeland et al. in 2006[104] offers an extensive review of both theoretical and observational perspectives on DE. It covers the evidence for cosmic acceleration from Type Ia Supernovae, the Cosmic Microwave Background, and Large Scale Structure, alongside methods like luminosity distance and redshift relations to measure expansion. The paper examines various models for DE, including the Cosmological Constant (Λ), which faces fine-tuning and coincidence issues, and scalar field models such as quintessence and phantom energy. Additionally, it discusses coupled DE models that interact with dark matter and modified gravity theories, such as $f(R)$ and DGP models, as alternatives to DE. The review also delves into the dynamics of these models using a dynamical systems approach, highlighting scaling solutions and the potential for future singularities like the Big Rip. While the ΛCDM model remains the simplest, the paper notes that dynamical models offer greater flexibility, with cosmological perturbations and observational data still allowing for various possibilities.

Linder (2008)[32] presents a comprehensive study of quintessence models, which interpret DE as a time-evolving scalar field rather than a static cosmological constant. The paper classifies these models into thawing, freezing, tracking, and oscillating types based on their behavior in the phase space of the equation of state w and its derivative w'.

It defines physically motivated boundaries in this space to distinguish model dynamics and evaluates how future cosmological observations might separate these from the standard ΛCDM model. Linder also discusses model-independent parametrizations such as the $w_0 - w_a$ form and principal component analysis as tools to capture DE behavior without relying on specific potentials. The paper highlights challenges in reconstructing scalar field properties due to observational limitations and shows how combinations of different components can obscure the fundamental nature of DE. Overall, the study underscores the value of analyzing DE dynamics to better understand the cause of cosmic acceleration.

Ureña-López (2009)[105] investigates the conditions under which a Bose-Einstein condensate (BEC) of scalar field dark matter (SFDM) could have formed in the early universe. By analyzing the thermodynamics of an ideal relativistic Bose gas, the study reveals that BEC formation is only feasible if the scalar particles were extremely light and relativistic during decoupling. Contrary to the traditional notion that BECs arise in low-temperature, non-relativistic settings, this work emphasizes that a cosmological BEC would be inherently relativistic. A key finding is that the presence of both particles and antiparticles is essential for condensation to occur. The study derives a critical temperature condition linked to the particle mass and asymmetry, showing that a persistent BEC up to the present era requires particle masses below 10^{-14} eV. For heavier masses, the BEC would dissolve as the universe expands. Additionally, it confirms that non-relativistic decoupling prevents BEC formation due to rapid density suppression. Overall, the paper outlines a consistent thermal framework for SFDM models and sets clear mass constraints for viable cosmological BEC scenarios.

Verma and S. D. Pathak (2013)[106] proposed a cosmological model in which the universe evolves through two distinct phases driven by a tachyonic scalar field.

Phase I: The scalar field splits into radiation and a Shifted Cosmological Parameter (SCP). The SCP further divides into a cosmological constant and exotic matter, both evolving independently.

Phase II: Radiation becomes negligible, and the scalar field manifests as SCP (with a perturbed equation of state, $w_\lambda = -1 + \epsilon$) and Shifted Dust Matter(SDM), which interact through the term

$$Q = \gamma \dot{\rho}_m,$$

where γ is the interaction strength and $\dot{\rho}_m$ is the time derivative of the matter energy density.

This interaction influences structure formation and offers a potential resolution to the cosmological constant problem. By employing observational data such as the Cosmic Microwave Background Radiation (CMBR), Baryon Acoustic Oscillations (BAO), and the normalized Hubble function $E(z)$, the authors constrained the parameters γ and ϵ.

Khurshudyan et al. (2015)[33] investigated cosmological models involving an effective quintessence scalar field characterized by a power-law potential, interacting with either a barotropic fluid or a viscous polytropic gas. Their study aimed to understand the Universe's accelerated expansion and test model predictions against observational data. The barotropic fluid model, where the equation of state depends on the deceleration parameter, exhibited instability at late times. On the other hand, the viscous polytropic gas model showed improved stability under suitable parameter choices. Both models reproduced expected cosmic behavior, such as a declining Hubble parameter and a transition in the deceleration parameter from positive to negative values, indicating a shift from decelerating to accelerating expansion. The theoretical results were consistent with observational datasets including SNeIa, BAO, and CMB. The authors concluded that the interacting quintessence model with a viscous polytropic gas presents a viable alternative for explaining DE and late-time cosmic acceleration.

In 2015 ***Böehmer et al.*** [107] introduces a another way to study how DE and DM might interact. Instead of adding these interactions by hand into the equations, the authors build them directly into the Lagrangian. They use a variational approach, which means they derive all the EoS from this starting point, making the model more consistent and grounded in fundamental physics. One of the key features of this method is that it naturally leads to a "fifth force" which is an extra force beyond gravity, caused by the interaction between DE (a scalar field) and matter. This force could explain why galaxies rotate the way they do or why gravity seems to behave differently in some places. This is similar to the chameleon mechanism, where the scalar field becomes very heavy in dense areas (like Earth) and very light in space, allowing it to have a big impact on the universe's expansion without being detectable in lab experiments. The paper also shows that this framework supports both early universe matter domination

and late-time cosmic acceleration, making it a flexible and powerful tool for studying the universe.

In 2017 ***Valentino et al.*** [108] investigates whether an interaction between DE and dark matter can help resolve the well-known *Hubble tension*—the discrepancy between the expansion rate of the universe measured by early-universe data (such as from the Planck satellite) and local observations (like those from Riess et al.). The authors propose a model where DE transfers energy to dark matter through a coupling parameter ξ. Their analysis of various cosmological datasets shows that introducing such an interaction raises the predicted value of the Hubble constant H_0, reducing the tension between the two measurements. Additionally, allowing DE to have a dynamic (phantom-like) equation of state further improves the agreement with observational data. An important consequence of the model is the appearance of a *fifth force*—an additional force acting on dark matter due to its interaction with DE. This force, while subtle, influences how structures in the universe grow and can be constrained through cosmological observations. The results suggest that interacting DE is a promising framework for addressing key tensions in modern cosmology and may point toward new physics in the dark sector.

In 2020 ***Cheng et al.*** [109] proposes a model where the interaction strength depends on the product of DM and DE densities raised to certain powers. This physically motivated form is inspired by interactions in particle physics. Unlike many earlier works that focused only on the background evolution, this study includes effects on cosmic perturbations and DM temperature. Using a range of observational data including CMB, BAO and supernovae the authors constrain the interaction parameters and find that their model, especially in the phantom DE regime ($w < -1$), fits the data better than the standard ΛCDM model. An interesting feature of the model is that it predicts a slight heating of DM due to the energy flow from DE. This interaction leads to better agreement with low-redshift structure formation data, offering a potential way to resolve the observed cosmological tensions. Overall, the paper provides strong evidence that dark sector interactions, when properly modeled, can significantly improve our understanding of the universe's evolution.

The DE Survey (DES) Year 3 cosmic shear analysis by ***Secco et al*** [110] in 2022 provides one of the most precise measurements of the large-scale structure of the universe

using over 100 million galaxy images. The study focuses on the weak lensing effect — tiny distortions in galaxy shapes caused by massive structures bending light — to infer cosmological information. This method is powerful because it is less sensitive to galaxy formation bias and can probe both the expansion of the universe and the growth of cosmic structures. This paper presents updated constraints on key cosmological parameters, especially S_8, a combination of the matter density and fluctuation amplitude. Interestingly, the DES result suggests a slightly lower S_8 compared to what is expected from cosmic microwave background data, indicating mild tension that could point to new physics. The study carefully tests for uncertainties from galaxy alignments, baryonic effects, and modeling choices. These systematics are shown to have a limited impact on the main conclusions, reinforcing the robustness of the findings. By comparing with other lensing surveys and Planck data, the paper highlights both consistency and potential hints toward extensions of the standard ΛCDM model. Overall, this work showcases the power of cosmic shear in testing cosmology and lays important groundwork for future surveys aiming to uncover the nature of dark matter and DE.

In the same year(2022) ***Storm et al.*** [111] explores a simple but intriguing model of DE called *inflection point quintessence*, where the scalar field evolves in a cubic potential of the form $V(\phi) = V_0 + V_3\phi^3$. Unlike traditional quintessence models, which are usually classified as either "freezing" or "thawing," this model displays a mix of both behaviors. It can lead to two different cosmic futures: a universe that expands forever like in ΛCDM (asymptotic de Sitter expansion), or one where acceleration is only temporary, potentially supporting cyclic cosmologies. The authors analyze the model's behavior using observational data from Planck (CMB), supernovae, and BAO surveys. Their results show that while most allowed parameter values lead to long-term acceleration similar to ΛCDM, a small region supports the idea of transient acceleration. Interestingly, this transitional scenario aligns with theoretical expectations from string theory, which often disfavors eternal expansion. Overall, the paper demonstrates that even simple potentials like the cubic one can offer rich dynamics and remain compatible with current observations, highlighting the importance of exploring beyond the standard cosmological model.

The standard ΛCDM model has been remarkably successful in explaining many features of our universe, yet it still faces challenges like the fine-tuning problem, the coincidence problem, and tensions in the values of H_0 and S_8. In light of this in 2024, the study by

Avsajanishvili et al. [112] reviews a broad class of alternatives known as dynamical DE models, especially those involving scalar fields, called ϕCDM models. These models assume that DE is not a fixed cosmological constant but evolves over time due to a scalar field. The paper divides them into two main types: quintessence models, where the field rolls slowly and causes late-time acceleration, and phantom models, where the field leads to even more rapid expansion and can produce extreme outcomes like the "big rip." The authors also discuss interacting DE (IDE) models, where DE and dark matter exchange energy. Such models can help solve the coincidence problem and ease the H_0 tension. Additionally, the paper explores quintessential inflation, where a single scalar field drives both the early inflationary period and today's accelerated expansion. While current observations still favor ΛCDM, this review highlights that many dynamical DE models remain viable and may offer deeper insights into the nature of the dark universe.

The question of whether DE is a simple cosmological constant or something more dynamic continues to spark debate in modern cosmology. The paper[20] by ***Carloni et al.*** in 2025 use the latest 2024 DESI data to test various DE models and examine how well they fit the observed expansion of the universe. They explore three broad categories of models: thermodynamic models like the Chaplygin gas and logotropic fluids, Taylor-expanded models like the CPL parametrization, and more standard parametrizations including ΛCDM and wCDM. Their analysis compares these models using observational data from DESI, supernovae (Pantheon), and Hubble measurements. They find that while the ΛCDM model remains statistically favored in some scenarios, alternative models—especially log-corrected DE models—fit the data even better when all datasets are considered. Notably, the often-used CPL model does not perform as well under the new data. Overall, this study suggests that some dynamic DE models may be making a comeback, especially when tested against the most recent and precise datasets. Future observations will be essential to determine whether these models are truly better or if the cosmological constant still holds strong.

The standard cosmological model, ΛCDM, has been successful in describing many features of our universe. However, ongoing tensions—particularly the Hubble tension—have led researchers to explore models where DE evolves over time. In this context, ***Roy*** [113] in (2025) proposes a new two-parameter equation of state (EoS) for DE inspired by quintom models, which combine both quintessence and phantom behaviors. This new parameterization behaves like a cosmological constant at high redshifts but allows for

richer dynamics at late times. It also mimics the widely used CPL form at intermediate redshifts, offering a smooth transition between different cosmic epochs. The model is tested using a wide range of observations, including DESI 2024 BAO data, Pantheon+ supernovae, SH0ES, and Planck measurements. The results show a clear preference for this dynamical model over ΛCDM. It slightly increases the Hubble constant value and reduces the Hubble tension to about 2.8σ. Importantly, the model captures a recent transition in DE's behavior—from phantom to quintessence—near redshift $z \approx 0.35$, supporting other recent studies. These findings suggest that DE might be more dynamic than previously thought, offering new insights into the universe's evolution.

2.1 Motivation and Research Gaps

The discovery that our universe is not only expanding but doing so at an accelerating rate has fundamentally changed our understanding of cosmology. This phenomenon, supported by a range of observational data such as Type Ia supernovae, cosmic microwave background (CMB) measurements, baryon acoustic oscillations (BAO) and DESI [1–3, 5] points toward the existence of an unknown form of energy—termed DE(DE) that dominates the energy content of the universe.

Despite accounting for nearly 70% of the total energy budget, the true nature of DE remains elusive. Alongside it we have another mysterious component called dark matter(DM) constitutes about 25% of the universe that influences structure formation and galaxy dynamics. These two dark components, though very different in behavior, intriguingly appear to evolve in such a way that their energy densities are comparable in the present epoch often referred to as the "cosmic coincidence problem" which raises the possibility that DE and DM might not be completely independent, but may instead interact with each other.

Motivated by this idea, the present work focuses on exploring the possible interaction between DE and matter. In particular, the study investigates whether such interaction can be modeled effectively through coupling terms within scalar field frameworks. Scalar fields are compelling candidates for DE because they offer dynamical flexibility and can mimic the effects of a cosmological constant under suitable conditions. One especially interesting regime is when the field evolves near an "inflection point" in its potential,

where the potential flattens and the field slows down, giving rise to a period of accelerated expansion.

This thesis is motivated by three central goals:

- To study how DE and dark matter might interact and how such an interaction could help explain the observed balance between their energy densities today.
- To examine the evolution of DE near the inflection point of its potential, both in the presence and absence of interaction with the matter sector.
- To explore whether the interaction between DE and dark matter can be interpreted as a new "fifth fundamental interaction" and the study of coupling parameters.

By addressing these questions, this work aims to deepen our understanding of the dark sector and provide insights into the mechanisms that might be driving the accelerated expansion of the universe. It also contributes to the broader effort in theoretical cosmology to go beyond standard models and uncover the fundamental principles governing cosmic evolution.

2.1.1 Research Objectives:

The primary aim of this research is to investigate the dynamics of DE through scalar field models, with a special focus on its interaction with matter, its behavior near the inflection point of the potential and the possibility of interpreting this interaction as a fifth fundamental interaction using a generalized Lagrangian framework. The specific objectives of this study are outlined as follows:

1. To investigate the interaction of DE and Dark Matter.
2. To investigate the behaviour of DE near inflection point in coupled and uncoupled DE.
3. To obtain a theory as a fifth fundamental interactions between DE and Dark Matter and obtain observationally consistent coupling parameter.

Chapter 3

Inflection point of Interacting Canonical Scalar fields

3.1 Introduction

As we have discussed, one of the known facts is that the universe is accelerating. In the framework of late-time cosmic acceleration, scalar field models have emerged as a compelling candidate to describe the DE responsible for this acceleration. Among various proposed dark energy scalar field models, quintessence stands out as being a well-motivated candidate of dynamic dark energy. Unlike comological constant which assumes a fixed or non-dynamic nature, quintessence can vary with time, and potentially it can address some of the major theoretical challenges associated with the cosmological constant, Λ such as the fine-tuning or the coincidence problem. There can be two scenarios: either the field under consideration can be minimally coupled to gravity with self-interacting potential, or the field can be interacting via some interacting or coupling parameter Q. One of the important points to be taken into account is the form of the potential, which could provide a flexible framework that could enhance the ability of the scalar field to "track" or"thaw," depending on its shape, while still producing observationally consistent acceleration.

This chapter is based on my published work titled "Inflection Point of Coupled Quintessence," in which a dynamical model having interacting quintessence scalar field in the presence of interaction between dark energy and dark matter is constructed. In particular, this

project focuses on the evolution of the interacting scalar field model near an inflection point of the potential where, as discussed previously, an inflection point in the potential is a region where the slope of the potential becomes nearly flat. In such a region, the field experiences a slow evolution, which could lead to a quasi-static behavior where the kinetic energy of the field becomes negligible compared to its potential energy. This kind of evolution is of theoretical interest because such a flat region could enable the field to temporarily behave as that of Λ. In other words, during this "slow-roll" phase near the inflection point, the EoS parameter can approach -1, which can provide the condition to derive the observed late-time acceleration. But then the question arises, what distinguishes this mechanism from the traditional Λ? The answer lies in the fact that, unlike Λ (which is fixed and unchanging), quintessence (canonical scalar field), it has a dynamical nature that allows the field to evolve with cosmic time, and it does so in a way that it naturally leads to the acceleration without doing extreme fine-tuning. Moreover, by introducing interaction, one extra layer of dynamical interaction is added, where there is energy exchange between dark sector. This framework opens up new possibilities for addressing the cosmological problems like the coincidence problem, while remaining consistent with the observational data.

In this study, two distinct interacting models are derived, each defined by different form of energy exchange as follow:

- Model-I: $Q = 3\alpha H \rho_m$
- Model-II: $Q = 3\beta \dot{\rho}_m$

Both of these coupling schemes aim to capture the possibility that DE and matter may not evolove independently but could instead influence each other over cosmic time. This idea in particular could address the coincidence problem i.e. the puzzling fact that despite different evolution why the densities of DE and matter are of the same order in the current epoch. So, by allowing energy exchange between these two components, this model provides a framework that can naturally slow down or speed up the evolution of the one component relative to other at different epochs.

An important outcome of introducing such coupling is that it alter the standard scaling solutions for both DE and matter. Unlike the non-interacting case, where each component evolves independently according to the respective EoS, here in the interacting case these coupled models evolve in a mutually dependent way, which can lead to a more

richer and more flexible cosmic dynamics which could shed light on the nature of DE and its connection with matter content of the universe.

3.1.1 Background Theory Modeling

As mentioned in Sec.(1.1.1) the background modeling starts with the well known "Cosmological Principle," which leads to the following FRLW geometry of the homogeneous, isotropic and flat ($K = 0$) universe, which states that the line element as mentioned in Eq.(1.3) in terms of co-moving coordinates $x^\mu = (t, x^i)$ and in natural units ($c = 1$), is given :

$$ds^2 = g_{\mu\nu}dx^\mu dx^\nu \equiv -dt^2 + a^2(t)\left(dr^2 + r^2(d\theta^2 + \sin^2\theta d\Phi^2)\right) \tag{3.1}$$

here again in the above equation $a(t)$ is the scale factor and k is the curvature parameter having values $k = -1, 0, 1$ corresponding to spatially open, flat, and closed geometry respectively Here in this chapter modelling is done for flat universe only. In this work, we model the DE component using a spatially homogeneous scalar field $\phi(t)$, minimally coupled to gravity but allowed to interact with the matter component. This scalar field evolves under a Lagrangian density of the form given as:

$$\mathcal{L}_\phi = -\frac{1}{2}g^{\mu\nu}\partial_\mu\phi\partial_\nu\phi - V(\phi). \tag{3.2}$$

and energy momentum tensor $T_{\mu\nu}$ for Lagrangian $\mathcal{L}_\phi$ is defined as

$$T^{\mu\nu} = \frac{\partial\mathcal{L}_\phi}{\partial(\partial_\mu\phi)}\partial^\nu\phi - g^{\mu\nu}\mathcal{L}_\phi. \tag{3.3}$$

here, ∂^ν and ∂_μ represents the contravariant and covariant derivative with respect to co-moving coordinates. Einstein's field equation for a spatially flat universe($K = 0$) gives the Friedmann equations as:

$$H^2 = \left(\frac{\dot{a}}{a}\right)^2 = \frac{8\pi G}{3}\rho \tag{3.4}$$

and

$$\frac{\ddot{a}}{a} = -\frac{4\pi G}{3}(\rho + 3p) \tag{3.5}$$

here $\rho = \rho_\phi + \rho_m$ and $p = p_\phi + p_m$ is the total energy density and total pressure of the model under cosideration, where ρ_ϕ, p_ϕ and ρ_m, p_m is the energy density and pressure of canonical field and matter component. $H(t)$ is the Hubble parameter. Now to attain cosmic acceleration, the brackted term in Eq.(3.5) needs to be negative i.e. $\rho + 3p < 0$ which provide us the EoS parameter of the model as:

$$w = \frac{p}{\rho} < -\frac{1}{3} \tag{3.6}$$

The continuity equation without interaction is given as

$$\dot{\rho} + 3H(1+w)\rho = 0. \tag{3.7}$$

For constant EoS w one can obtain from (3.7) the following "scaling solution" of ρ for constant w as given by:

$$\rho = \rho_0 \left(\frac{a}{a_0}\right)^{-3(w+1)} \tag{3.8}$$

where ρ_0, a_0 are present value of ρ and a respectively. The scaling solution discussed in (3.8) is valid for a single perfect fluid. If there are multiple components (we consider two components one is pressure-less matter and the other one is scalar field as a source of dynamical DE) interacting with each other then the scaling behavior of components will be changed. In the next section we obtain the scaling solutions of these two components with a given coupling parameter Q.

In this chapter, two components of the universe: matter + DE are considered. For spatially homogeneous quintessence minimally coupled with matter and in this coupling, we consider the transfer of energy between matter and canonical scalar field.

The chapter is organized as follows: In the next section, the scaling solutions of two dominating components of the universe with two coupling terms: Two different forms of coupling are considered: Two different forms of coupling are considered:

1. A coupling proportional to the Hubble parameter and the scalar field energy density:

   $$Q = 3H\alpha\rho_m$$

   where α is the coupling constant, H is the Hubble parameter, and ρ_m is the matter energy density.

2. A coupling that depends on the time derivative of the scalar field energy density:

$$Q = 3\beta\dot{\rho}_m,$$

where β is a coupling parameter and $\dot{\rho}_m$ represents the time derivative of the matter energy density.

These two expressions represent distinct phenomenological approaches for describing how energy might be exchanged between the dark energy component (represented by the canonical scalar field) and the matter sector of the universe. In section: (3.3), ϕ in the presence of two coupled models is obtained and the behavior of coupled quintessence is analyzed by considering the potential $V(\phi) = V_3(\phi - \phi_0)^3$ near the inflection point. Section:(3.4) presents the comparison between the results so obtained and current observational data, In particular, the analysis includes the calculation of key cosmological quantities such as the slow-roll parameters and the scalar spectral index. These theoretical predictions are then compared against the latest observational constraints from the Planck 2018 mission, providing a crucial link between the model and empirical data and reinforcing its potential viability, and at last section:(3.5) summarizes the key findings of the chapter, reflects on their implications, and discusses possible directions for future work. The chapter as a whole provides a detailed investigation into how coupling between dark energy and matter, combined with a suitably chosen scalar potential, can give rise to an accelerated cosmic expansion consistent with observations.

3.2 Scaling Solution of Coupled ϕCDM Model

The interacting DE model proposed by several authors [51–57] motivated to solve the fine-tuning and cosmic coincidence problem by considering the transfer of energy between the two components of the universe and thus conservation of energy is locally violated while globally it is conserved. Thus, one can write [58] the energy-momentum tensor $T^{(1)}_{\mu\nu}$ and $T^{(2)}_{\mu\nu}$ for the two respective components as:

$$\nabla^{\mu} T^{(1)}_{\mu\nu} = Q_{\nu} \tag{3.9a}$$

and

$$\nabla^{\mu} T^{(2)}_{\mu\nu} = -Q_{\nu} \tag{3.9b}$$

here $Q_{\nu} \neq 0$ and denotes the energy-momentum exchanged between two components.

For the case of spatially homogeneous quintessence field, we have the following form of energy density and the pressure as:

$$\rho_{\phi} = \frac{1}{2}\dot{\phi}^2 + V(\phi) \tag{3.10a}$$

$$p_{\phi} = \frac{1}{2}\dot{\phi}^2 - V(\phi) \tag{3.10b}$$

with EoS

$$w_{\phi} = \frac{p_{\phi}}{\rho_{\phi}} = \frac{\frac{1}{2}\dot{\phi}^2 - V(\phi)}{\frac{1}{2}\dot{\phi}^2 + V(\phi)} \tag{3.11}$$

In the coupled quintessence model, total global energy is conserved, but locally there is a violation of the conservation of energy. Thus, the expressions (3.9a) and (3.9b) take the form:

$$\dot{\rho_{\phi}} + 3H(1 + w_{\phi})\rho_{\phi} = -Q \tag{3.12a}$$

$$\dot{\rho_{m}} + 3H(1 + w_{m})\rho_{m} = Q \tag{3.12b}$$

where Q is the time component of Q_{ν} dubbed as the coupling parameter between matter and field ϕ. One can obtain the following equation of motion of quintessence from (3.10a) and (3.12a) with coupling parameter Q as

$$\ddot{\phi} + 3H\phi + \frac{dV}{d\phi} - \frac{Q}{\dot{\phi}} = 0. \tag{3.13}$$

Recently, in interacting DE, the different forms of coupling parameter Q have been proposed and analyzed by different authors [114–121]. They consider the linear and nonlinear forms of coupling strengths. In [122] author consider the two stable interacting DE model by considering interaction strength as a linear combination of energy densities of components.

3.2.1 Interacting Model- I

The choice of Q is one of the major challenges in the all-interacting DE model. In the absence of a fundamental theory of the dark sector(dark matter and DE), we consider the following heuristic form of Q used in [123] as:

$$Q = 3H\alpha\rho_m \tag{3.14}$$

where α is taken as constant. With Eq.(3.14) the continuity equations (3.12a) and (3.12b) becomes

$$\dot{\rho_\phi} + 3H(1+w_\phi)\rho_\phi = -3H\alpha\rho_m \tag{3.15a}$$

$$\dot{\rho_m} + 3H(1+w_m)\rho_m = 3H\alpha\rho_m \tag{3.15b}$$

from (3.15b) we have

$$\frac{\rho_m}{\rho_m^0} = \left(\frac{a}{a_0}\right)^{-3(1+w_m-\alpha)}. \tag{3.16}$$

One can obtain the general solution of Eq. (3.15a) as follows

$$\frac{\rho_\phi}{\rho_\phi^0} = \left(\frac{a}{a_0}\right)^{-3(1+w_\phi)} + \frac{\alpha\rho_m^0}{\rho_\phi^0(w_m-\alpha-w_\phi)}\left[\left(\frac{a}{a_0}\right)^{-3(1+w_m-\alpha)} - \left(\frac{a}{a_0}\right)^{-3(1+w_\phi)}\right] \tag{3.17}$$

In the absence of interaction i.e. $\alpha \longrightarrow 0$ and considering constant EoS $w_\phi = -1$, we have from Eq.(3.17) $\rho_\phi \longrightarrow \rho_\phi^0 =$ constant and quintessence becomes mimic of the cosmological constant and matter energy density Eq. (3.16) reduced to $\rho_m \sim (a)^{-3(1+w_m)}$ for EoS $w_m = 0$, consistent with ΛCDM model as expected.

3.2.2 Interacting Model- II

There are several possible forms of interaction strength and a few of them were recently discussed by authors [53–57, 114–122] in their interacting DE model. Here, we consider other possible heuristic forms of Q used in literature [123]

$$Q = 3\beta\dot{\rho_m} \tag{3.18}$$

where β is taken as constant.

With Eq.(3.18) the continuity equations (3.12a) and (3.12b) reads as

$$\dot{\rho_\phi} + 3H(1+w_\phi)\rho_\phi = -3\beta\dot{\rho_m} \tag{3.19a}$$

$$\dot{\rho_m} + 3H(1+w_m)\rho_m = 3\beta\dot{\rho_m} \tag{3.19b}$$

in solving Eq.(3.19b) we have the following scaling solution

$$\left(\frac{\rho_m}{\rho_m^0}\right) = \left(\frac{a}{a_0}\right)^{-3A} \tag{3.20}$$

where $A = \left(\frac{1+w_m}{1-3\beta}\right)$ taken as constant. From (3.19a) and (3.20) one can obtain the following functional form of the energy density:

$$\frac{\rho_\phi}{\rho_\phi^0} = \left(\frac{a}{a_0}\right)^{-3(1+w_\phi)} + \frac{3A\beta\rho_m^0}{\rho_\phi^0(1+w_\phi-A)}\left[\left(\frac{a}{a_0}\right)^{-3A} - \left(\frac{a}{a_0}\right)^{-3(1+w_\phi)}\right]. \tag{3.21}$$

In the absence of coupling as $\beta = 0$, (3.20) and (3.21) reduces to $\rho_m \sim (a)^{-3(1+w_m)}$ and $\rho_\phi \sim (a)^{-3(1+w_\phi)}$ which is again reduced to ΛCDM in the absence of coupling/interaction between matter and DE component.

3.3 Inflection Point for potential $V(\phi) = V_3(\phi - \phi_0)^3$

DE as a scalar field with an inflection point has been contemplated by a number of authors [91, 124–131] in the cosmic inflation theory. Near the inflection point, one may refer to a specific set of situations where in the inflationary expansion changes behaviour. The early inflation theory is triggered by cosmological constant or real scalar fields under the slow roll approximations[132, 133]. In [134] authors investigate the inflection point inflation by considering a canonical scalar field in the absence of coupling with background matter. In this section, we analyze the inflection point inflation in the presence of coupling between the spatially homogeneous canonical scalar field (quintessence) and background matter in the late time acceleration (DE-dominated universe).

3.3.1 Cubic Inflection point for Interacting Model-I ($Q = 3H\alpha\rho_m$)

Friedmann (00) equation can be written as:

$$\left(\frac{H}{H_0}\right)^2 = \frac{1}{\rho_c^0}\rho = \frac{1}{\rho_c^0}(\rho_\phi + \rho_m) \tag{3.22}$$

where $\frac{3H_0^2}{8\pi G} = \rho_c^0$ is the critical energy density and $\rho = \rho_\phi + \rho_m$. From (3.16) and (3.17) the Hubble parameter reads:

$$H = H_0\left[\Omega_m^0 X^{3(1+w_m-\alpha)}\left(\frac{w_m - w_\phi}{w_m - \alpha - w_\phi}\right) + X^{3(1+w_\phi)}\left(\Omega_\phi^0 - \frac{\Omega_m^0\alpha}{(w_m - \alpha - w_\phi)}\right)\right]^{\frac{1}{2}} \tag{3.23}$$

where $X = 1 + z = \left(\frac{a_0}{a}\right)$ and $\Omega_m^0, \Omega_\phi^0$ are the density parameters of matter and quintessence (DE) at the present epoch, respectively. The equation of motion of coupled quintessence from Eq.(3.13) given as

$$\ddot{\phi} + 3H\dot{\phi} + \frac{dV}{d\phi} - \frac{3H\alpha\rho_m}{\dot{\phi}} = 0. \tag{3.24}$$

The evolution of ϕ is specified by the initial values of ϕ_i and $\dot{\phi}$, α and V. In order to solve Eq.(3.24) we assumed that the kinetic term of the scalar field is approximately constant with time as $\dot{\phi}^2 \approx$ constant (under slow roll approximated in late time accelerated expansion of the universe) and thus, we have $\ddot{\phi} \simeq 0$. The equation of motion Eq.(3.24) can be solved by considering different choices of potential. We consider the cubic power law potential given as

$$V(\phi) = V_3(\phi - \phi_0)^3 \tag{3.25}$$

having $\phi = \phi_0$ at inflection point with $V' = \frac{dV}{d\phi} = 0$. We are interested in calculating the behavior of this coupled quintessence near the inflection point at which $\phi = \phi_0$. On substituting the value of potential in equation (3.24) we are left with:

$$\dot{\phi}^2 + \frac{V_3(\phi - \phi_0)^2}{H}\dot{\phi} - \alpha\rho_m^0 X^{3(1-\alpha)} = 0. \tag{3.26}$$

Where equation (3.16) and (3.17) in terms of X can be written as

$$\rho_m = \rho_m^0 X^{3(1-\alpha)} \tag{3.27}$$

$$\rho_\phi = X^{3(1+w_\phi)}\left[\rho_\phi^0 + \left(\frac{\alpha}{\alpha+w_\phi}\right)\rho_m^0\right] - \rho_m^0 X^{3(1-\alpha)}\left(\frac{\alpha}{\alpha+w_\phi}\right). \tag{3.28}$$

Using above Eqs.(3.27) and (3.28) and when $w_\phi \approx -1$; then equation (3.23) takes the form

$$H = H_0\left[\frac{\Omega_m^0 X^{3(1-\alpha)}}{(1-\alpha)} + \Omega_\phi^0 - \frac{\alpha\Omega_m^0}{(1-\alpha)}\right]^{1/2} \tag{3.29}$$

and thus energy density of field Eq.(3.28) reads:

$$\frac{\rho_\phi}{\rho_\phi^0} = 1 + \frac{\alpha\rho_m^0}{(1-\alpha)\rho_\phi^0}\left(X^{3(1-\alpha)} - 1\right). \tag{3.30}$$

From Eqs.(3.27), (3.29), (3.30) with (3.26) one can numerically solve the equation and we have solution for the scalar field $\phi(X)$ given as

$$\phi(X) = \left[\frac{2\alpha\rho_m^0}{3V_3(1-\alpha)}\left(\frac{PB(X^{3(1-\alpha)}-1)}{(3P+2B)(3PX^{3(1-\alpha)}+2B)}\right)\right]^{1/3} + \phi_0 \tag{3.31}$$

where $P = \frac{\Omega_m^0}{1-\alpha}$ and $B = \Omega_\phi^0 - \left(\frac{\alpha\Omega_m^0}{1-\alpha}\right)$ and ϕ_0 is the value of coupled quintessence near the inflection point of the cubic potential. As $X \to 1$ (present epoch) then $\phi(X) \to \phi_0$ means our coupled ϕ evolves from the inflection point giving present acceleration of the universe.

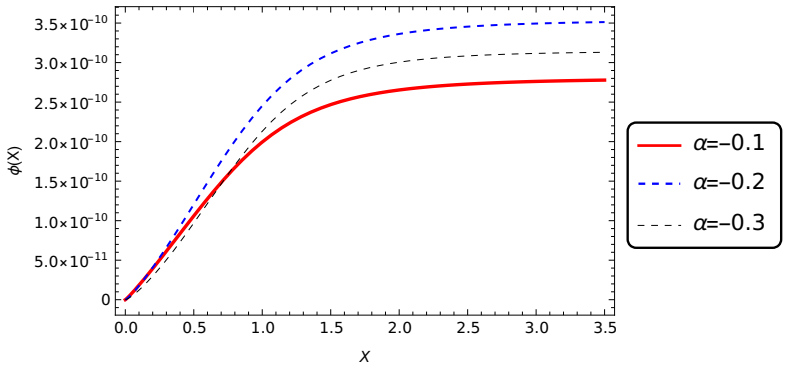

FIGURE 3.1: For negative coupling parameter ($\alpha < 0$) numerical plot shows the evolution of coupled scalar field ϕ with respect to the redshift $X(= 1 + Z)$ showing energy transfers from matter to quintessence for potential $V(\phi) = V_3(\phi - \phi_0)^3$ with $\phi_0 = 0$ at inflection point. The present value of density parameters are taken as $\Omega_m^0 = 0.3$ and $\Omega_\phi^0 = 0.7$ [13].

The numerical plot of coupled ϕ in the presence of the coupling (with negative coupling constant α) is shown in the Fig.(3.1), for this negative coupling parameter the transfer of energy is taking place from matter to the quintessence. In the case of positive coupling

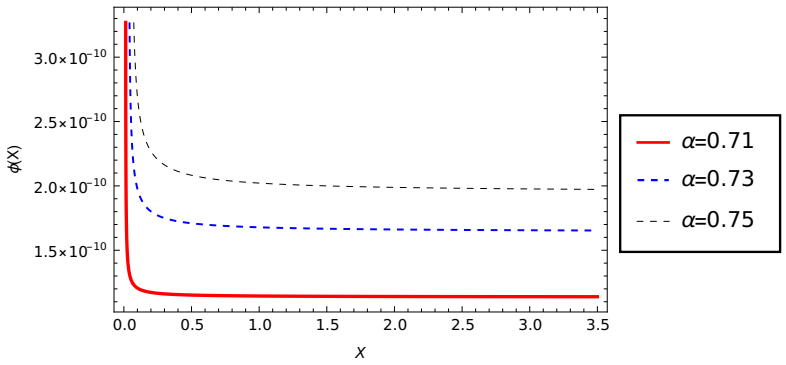

FIGURE 3.2: For positive coupling parameter ($\alpha > 0$) the numeric plots shows the evolution of coupled scalar field $\phi(X)$ near inflection point for the cubic potential $V(\phi) = V_3(\phi - \phi_0)^3$ leads to transfer of energy from quintessence to matter component. Here $\Omega_m^0 = 0.3, \Omega_\phi^0 = 0.7$ as mentioned in [13].

constant Fig.(3.2) coupled scalar field evolves asymptotically with Xnear the inflection point with $w \approx -1$. This asymptotic behavior near the inflection point of the cubic potential is noteworthy, as it mirrors certain characteristics observed in the ΛCDM model signifying the accelerated expansion of the universe as seen in ΛCDM.

3.3.2 Cubic Inflection point Interacting Model-II ($Q = 3\beta\dot{\rho_m}$)

Using Eqs.(3.16) and (3.17) we can solve the Hubble parameter in terms of coupling constant for interacting model-II as:

$$H = H_0 \left[X^{3A}\Omega_m^0 \left(1 + \frac{3\beta A}{(1 + w_\phi - A)}\right) + X^{3(1+w_\phi)} \left(\Omega_\phi^0 - \frac{3\beta A \Omega_m^0}{(1 + w_\phi - A)}\right)\right]^{\frac{1}{2}} \tag{3.32}$$

here $A = \left(\frac{1}{1-3\beta}\right)$ and as $X \to 1$; $H \to H_0$. Scaling solution of energy density in interacting model-II for $w_\phi \approx -1$ can be written as:

$$\rho_m = \rho_m^0 X^{3A} \tag{3.33a}$$

$$\frac{\rho_\phi}{\rho_\phi^0} = 1 + \frac{3\beta\rho_m^0}{\rho_\phi^0}(1 - X^{3A}) \tag{3.33b}$$

The equation of motion of quintessence with coupling parameter takes the form:

$$\dot{\phi}^2 + \frac{V_3(\phi - \phi_0)^2}{H}\dot{\phi} + \left(\frac{3\beta}{1 - 3\beta}\right)\rho_m = 0 \tag{3.34}$$

When $w_\phi \approx -1$ Eq.(3.32) takes the from:

$$H = H_0 \left[\Omega_\phi^0 + 3\beta\Omega_m^0 + X^{3A}\Omega_m^0(1-3\beta)\right]^{1/2} \tag{3.35}$$

Eq.(3.34) solved numerically provides the following expression:

$$\phi(X) = \left[\frac{2\beta\rho_m^0 RS(1-X^{3A})}{V_3(3R+2S)(3RX^{3A}+2S)}\right]^{1/3} + \phi_0 \tag{3.36}$$

From Eq.(3.36); we can see that as $X \to 1$ the coupled scalar field $\phi(X) \to \phi_0$ at the inflection point.Here in the above equation $R = \Omega_m^0(1-3\beta)$ and $S = \Omega_\phi^0 + 3\beta\Omega_m^0$.

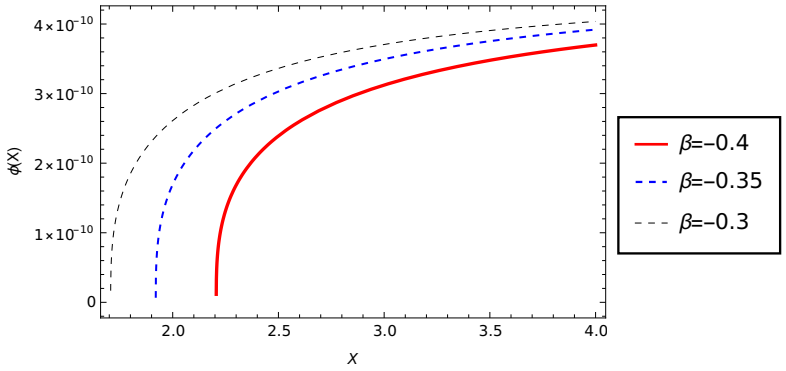

FIGURE 3.3: The numerical plot of ϕ with X be considering negative coupling constant $\beta < 0$ shows the evolution of coupled scalar field (quintessence) $\phi(X)$ for the cubic potential $V(\phi) = V_3(\phi - \phi_0)^3$ with inflection point at $\phi_0 = 0$. $\Omega_m^0 = 0.3, \Omega_\phi^0 = 0.7$ as mentioned in [13].

Fig.(3.3) shows the numerical plot for the case of negative coupling parameter ($\beta < 0$) showing the transfer of energy from matter to quintessence and the numerical plot of ϕ with X for positive β is shown in Fig.(3.4)

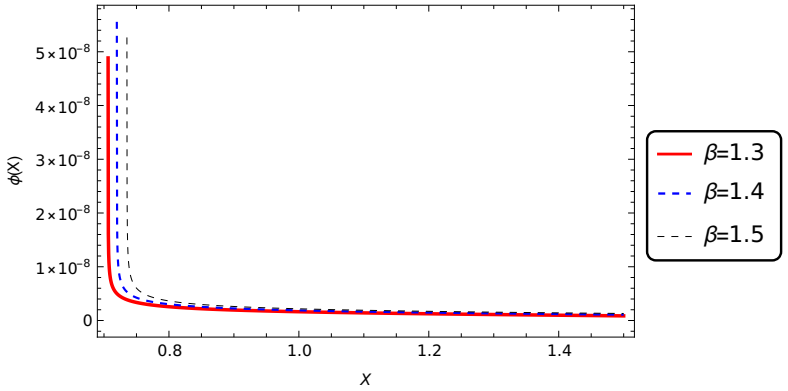

FIGURE 3.4: shows the numerical plot for the evolution of coupled quintessence $\phi(X)$ for the cubic potential $V(\phi) = V_3(\phi - \phi_0)^3$ with $\phi_0 = 0$ at inflection point ; for the positive coupling constant i.e. $\beta > 0$. $\Omega_m^0 = 0.3$ and $\Omega_\phi^0 = 0.7$ as mentioned in [13].

From Fig.(3.4) we can see that as the X approachs to 0 the coupled quintessence evolves asymptotically to infinity in the DE-dominated era with the accelerated expansion of the universe and mimics ΛCDM model when the coupling constant is taken to be positive. Thus, for both models the negative coupling constant (α and β) case as $\phi(X) \to 0$ near the inflection point while for the positive coupling constant both models shows the assymptotic evolution of the universe. So both ϕCDM models with positive coupling evolves assymptolically in the DE-dominated epoch, representing the possibility of an eternally accelerated universe.

3.3.3 Inflection Point for Potential ($V(\phi) = V_n(\phi - \phi_0)^n$)

Inflection point of this generalized potential $V(\phi) = V_n(\phi - \phi_0)^n$ obtain by solving Eq.(3.13) with two coupling term Q. In this section, we have taken a generalized case of the nth-order potential and we calculated the evolution equations of coupled quintessence for both models near the inflection point of the potential. For different values of n, the behavior of the coupled ϕ is calculated $\phi = \phi_0$ at the inflection point.

3.3.3.1 Interacting Model- I: ($Q = 3H\alpha\rho_m$)

Using Eq.(3.13) for the above general form of scalar potential, we get the evolution of $\phi(X)$ as:

$$\phi(X) = \left[\frac{2\alpha\rho_m^0}{3V_n(1-\alpha)}\left(\frac{PB(X^{3(1-\alpha)}-1)}{(3P+2B)(3PX^{3(1-\alpha)}+2B)}\right)\right]^{1/n} + \phi_0 \tag{3.37}$$

where $P = \frac{\Omega_m^0}{(1-\alpha)}$ and $B = \Omega_\phi^0 - \left(\frac{\alpha\Omega_m^0}{(1-\alpha)}\right)$

For different values of n, we can find different inflection points in coupled quintessence models. As we increase the value of n the coupled quintessence ϕ_0 evolves through the inflection point with a higher value of $\phi(X)$ for the positive coupling constant. From Fig.(3.5) we found that for different value of n i.e. for different power potentials we have different inflection points, although the coupled quintessence shows similar asymptotic evolution through their respective inflection points.

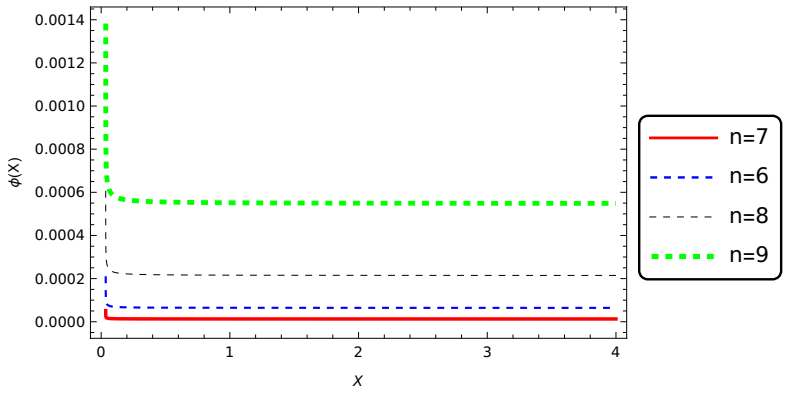

FIGURE 3.5: The numerical plot of ϕ with X by considering positive coupling constant $\alpha > 0$ shows the evolution of coupled scalar field (quintessence) $\phi(X)$ for the potential $V(\phi) = V_n(\phi - \phi_0)^n$ for different values of n. $\Omega_m^0 = 0.3, \Omega_\phi^0 = 0.7$ as mentioned in [13].

3.3.3.2 Interacting Model- II: ($Q = 3\beta\dot{\rho_m}$)

In this section, a generalized case is taken for the interacting model-II in which β is our coupling parameter. We find the evolution of coupled quintessence (with respect to the cosmological redshift) for the generalized case as follows:

$$\phi(X) = \left[\frac{2\rho_m^0\beta}{V_n}\left(\frac{RS(X^{3A}-1)}{(3R+2S)(3RX^{3A}+2S)}\right)\right]^{1/n} + \phi_0 \tag{3.38}$$

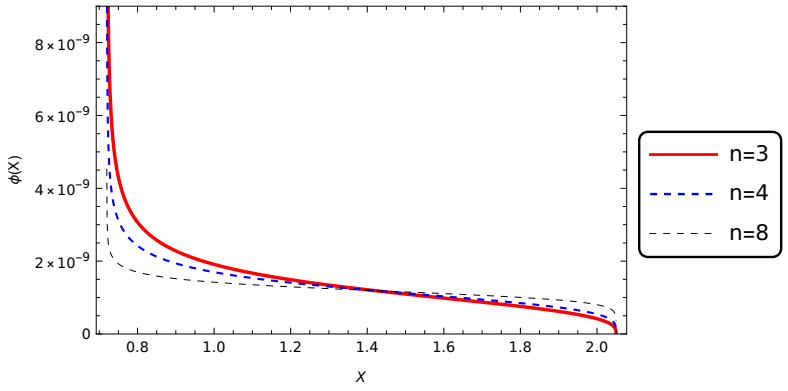

FIGURE 3.6: The numerical plot of ϕ with X be considering positive coupling constant $\beta > 0$ shows the evolution of coupled scalar field (quintessence) $\phi(X)$ for the potential $V(\phi) = V_n(\phi - \phi_0)^n$ for different values of n. $\Omega_m^0 = 0.3, \Omega_\phi^0 = 0.7$ as mentioned in [13].

In this model of the different values of n the behaviour of coupled quintessence near the inflection point ($\phi = \phi_0$) can be seen. Again here in this second interacting model for different n we have different inflection points but Fig.(3.6) shows as $z \to 1$ the scalar

field changes its behaviour and evolves past the inflection point and in late time era again we got asymptotic behaviour of the coupled quintessence.

3.4 Observational Consistency

In this section we compare our results with the observational data from Planck 2018 [13]. The quantities that characterize the dynamics of the scalar field during the inflationary [135–137] epoch are the "slow roll" parameters ξ and η [138] and are given as follows:

$$\xi = \frac{1}{2}\left[\frac{V'(\phi)}{V(\phi))}\right]^2 << 1 \tag{3.39}$$

$$\eta = \frac{V''(\phi)}{V(\phi)} << 1 \tag{3.40}$$

Here the derivative is with respect to ϕ. In our case for the cubic potential at the inflection point, these slow-roll parameters take the form

$$\xi = \frac{9}{2}\left[\frac{\phi^2}{\frac{V_0}{V_3}+\phi^3}\right]^2, \eta = \frac{6\phi}{\frac{V_0}{V_3}+\phi^3} \tag{3.41}$$

The accelerated expansion occurs when $\xi < 1$ [138] and this accelerated expansion will sustain for a sufficiently long period only if the second order derivative of ϕ is small which requires the smallness of $\eta < 1$. Here we have taken the value of $\frac{V_0}{V_3} = 0.77$ as obtained in [134].The other parameter is the "scalar spectral index" which characterizes the density fluctuation in the early universe which is given as:

$$n_s = 1 - 6\xi - 2\eta \tag{3.42}$$

After doing the numerical calculation the results are shown in the Table(3.1) for both ϕCDM interacting models corresponding to the various values of redshift parameter X. For both models the value of both slow-roll parameters are coming out to be very less than 1 signifying the inflation consistent with observations. Moreover, the values of the scalar spectral index for our current ϕCDM models is approximately 1.

Interacting Model-I			
X	$\phi(X)$	ξ	η
10	1.1372×10^{-10}	1.2693×10^{-39}	8.8613×10^{-10}
9	1.13731×10^{-10}	1.2698×10^{-39}	8.86208×10^{-10}
7	1.13762×10^{-10}	1.2711×10^{-39}	8.86442×10^{-10}
Interacting Model-II			
X	$\phi(X)$	ξ	η
10	5.7262×10^{-10}	8.1603×10^{-37}	4.462×10^{-9}
9	5.6950×10^{-10}	7.9841×10^{-37}	4.43772×10^{-9}
7	5.6005×10^{-10}	7.46718×10^{-37}	4.36407×10^{-9}

TABLE 3.1: Slow roll parameters and scalar spectral index has been calculated for Interacting Model-1 when the coupling parameter $\alpha = 0.71$ and for the Interacting Model-II when the coupling parameter $\beta = 1.3$ and the ratio $V_0/V_3 = 0.77$ [134].

3.5 Conclusion

The canonical scalar field, often referred to as *quintessence*, is one of the leading theoretical candidates for modeling dynamical dark energy (DE). Unlike the cosmological constant in the standard ΛCDM model, quintessence allows for a time-evolving energy component that can potentially address some of the puzzles in cosmology, such as the coincidence problem and the nature of late-time cosmic acceleration.

In our work, we explore a scenario where this quintessence field is not completely isolated but interacts with the matter sector specifically with both baryonic and dark matter components. We introduce two distinct forms of coupling between the quintessence field and matter. These coupling forms are represented through interaction terms in the continuity equations as follows:

- $Q = 3H\alpha\rho_m$
- $Q = 3\beta\dot{\rho}_m$

These interaction terms, Q, are not derived from any underlying fundamental theory, since, as of now, the true nature of the dark sector remains unknown. Instead, the forms we use are based on heuristic reasoning, chosen for their mathematical convenience and consistency with the dimensional structure of the continuity equations. They are constructed using the physically relevant quantities: the Hubble parameter H, the matter energy density ρ_m, and their time derivatives. Of course, other functional forms of Q are also plausible, including those involving combinations such as ρ_ϕ, $\dot{\rho}_\phi$, and mixed

terms. However, for this study, we focus on these two commonly used forms that allow for analytical and numerical tractability.

In the limiting case where no coupling is present, the system naturally reduces to the standard ΛCDM, providing a consistent baseline.

Our analysis is centered on the late-time universe specifically, the epoch dominated by DE where cosmic acceleration becomes significant. At this stage, we find that the scalar field, even when coupled to matter, behaves in such a way that the effective interaction weakens, and the field becomes *asymptotically decoupled*. This means that the field evolves almost independently, approaching a stable phase known as the inflection point. This transition leads to an asymptotic de Sitter expansion, which aligns with observations of the universe's accelerated expansion.

Previous studies, notably by Chang *et al.*[134] and Strom[111], have investigated inflection point dynamics in uncoupled quintessence models using various power-law potentials. Building upon their work, we aim to understand how introducing coupling alters the behavior near these inflection points during the dark energy-dominated era.

To do this, we employ a specific form of the potential; namely, a *cubic potential* defined earlier in Eq.(3.25). Additionally, we generalize this to a broader class of *power-law potentials* of the form:

$$V(\phi) = V_n(\phi - \phi_0)^n,$$

where n determines the steepness and curvature of the potential around the inflection point. Through numerical simulations, we evaluate important cosmological parameters, such as the slow-roll parameters ξ and η, as well as the scalar spectral index n_s, and compare these predictions with current observational data from Planck [13] and Baumann [138]. Encouragingly, our model shows good consistency with the data.

In summary, by considering the simplest cubic and its generalized power-law extensions, we demonstrate that coupled quintessence models can also exhibit inflection points in their scalar field evolution, similar to uncoupled cases. These inflection points play a critical role in shaping the late-time acceleration of the universe. While our focus here has been on canonical scalar fields, similar phenomena are expected to occur in non-canonical models such as *phantom* and *tachyon* fields. The investigation of those models,

both with and without coupling, is a natural next step and will be the subject of future work.

Chapter 4

Inflection Point of Minimally Coupled Tachyonic Field

4.1 Introduction

Another candidate of DE is the Tachyon scalar field which in context of inflation was investigated by [102] in 2004 and A. Sen in 2002 [40]. This scalar field, originating in string theory, have emerged as compelling candidates for explaining the late-time cosmic acceleration observed in the universe, often associated with DE. When incorporated into a cosmological framework, these fields are described by a Dirac–Born–Infeld (DBI)-type action, which introduces a non-canonical kinetic term. This feature distinguishes them from traditional canonical scalar fields such as quintessence. The action for a minimally coupled tachyonic field takes the form:

$$S_{tachyon} = \int d^4x\sqrt{-g}\, V(\phi)\sqrt{1-\partial_\mu\phi\partial^\mu\phi} \tag{4.1}$$

where $V(\phi)$ is the tachyon potential, and the square root is the non-canonical kinetic behaviour, this non-linearity leads to a rich dynamical phenomenon. Tachyon fields naturally support a slow-roll regime when the field evolves through flat regions of the potential, which is a desirable feature for modeling both early inflation and late-time acceleration (see [46, 104]), In particular, potentials with inflection points offer an extended phase of ultra slow-roll evolution. Near such points, the flatness of the potential causes the kinetic term to remain small, allowing the field's potential energy to dominate.

This results in an effective EoS close to $w_\phi \sim -1$, mimicking DE behaviour. Another interesting feature that we found is that tachyonic scalar field can dynamically interpolate between different cosmic eras, behaving like dust-like matter in certain regimes and DE in others and the flexibility of tachyon dynamics has been presented in various cosmological scenarios, including models of DE, unified dark matter–DE frameworks, and inflationary models based on string-inspired constructions [42, 47, 102]. These characteristics make tachyonic scalar fields particularly compelling for investigating scenarios where cosmic acceleration arises naturally from the dynamics of a single scalar field. The presence of an inflection point in the potential further enhances this picture, providing a controlled transition between kinetic and potential-dominated phases and allowing for a unified description of different expansion histories within a single theoretical setup.

Dynamical Setup

In this section presents the mathematical framework on which the dynamics are based. Again using FRLW metric Eq.(3.1) for a flat, homogenous and isotropic universe, we have

$$ds^2 = g_{\mu\nu}dx^\mu dx^\nu \equiv -dt^2 + a^2(t)\left(dr^2 + r^2 d\theta^2 + r^2 \sin^2\theta d\Phi^2\right). \tag{4.2}$$

Here, as mentioned earlier, all calculations are in natural units with $c = 1$. In the above equation, $a(t)$ is the scale factor. Now, the effective four-dimensional action for the tachyonic field is given as follows [44, 45]:

$$S_\phi = \frac{1}{2\kappa^2}\int d^4x f(\phi)\sqrt{-g}R + \int d^4x V(\phi)\sqrt{-g}\sqrt{(1 + g^{\mu\nu}\partial_\mu\phi\partial_\nu\phi)}, \tag{4.3}$$

where $V(\phi)$ represents the potential, $\kappa^2 = \frac{1}{M_p^2} = 1$, and $f(\phi) = 1$ under minimal coupling. This action introduces a non-canonical scalar field with a modified (DBI) kinetic term, often inspired by high-energy theories. The square-root structure resembles the DBI action in string theory. The energy–momentum tensor for Eq.(4.3) can be written as follows:

$$T^{(\phi)}_{\mu\nu} = \frac{V(\phi)\partial_\mu\phi\partial_\nu\phi}{\sqrt{1 + g^{\alpha\beta}\partial_\alpha\phi\partial_\beta\phi}} - g_{\mu\nu}V(\phi)\sqrt{1 + g^{\alpha\beta}\partial_\alpha\phi\partial_\beta\phi}. \tag{4.4}$$

Here, again for a spatially flat universe ($K = 0$), Einstein's field equation gives the following Friedmann equations:

$$H^2 = \left(\frac{\dot{a}}{a}\right)^2 = \frac{8\pi G}{3}\rho, \tag{4.5}$$

and

$$\frac{\ddot{a}}{a} = -\frac{4\pi G}{3}(\rho + 3p), \tag{4.6}$$

where $H(t) \equiv \frac{da}{dt}$ is the Hubble parameter and $\rho = \rho_\phi + \rho_m$ and $p = p_\phi + p_m$ denote the total energy and the pressure of this model, respectively. In general, multiple components, such as matter, radiation, and DE, can contribute to the energy–momentum tensor, each with a different EoS. However, during early time periods, radiation dominated, after which matter started dominating more effectively. At later time periods ($z \longrightarrow 0$), DE dominated the universe, leading to cosmic acceleration. We are therefore driven to focus on only two components: pressureless matter and DE. For cosmic acceleration, we have $\rho + 3p < 0$. The continuity equation is given as follows:

$$\dot{\rho} + 3H(1 + w)\rho = 0. \tag{4.7}$$

where

$$\rho_{=}\rho_m + \rho_\phi \tag{4.8a}$$

and

$$p_{=}p_m + p_\phi \tag{4.8b}$$

In the next section, we will investigate the behaviour of the tachyonic scalar field near the inflection point of potential by considering three different possibilities of cosmic behaviours; the first two cases involve conventional power-law expansion and pure exponential growth, i.e., and $a(t) = \alpha t^n, a(t) = \gamma e^{\beta t}$, respectively, and the third case is of quasi-exponential expansion of the scale factor $a(t) = \eta t^n e^{\beta t}$. For these three cases, we will calculate the respective potentials and then investigate the behaviour of that particular model near their respective inflection points. In Section (4.3), we will do the dynamical analysis of the model.

4.2 Inflection Point of Tachyonic Scalar Field

Using Eq.(4.4) for a flat ($K = 0$) FRLW universe using, the energy density and pressure for the spatially homogeneous tachyonic scalar field are given as:

$$\rho_\phi = \frac{V(\phi)}{\sqrt{1-\dot{\phi}^2}}, \tag{4.9}$$

$$p_\phi = -V(\phi)\sqrt{1-\dot{\phi}^2}. \tag{4.10}$$

Here, the overdot denotes the derivative with respect to cosmic time (t). $V(\phi)$ is the potential associated with the tachyonic field that we are going to calculate in the upcoming subsections for each case.

Using Eqs.(4.5) and (4.6), we get:

$$\frac{\ddot{a}}{a} = H^2 + \dot{H}, \tag{4.11}$$

on differentiating Eq.(4.6) with respect to time. we get:

$$\dot{H} = -\frac{8\pi G}{3}\frac{3\dot{\phi}^2 V(\phi)}{\sqrt{1-\dot{\phi}^2}} \tag{4.12}$$

and plugging Eqs.(4.5), (4.9) and (4.12) into Eq.(4.11) for the scalar field, we can obtain the following form of the second Friedmann equation:

$$\frac{\ddot{a}}{a} = \frac{\kappa^2 V(\phi)}{3\sqrt{1-\dot{\phi}^2}}\left(1-\frac{3}{2}\dot{\phi}^2\right) \tag{4.13}$$

Now, for the accelerated expansion of the universe, we have $\ddot{a} > 0$; thus, using Eqs. (4.13) and $\dot{\phi}^2 < \frac{2}{3}$, the EoS for ϕ becomes:

$$w_\phi = \frac{p_\phi}{\rho_\phi} = (\dot{\phi}^2 - 1) \tag{4.14}$$

In terms of Hubble parameter, the EoS w_ϕ can be written as follows:

$$w_\phi = -1 - \frac{2\dot{H}}{3H^2} \tag{4.15}$$

For cosmic acceleration, the possible range of the values of w_ϕ is $-1 \leq w_\phi < -\frac{1}{3}$ and $0 < \dot{\phi}^2 < \frac{2}{3}$. Using the continuity equation and plugging Eqs.(4.9) and (4.10), we can easily find the equation of motion for this tachyonic scalar field model, as follows:

$$\dot{\rho}_\phi + 3H(1 + w_\phi)\rho_\phi = 0$$

using Eq.(4.9)

$$\frac{\dot{V}(\phi)}{\sqrt{1-\dot{\phi}^2}} + \frac{V(\phi)\dot{\phi}^2\ddot{\phi}}{(1-\dot{\phi}^2)\sqrt{1-\dot{\phi}^2}} + 3H\frac{V(\phi)\dot{\phi}^2}{\sqrt{1-\dot{\phi}^2}} = 0$$

we get:

$$\frac{\ddot{\phi}}{1-\dot{\phi}^2} + 3H\dot{\phi} + \frac{1}{V}\frac{dV}{d\phi} = 0. \tag{4.16}$$

Now, using Eqs.(4.5) and (4.6), we can rewrite $\phi(t)$ and $V(\phi)$ in the forms of H and $\dot{H}$, as:

$$\phi(t) = \int \left(dt\sqrt{-\frac{2\dot{H}}{3H^2}} \right) \tag{4.17}$$

$$V(t) = \frac{3H^2}{\kappa^2}\sqrt{1 + \frac{2\dot{H}}{3H^2}} \tag{4.18}$$

Using the above two equations, we will find the potential and their respective inflection point behavior for the three cases.

4.2.1 For Case I: $a(t) = \alpha t^n$

In this subsection, let us consider the simplest model for describing the expansion of the universe in certain cosmological scenarios, namely, the power-law form of scale factor; this suggests that the universe's expansion follows a simple power-law relationship with time. i.e., $a(t) = \alpha t^n$. Here, α is a constant which describes the overall scale of the universe, and the exponent n determines the rate of expansion it has to be greater than 0 for the universe to experience accelerated expansion. For this kind of model, the Hubble parameter can be obtained as:

$$H = \frac{1}{a}\frac{da}{dt}$$

i.e.,

$$H = \frac{n}{t} \tag{4.19}$$

and on differentiating H with respect to t we get:

$$\dot{H} = -\frac{n}{t^2} \tag{4.20}$$

Upon substituting this value of H into Eq.(4.18) we get:

$$V(t) = \frac{3n^3}{\kappa t^2}\sqrt{1 - \frac{2n}{3}} \tag{4.21}$$

and using Eqs. (4.17) and (4.21), we can obtain the following form of the potential:

$$V(\phi) = V_0(\phi - \phi_0)^{-2}, \tag{4.22}$$

where $V_0 = \frac{2n}{\kappa^2}\sqrt{1 - \frac{2}{3n}}$. From the above Eq.(4.22), we found that there is no such inflection point for this particular model; we can also see in Fig.(4.1) that the curve shows no inflection, but we can observe that the scalar field is rolling slowly along the potential and when applying slow roll approximation directly into Eq.(4.16) using $\dot{\phi}^2 << 1 \implies 1 - \dot{\phi}^2 \approx 1$ and we can find the evolution of the scalar field with respect to time, but, in this case, w_ϕ will be very close to -1. However, in our case, we have calculated the evolution equation directly from Eq.(4.17), resulting in the following equation:

$$\phi(t) = \sqrt{\frac{2}{3n}(t^2 - t_0^2)} + \phi_0 \tag{4.23}$$

where $t = t_0$ when $\phi = \phi_0$, and the EoS (Eq.(4.15)) is as follows:

$$w_\phi = -1 + \frac{2}{3n} \tag{4.24}$$

For $n = 2/3$, the scale factor evolves as $a \propto t^{2/3}$, corresponding to a matter-dominated universe, and as we can see from Fig.(4.1) the potential corresponding to this case vanishes. This, in return, leads to $p_\phi = 0$, which corresponds to pressureless fluid with $w_\phi = 0$. For $n > 2/3$, the EoS satisfies $w_\phi > -1$, indicating a quintessence-like behaviour. If we set $n > 1$, then the EoS satisfies $w_\phi < -1/3$, which is a necessary condition for late-time cosmic acceleration. This supports an expanding universe consistent with observations of DE-driven acceleration.

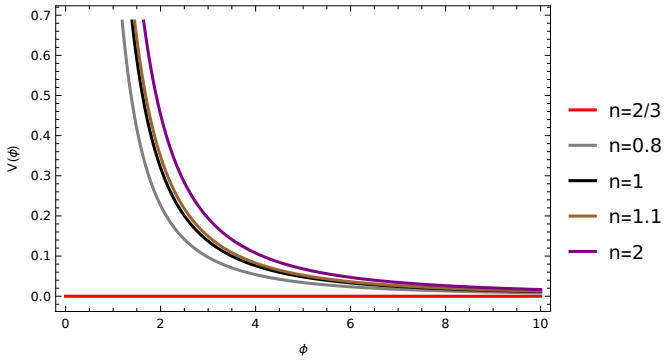

FIGURE 4.1: The plot shows the variation of ϕ with potential $V(\phi)$ for different values of the exponent factor n ($n = 2/3$, $n = 0.8$, $n = 1$, $n = 1.1$, and $n = 2$) for fixed value of $\phi_0 = 0.1$.

In terms of cosmological redshift, we can also rewrite the above Eq.(4.23) as follows:

$$\phi(1+z) = \sqrt{\frac{2}{3n\alpha^{2/n}}}\sqrt{\left(\left(\frac{1}{1+z}\right)^{2/n} - \left(\frac{1}{1+z_0}\right)^{2/n}\right)} + \phi_0 \tag{4.25}$$

Here, the initial value of the redshift is taken to be $z_0 \longrightarrow 1100$. Fig.(4.2) shows the evolution of ϕ for different values of n. Also, α is a normalization constant and, for simplicity, is taken to be unity. We examine the behaviour of a scalar field ϕ with respect to redshift z. As the redshift z approaches zero, $\phi(z)$ increases asymptotically with $z \longrightarrow 0$, corresponding to the late-stage evolution of the universe. The field is characterized by a unique potential which is derived from the scale factor; this potential governs its dynamics and the corresponding impact on cosmic expansion. Here, the case $n < 1$ is of interest, as it provides a smooth/slow evolution of the scalar field ϕ at a late epoch, resulting in the accelerated expansion at later stage. This slow-roll regime results in the field behaving similarly to a cosmological constant, with a near-constant energy density. As a consequence, the universe continues to expand at an accelerating pace.

4.2.2 For Case II: $a(t) = \gamma e^{\beta t}$

Another simple case is the exponential form of the scale factor $a(t) = \gamma e^{\beta t}$, where γ and β are the constants. β determines the overall rate at which the scale factor changes and can have two possibilities for its values, as follows: the first possibility is $\beta > 0$, which implies the exponential growth of the universe, i.e., an expanding universe; the second possibility is $\beta < 0$, which implies exponential decay, i.e., a contracting universe. As we

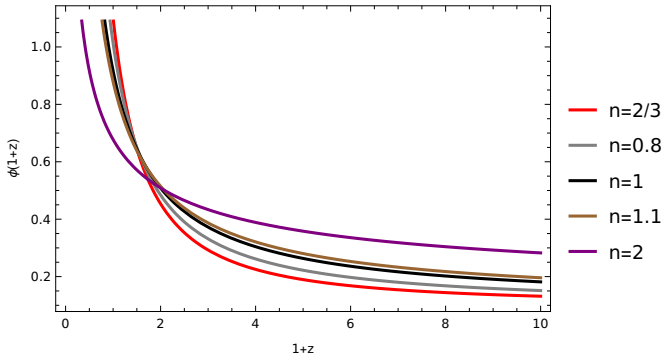

FIGURE 4.2: The plot shows the evolution of ϕ with cosmological redshift z for different values of the exponent factor n ($n = 2/3$, $n = 0.8$, $n = 1$, $n = 1.1$, and $n = 2$), with the normalization constant $\alpha = 1$ (for simplicity) and $\phi_0 \sim 0.1$.

know, during early epochs the universe experienced expansion, so we can discard the second possibility. Now, the second constant γ is a normalization factor that sets the overall scale of the universe at a particular cosmic time t, and H for this exponentially expanding universe is proportional to the constant below:

$$H = \beta. \tag{4.26}$$

Now, using this value of H in Eqs.(4.17) and (4.18), we can obtain the following form of potential:

$$V(\phi) = \frac{3\beta^2}{\kappa^2} \tag{4.27}$$

Therefore, for this particular model, again there is no inflection point because the potential is revealed to be constant; this is consistent with the quintessence model (as if the same calculations are carried out for the quintessence model with the same scale factor). Using Eqs.(4.16) and (4.27) and after applying the slow roll approximation, the scalar field ϕ is also revealed to be a constant.

4.2.3 For Case III: $a(t) = \eta t^n e^{\beta t}$

Now this case is of our particular interest, as in this case, we are considering the universe to have a mixed form of the scale factor given by $a(t) = \eta t^n e^{\beta t}$, i.e., the product of power-law and exponential terms, where η, n and β are the constants determining the overall rate at which the scale factor changes. For this model, the Hubble parameter is obtained as follows:

$$H = \frac{n}{t} + \beta = \frac{n + \beta t}{t} \tag{4.28}$$

and its derivative with respect to cosmic time is:

$$\dot{H} = -\frac{n}{t^2}. \tag{4.29}$$

Using Eqs.(4.17), (4.18), and (4.28), we can derive the following form of potential and the scalar field, in terms of t, as follows:

$$V(t) = \frac{3(n+\beta t)^2}{\kappa^2 t^2}\sqrt{1-\frac{2n}{3(n+\beta t)^2}}. \tag{4.30}$$

Now, using Eq.(4.17), the evolution of the scalar field with respect to cosmic time can be written as:

$$\phi(t) = \frac{1}{\beta}\sqrt{\frac{2n}{3}}\log|n+\beta t| + \mathcal{C}, \tag{4.31}$$

where $\mathcal{C}$ is some integration constant. Let's assume that, at some $t = t_0 = 0$, the scalar field is $\phi = \phi_0$; thus, the above equation can be rewritten as,

$$\phi(t) = \frac{1}{\beta}\sqrt{\frac{2n}{3}}\log\left(\frac{n+\beta t}{n}\right) + \phi_0. \tag{4.32}$$

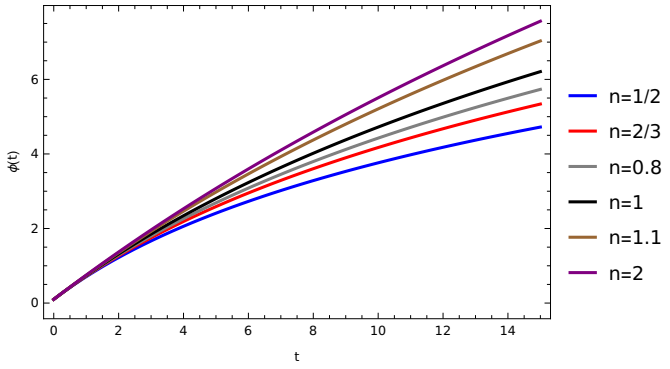

FIGURE 4.3: The plot shows the evolution of ϕ with cosmic time t for different values of n, $\beta = 0.1$, and $\phi_0 = 0.1$

Fig.(4.3) shows the scalar field is increasing with cosmic time t for all set of values of n as mentioned in plot and for fixed $\beta = 0.1$. Now, the EoS (Eq. (4.15)) for this case follows:

$$w_\phi(t) = -1 + \frac{2n}{3(n+\beta t)^2} \tag{4.33}$$

which is dynamic and varies with cosmic time t. Fig.(4.4) shows the variation in EoS with respect to cosmic time, which is in Gyr. Within the plot, the straight dotted black line shows today's cosmic time. One can observe from the Fig.(4.4) that the EoS varies

with time and that $w_\phi \longrightarrow -1$ at a late time period (a point to remember here is that w_ϕ has both DE and matter components).

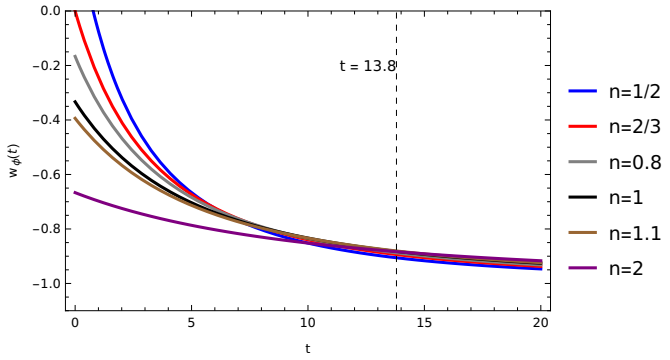

FIGURE 4.4: The plot shows the evolution of w_ϕ with cosmic time t (Gyr) for different values of n, $\beta = 0.1$, and $\phi_0 = 0.1$

.

Eq. (4.32), in terms of t, can be rewritten as follows:

$$t = -\frac{n}{\beta} + \frac{n}{\beta}\exp\left(\beta\sqrt{\frac{3}{2n}}(\phi - \phi_0)\right) \tag{4.34}$$

Upon substituting Eq. (4.34) into (4.30), we can obtain the following form of potential $V(\phi)$, which depends on the scalar field ϕ, as follows:

$$V(\phi) = \frac{3\beta^2 \exp\left(2\beta\sqrt{\frac{3}{2n}}(\phi - \phi_0)\right)}{\kappa^2\left(\exp\left(\beta\sqrt{\frac{3}{2n}}(\phi - \phi_0)\right) - 1\right)^2}\sqrt{1 - \frac{2}{3n\exp\left(2\beta\sqrt{\frac{3}{2n}}(\phi - \phi_0)\right)}} \tag{4.35}$$

Using binomial expansion and simplification, Eq. (4.35) can be rewritten as follows:

$$V(\phi) = \frac{3\beta^2}{\kappa^2}\left(\frac{\exp\left(2\beta\sqrt{\frac{3}{2n}}(\phi - \phi_0)\right) - 1/3n}{\left(\exp\left(\beta\sqrt{\frac{3}{2n}}(\phi - \phi_0)\right) - 1\right)^2}\right) \tag{4.36}$$

where, for the simple case, we use the following assumption:

$$\exp\left(\beta\sqrt{\frac{3}{2n}}(\phi - \phi_0)\right) \approx 1 + \left(\beta\sqrt{\frac{3}{2n}}(\phi - \phi_0)\right). \tag{4.37}$$

This above assumption constrains the parameter β as $0 < \beta << 1$, so that, with an increase in power, the higher-order terms become negligibly small and the relationship

between potential and scalar field can be written as:

$$V(\phi) = \frac{2n}{\kappa^2}\frac{\left((1-\frac{1}{3n}) + 2\beta\sqrt{\frac{3}{2n}}(\phi-\phi_0) + \frac{3\beta^2}{2n}(\phi-\phi_0)^2\right)}{(\phi-\phi_0)^2}. \tag{4.38}$$

Solving Eq. (4.38) above using the approximation mentioned in Eq. (4.37) results in the above potential showing inflection at the following point:

$$\phi_{inflection} = \left(\frac{1-3n}{2n\beta}\right)\sqrt{\frac{2n}{3}} + \phi_0. \tag{4.39}$$

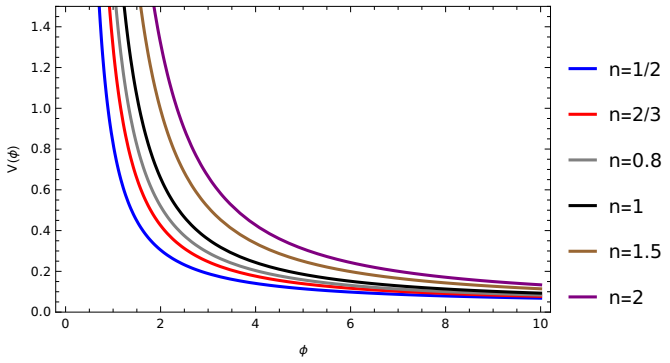

FIGURE 4.5: The plot shows the variation in the scalar field ϕ with respect to the potential $V(\phi)$ for different sets of values of n with a fixed value of $\beta << 1$, specifically $\beta = 0.1$ and $\phi_0 = 0.1$.

The above equation, Eq. (4.39), is the inflection point which provides a flat region and this inflection point serves as a critical location where the field experiences slow rolling. Using the Lambert $\mathcal{W}$ function and the scale factor $a(t) = \eta t^n \exp\beta t$, the redshift z and cosmic time t are related, as shown below:

$$t = \frac{n}{\beta}\mathcal{W}\left(\frac{\beta}{n}(\eta(1+z))^{-1/n}\right) \tag{4.40}$$

where the Lambert $\mathcal{W}$ function is defined as the root of a transcendental equation of the form $\mathcal{W}(y)\exp\mathcal{W}(y) = y$ and has distinct branches, among which two are real; for more information, readers can refer to [111, 139, 140]. On setting the value of cosmic time t in Eq. (4.32), the evolution of the EoS and the scale factor, in terms of redshift z, can be obtained, respectively, as follows:

$$w_\phi(z) = -1 + \frac{2n}{3(n + n\mathcal{W}(\frac{\beta}{n}(\eta(1+z))^{-1/n})^2} \tag{4.41}$$

and

$$\phi(z) = \frac{1}{\beta}\sqrt{\frac{2n}{3}}\log\left[1+\mathcal{W}\left(\frac{\beta}{n}(\eta(1+z))^{-1/n}\right)\right]+\phi_0. \tag{4.42}$$

Using Eqs. (4.30) and (4.40) we can write potential in terms of redshift as:

$$V(z) = \frac{3\beta^2}{\kappa^2}\frac{\left(1+\mathcal{W}\left(\frac{\beta}{n}(\eta(1+z))^{-1/n}\right)\right)^2}{\mathcal{W}\left(\frac{\beta}{n}(\eta(1+z))^{-1/n}\right)^2}\sqrt{1-\frac{2}{3n(1+\mathcal{W}\left(\frac{\beta}{n}(\eta(1+z))^{-1/n}\right)^2}}. \tag{4.43}$$

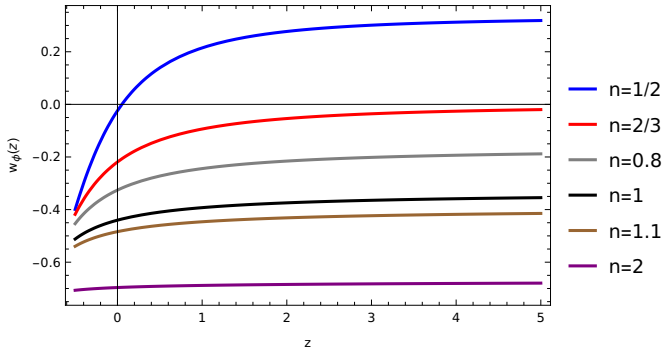

FIGURE 4.6: The plotshows the variation in EoS w_ϕ with respect to cosmological redshift z for different sets of values of n ($n = 1/2, n = 2/3, n = 0.8, n = 1, n = 1.1$ and $n = 2$ from top to bottom) with a fixed value of $\beta << 1$, specifically $\beta = 0.1$ and $\phi_0 = 0.1$. Here in plot vertical solid black line represents the present epoch with $z = 0$ while the horizontal blacksolid line represents null value of EoS parameter w_ϕ.

Fig.(4.5) shows how the scalar field is varying with potential and Fig.(4.6) shows the variation in EoS with respect to cosmological redshift z. From this figure, we observe that, for lower values of n, the EoS remains close to $w_\phi \approx 0$, resembling the matter-dominated era, while the field itself behaves similarly to dust-like matter. For small n values, the EoS falls below $-1/3$, suggesting that the same field can transition into a DE-like component at late time periods, driving accelerated expansion. Fig.(4.7) illustrates the behavior of the scalar field with respect to redshift, indicating that, ϕ takes higher values during late time as compared to a higher redshift. Fig.(4.8) illustrates the evolution of the potential $V(z)$ as a function of redshift. At lower redshifts, corresponding to late-time cosmology, the potential flattens due to the presence of an inflection point. This behaviour allows the scalar field to enter a slow-roll phase, or we can say an ultra slow-roll, which can drive the accelerated expansion of the universe.

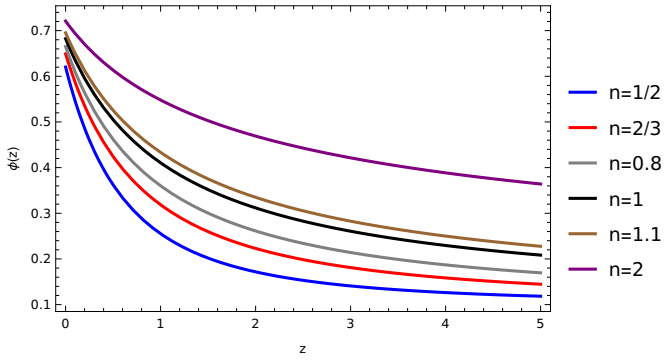

FIGURE 4.7: The plot shows the variation in the scalar field ϕ with respect to cosmological redshift z for different sets of values of n with a fixed value of $\beta << 1$, specifically $\beta = 0.1$ and $\phi_0 = 0.1$.

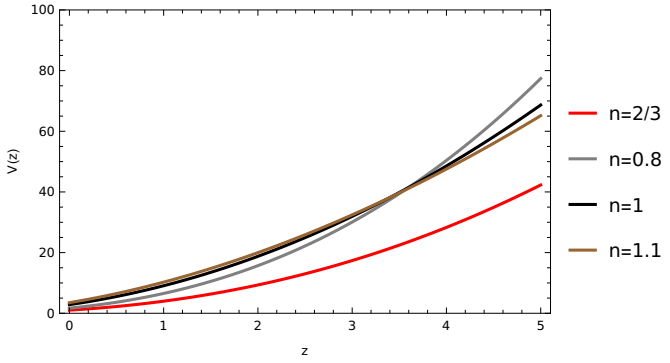

FIGURE 4.8: The plot shows the variation in potential $V(\phi(z))$ with respect to cosmological redshift z for different sets of values of n with a fixed value of $\beta << 1$, specifically $\beta = 0.1$, $\eta = 1$, and $\phi_0 = 0.1$.

4.3 Dynamical Analysis at Inflection Point

In this section, Let's perform a dynamical analysis of our inflection point tachyon model, but first lets learn what is dynamical system analysis.

4.3.1 Dynamical System Analysis:

Dynamical analysis [58, 141, 142] is a powerful tool used to study the dynamics of a given model under consideration and its behaviour over time, thereby providing insights into its long-term behaviour. In cosmology, dynamical system analysis allow us to analyze the contribution of various components of the universe, including DM, DE, and ordinary matter, by transforming complex differential equations into a phase space, which helps to understand the qualitative nature of cosmological models. A general dynamical system can be expressed in the form:

$$\frac{d\mathbf{x}}{dt} = \mathbf{f}(\mathbf{x}), \tag{4.44}$$

where $\mathbf{x} \in \mathbb{R}^n$ represents the state variables of the system and $\mathbf{f} : \mathbb{R}^n \to \mathbb{R}^n$ is a vector-valued function that governs the evolution.

To analyze the system, one first identify the *critical points* (or fixed points)- the point $\mathbf{x}_c$ where our function $\mathbf{f}(\mathbf{x})$ vanishes, satisfying:

$$\mathbf{f}(\mathbf{x}_c) = 0. \tag{4.45}$$

Stability of these points is examined by linearizing the system around each critical point $\mathbf{x}_c$ and then by calculating the Jacobian matrix which is write as:

$$J_{ij} = \left.\frac{\partial f_i}{\partial x_j}\right|_{\mathbf{x}=\mathbf{x}_c}. \tag{4.46}$$

The nature of the eigenvalues of this matrix determines the stability: if all eigenvalues are negative and real, the critical point is stable; if any one of the eigenvalues is positive and real, then the corresponding critical point is unstable and if all eigenvalues are positive and real then the critical point is unstable node.

In cosmology, dynamical system analysis allows for a qualitative understanding of cosmic evolution. It can distinguish between phases such as matter domination, radiation domination, or accelerated expansion by identifying the nature of critical points in the phase space. This approach is particularly useful in scalar field cosmology, where exact solutions are difficult to obtain, and qualitative behavior is more insightful. Now lets move to our inflection point model, the background equations governing the model are as follows:

$$H^2 = \frac{\kappa^2}{3}\rho \tag{4.47a}$$

$$\frac{\ddot{a}}{a} = \frac{-\kappa^2}{6}(\rho + 3p) \tag{4.47b}$$

Here again, as mentioned earlier, ρ and p contain two components, namely scalar field and matter. Let's set the dimensionless variables [58] as follows:

$$X = \dot{\phi} \equiv H\phi' \tag{4.48a}$$

$$Y = \frac{\kappa\sqrt{V}}{\sqrt{3}H} \tag{4.48b}$$

$$\Gamma = \frac{V(d^2V/d\phi^2)}{(dV/d\phi)^2} \tag{4.48c}$$

Here, the scalar field has inverse mass dimensions and $'$ signifies the derivative with respect to $\eta = \log a$. In the above equation, the term Γ naturally approaches zero at the inflection point of the potential. By definition, an inflection point is where the second derivative of the potential vanishes, i.e., $d^2V/d\phi^2 = 0$. This condition ensures that the potential flattens out locally, allowing the scalar field to undergo slow roll. The slow-roll behaviour, in turn, facilitates a smooth transition between different cosmological phases, making the inflection point a crucial feature in models describing cosmic acceleration. The vanishing of Γ at this point further simplifies the dynamical system.

$$\lambda = -\frac{dV/d\phi}{\kappa\sqrt{V^3}} \tag{4.48d}$$

Upon introducing the inflection point from Eq. (4.39) into Eq. (4.48d), we can obtain the following value of λ:

$$\lambda = \frac{1}{\sqrt{2n}}\left(\frac{3\beta^2}{2n} + \frac{2\beta}{3}\sqrt{\frac{3}{2n}}\right)\left(\frac{4\beta}{3}\sqrt{\frac{3}{2n}} + \frac{3\beta(1-3n)}{4n^2}\sqrt{\frac{2n}{3}}\right)^{-3/2} \tag{4.49}$$

Here, we obtain an autonomous two-dimensional system which has been previously studied by [43]. Two other parameters (see Eq. (4.48d)) still have ϕ dependency; upon differentiating these aforementioned dimensionless equations, namely Eqs. (4.48a), (4.48b), and (4.48d) with respect to $\eta = loga$ and using Eq. (4.47a) and (4.47b), one can obtain the following equations:

$$X' = \frac{dX}{d\eta} = (X^2 - 1)(3X - \lambda\sqrt{3}Y) \tag{4.50a}$$

$$Y' = \frac{dY}{d\eta} = \frac{-Y}{2}\left(3Y^2\frac{(1 + w_m - X^2)}{\sqrt{1 - X^2}} - 3(1 + w_m) + \sqrt{3}\lambda XY\right) \tag{4.50b}$$

$$\lambda' = \frac{3\sqrt{3}}{2}\lambda^2 XY \tag{4.50c}$$

Using the following constraint equation:

$$\Omega_\phi = \frac{Y^2}{\sqrt{1-X^2}} \tag{4.51}$$

the EoS and the energy density of the tachyonic scalar field, in terms of these dimensionless parameters, can be written as follows:

$$w_\phi = X^2 - 1 \tag{4.52}$$

$$\Omega_m = 1 - \frac{Y^2}{\sqrt{1-X^2}} \leq 1 \tag{4.53}$$

and the effective equation of motion can be written as follows:

$$w_{eff} = w_m\left(1 - \frac{Y^2}{\sqrt{1-X^2}}\right) - Y^2\sqrt{1-X^2} \tag{4.54}$$

The critical points for Eq. (4.48a) and (4.48b) are discussed below and are listed in Table (4.1):

X	Y	*Existence*	w_{eff}	Stability
0	0	$\forall n, (1+w_m)$ $w_m = 1$	w_m 1	Unstable Saddle point Stable Node
± 1	0	$\forall n, (1+w_m)$	–	Unstable Nodes
$\frac{Y_c\lambda}{\sqrt{3}}$	$Y_c = \sqrt{\frac{-\lambda^2+\sqrt{\lambda^4+36}}{6}}$	$\forall(1+w_m)$, $0 < n < 1$	$-Y_c^2\sqrt{1-\frac{\lambda^2 Y_c^2}{3}}+$ $w_m\left(1-\frac{Y_c^2}{\sqrt{1-\frac{\lambda^2 Y_c^2}{3}}}\right)$	Stable node

TABLE 4.1: The table shows the critical points of the system (4.48a)–(4.53) at the inflection point with λ.

There are five critical points within the dynamical analysis at the inflection point, as shown in Fig.(4.9) and discussed below:

(a.) Point O: For this critical point, $X = 0$ and $Y = 0$; the energy density of the tachyonic scalar field is revealed to be 0, thereby signifying the matter-dominated epoch. From the Friedmann constraint equation, Eq.(4.53), we can see that $\Omega_m = 1$ and $w_{eff} = w_m$ again signify the matter-dominated epoch; thus, this origin point of the phase space refers to the unstable saddle point, which has the following eigenvalues:

$$\nu_1 = -3 < 0 \tag{4.55}$$

and

$$\nu_2 = \frac{3}{2}(w_m + 1) \tag{4.56}$$

. For this critical point, if $(1 + w_m) > 0$, the point is an unstable saddle point. This saddle point demonstrates attractor behaviour, as shown in Fig.(4.9) and at this point, the value of $w_\phi = -1$ imitates the cosmological constant behaviour.

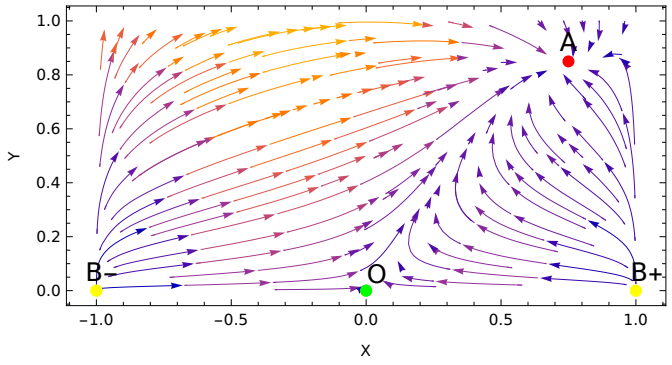

FIGURE 4.9: A phase portrait of the dynamical system for $n = 1/3$ with $\lambda \longrightarrow 1$ and $w_m = 0$, near the inflection point $\phi_{inflection}$ with $\beta << 1$ ($\beta = 0.1$). In plot A, O, B_- and B_+ represents the critical points. Here, stable point A in the phase space shows the region where the universe undergoes accelerated expansion.

(b.) Point B$_-$: For this point, we obtain the following critical points: $X = -1$ and $Y = 0$. At this critical point, the tachyonic EoS vanishes, i.e., $w_\phi = 0$; we also obtain the following eigenvalues:

$$\nu_1 = 6 > 0 \tag{4.57a}$$

and

$$\nu_2 = \frac{3}{2}(w_m + 1) > 0; if (1 + w_m) > 0. \tag{4.57b}$$

Therefore, the critical point B$_-$ is an unstable node representing the past attractor, but, here, the tachyon field behaves like dust-like matter, as in the case with $w_\phi = 0$ and $w_{eff} = w_m$.

(c.) Point B$_+$: X = 1, Y = 0. This point also represents an unstable node with the same eigenvalues as mentioned above, as follows:

$$\nu_1 = 6 > 0 \tag{4.58a}$$

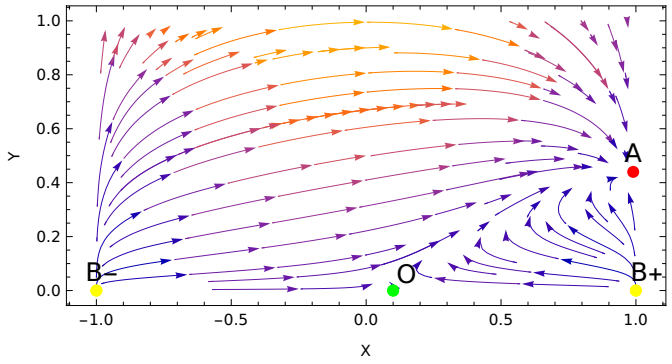

FIGURE 4.10: Phase portrait of the dynamical system for $n = 2/3$ with $\lambda > 1$ and $w_m = 0$, near the inflection point $\phi_{inflection}$ with $\beta << 1$ ($\beta = 0.1$). In plot A, O, B_- and B_+ represents the critical points. The stable point A in the phase space shows the region where universe undergoes accelerated expansion; however, because of the increase in n, point A is shifting towards $X \sim 1$.

and

$$\nu_2 = \frac{3}{2}(w_m + 1) > 0; if (1 + w_m) > 0 \tag{4.58b}$$

This point also shows the same past attractor behaviour, and the field shows dust-like behaviour, with $w_{eff} = w_m$.

(d.) Point A: $(X = \frac{\lambda Y_c}{\sqrt{3}}, Y_c = \sqrt{\frac{-\lambda^2+\sqrt{\lambda^4+36}}{6}})$ is the stable node, with the following eigenvalues:

$$\nu_1 = -3 + \frac{(-\lambda^4 + \lambda^2\sqrt{\lambda^4 + 36})}{12} \tag{4.59}$$

$$\nu_2 = -3(1 + w_m) + 2\frac{(-\lambda^4 + \lambda^2\sqrt{\lambda^4 + 36})}{12} \tag{4.60}$$

We obtain a stable point when $(1+w_m) > \frac{(-\lambda^4+\lambda^2\sqrt{\lambda^4+36})}{18}$; for this case, $\Omega_\phi = \frac{3(-\lambda^2+\sqrt{\lambda^4+36})}{18\sqrt{1-\frac{-\lambda^4+\sqrt{\lambda^4+36}}{18}}}$, thereby showing DE-like behaviour at this point. This stable point also depends on the values of n; as the value of n increases, this stable point is shifting more towards $X = 1$, and this behaviour can be seen in the phase portraits for different values of n. The critical point A, as shown in Figs.(4.9), (4.10) and (4.11), represents the stability of the derived dynamical system of equations and shows the accelerated expansion of the universe at the inflection point, which is incorporated in the system via the variable λ, and the field experiences accelerated expansion at a late time period.

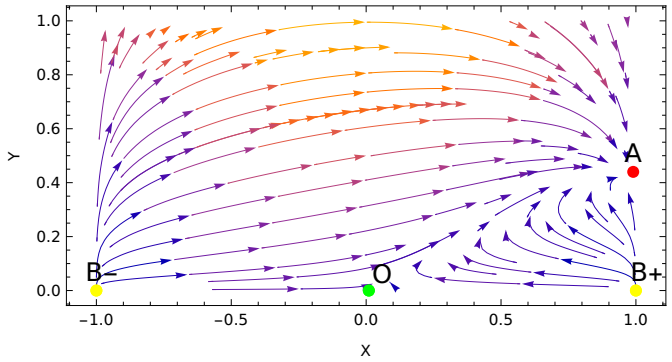

FIGURE 4.11: Phase portrait of the dynamical system for $n = 0.8$ with $\lambda \sim 5$ and $w_m = 0$, near the inflection point $\phi_{inflection}$ with $\beta << 1$ ($\beta = 0.1$). In plot A, O, B_- and B_+ represents the critical points. The stable point A in the phase space shows the region where universe undergoes accelerated expansion; however, because of the increase in n, point A is shifting more towards 1.

4.4 Conclusions

In this chapter, the evolution of a minimally coupled tachyonic scalar field at the inflection point has been investigated within an accelerating universe. The inflection point signifies a transition between regions of stability and instability and provides a flat region suitable for the ultra slow-roll approximation. In fact, inflection point models can also offer a robust framework for describing the inflationary phase as it can provide a prolonged period of slow-roll inflation. In this paper, the field's dynamics have been investigated for different forms of expansion factors, and by considering a different form of scale factor, a form of potential is derived; only the mixed form of potential has shown the inflection point. We have mainly considered the following three categories of scale (expansion) factor: (a) power-law expansion ($a(t) = \alpha t^n$); (b) the exponential form ($a(t) = \gamma e^{\beta t}$); and (c) the mixed form ($a(t) = \eta t^n e^{\beta t}$). For all these categories, the potentials and the corresponding possible inflection points have been calculated, and the dynamical system of equations for the model has been obtained. Out of these three categories, the mixed form shows inflection at $\phi_{inflection}$, as given in Eq.(4.39), and, near this point, under slow roll approximation, the evolution of the scalar field with cosmic time (t) and cosmological redshift (z) shows the accelerated expansion of the universe at late time periods near the inflection point. Fig.(4.8) also indicates that a potential with an inflection point can provide a near-flat region for the field to slow roll, which may derive the accelerated cosmic expansion.

In Section (4.3), the dynamical analysis carried out shows that the critical point A, as

shown in Figs.(4.9),(4.10) and (4.11), represents the stability of the derived dynamical system of equations and shows the accelerated expansion of the universe at an inflection point, which is incorporated in the system via the variable λ, and the field demonstrates accelerated expansion at late time periods.

Chapter 5

Generalizing Scalar fields

5.1 Introduction

Modern cosmology is fundamentally based on Einstein's General Relativity (GR), which provides a robust framework for describing the dynamics of the universe at the classical level, where gravity is the dominant force. GR effectively accounts for the coupled dynamics between the gravitational and matter sectors. Observations reveal that the evolution of the universe is characterized by successive epochs, each dominated by a specific component of matter. The physics underlying the radiation and matter dominated eras is understood quite well within the framework of the standard cosmological model. Beyond the inflationary paradigm, various forms of scalar field Lagrangians have been proposed to construct models aimed at explaining the late-time acceleration of the universe. Over the years, as discussed earlier, numerous observations have provided compelling evidence that the universe is undergoing an accelerated phase of expansion[2, 3, 13, 97–99, 143]. The simplest model is the ΛCDM framework. However, it faces unresolved issues such as the fine-tuning problem and the cosmological coincidence problem as already mentioned earlier in chapter-1.

Each model offers a distinct perspective on the underlying properties of DE, yet they face individual challenges, such as instabilities or incomplete phenomenological coverage. Many authors also work in order to unify matter and DE into a single framework [144–147]. The Lagrangian that we are going to define distinguishes itself from prior unified models by encapsulating quintessence, phantom and tachyon behaviors within a single,

two-parameter framework. Unlike Scherrer's unified DE-dark matter model [148], which uses a single scalar field with a specific potential, or Sahni and Sen's two-component fluid approach [144], our formalism avoids prescribing a unique potential form, offering greater flexibility via α and β.

Compared to K-essence or Chaplygin gas models [146, 149, 150], which unify dark sectors through non-linear kinetic terms, our approach explicitly recovers the canonical structures of three distinct scalar fields by tuning parameters, enabling direct comparisons within a cohesive mathematical structure. This reformulation, while not dynamically unifying the fields, provides a novel lens for studying their interrelations, as evidenced by the smooth transitions in $Om(z)$ diagnostics, setting the stage for deeper cosmological insights.

In this chapter, a generalized form of the Lagrangian is introduced which encapsulates three major classes of scalar field models: quintessence, phantom, and tachyon. This formulation offers a unifying two-parameter framework capable of reproducing the canonical forms of each field type by appropriate choices of parameters while maintaining a single cohesive mathematical structure.

5.2 Scalar field dynamics:

At the classical level, there are broadly two possible dynamical approaches to replicate an accelerated phase of cosmic expansion: either by modifying the gravity sector (i.e., modified gravity theories) or by altering the matter sector. In this work, we confine our analysis within the framework of general relativity, based on the Einstein-Hilbert action, and focus exclusively on modifications in the matter sector.

Scalar field models play a crucial role in modern cosmology, offering plausible and flexible mechanisms for explaining the observed late-time acceleration of the universe. These fields serve as dynamical alternatives to the cosmological constant and are capable of emulating a wide spectrum of DE behaviors. Beyond DE, the dynamical nature of scalar fields has also been instrumental in explaining early-universe inflation, where a scalar field with a sufficiently flat potential can drive exponential expansion. Moreover, scalar field dynamics have been successfully adapted to describe dark matter behavior

under specific conditions, further underscoring their versatility in addressing multiple fundamental aspects of the cosmic evolution.

The quest to understand the cosmos particularly the observed phenomenon of late-time accelerated expansion has led to extensive investigations into a wide array of scalar field models. While each of these models offers a compelling framework for describing DE, they are not without limitations, often constrained by specific assumptions about potentials or kinetic terms. Despite significant progress, a comprehensive formalism that can encompass all major scalar field models within a single theoretical structure remains elusive.

The development of such a generalized framework would mark a significant advance, enabling a unified approach to the treatment of DE phenomena. It would provide the flexibility to recover known models as special cases while offering new pathways to overcome their individual shortcomings. In response to this challenge, several researchers have proposed unified treatments of DE and dark matter by employing non-canonical scalar field models [144, 151]. These models typically introduce additional parameters to characterize a two-component fluid, where the kinetic term accounts for dark matter-like behavior and the potential term mimics a cosmological-constant.

5.3 Generalized Lagrangian of three classes of scalar fields:

A key element of this study is the introduction of a generalized Lagrangian formalism designed to unify several prominent scalar field models that describe DE. This framework incorporates two free parameters, namely α and β, which govern the dynamics and allow smooth transitions between different field behaviors specifically quintessence, phantom and tachyon fields. The generalized Lagrangian is expressed as:

$$\mathcal{L}_X = \alpha X^{\alpha^2} - V(\phi)(1-2X)^{\beta/2}, \tag{5.1}$$

where $X = \frac{1}{2}\partial_\mu\phi\partial^\mu\phi$ is the kinetic term, ϕ represents the scalar field, $V(\phi)$ is the potential, and the flexibility of the model arises from the tunability of the parameters α

and β , which recover well-known scalar field models for specific values:

$$\alpha, \beta = \begin{cases} \alpha = 0, \beta = 1; & \text{Tachyon} \\ \alpha = 1, \beta = 0; & \text{Quintessence} \\ \alpha = -1, \beta = 0; & \text{Phantom} \end{cases} \cdot \tag{5.2}$$

The generalized Lagrangian $\mathcal{L}_X = \alpha X^{\alpha^2} - V(\phi)(1-2X)^{\beta/2}$, where $X = \frac{1}{2}\partial_\mu\phi\partial^\mu\phi$, is proposed as a phenomenological framework to unify quintessence, phantom, and tachyon scalar fields. While not derived from a fundamental theory, its structure can be motivated by effective field theories and non-canonical scalar field models. The kinetic term αX^{α^2} generalizes the standard canonical form (as in quintessence) and resembles higher-order corrections found in string-inspired models, such as tachyon dynamics [47, 152–154]. The second term, involving the factor $(1 - 2X)^{\beta/2}$introduces non-linear modifications reminiscent of K-essence and tachyon Lagrangians, potentially representing low-energy effective limits of more fundamental theories or as an ad-hoc generalization to capture diverse DE behaviors. This form ensures covariance under coordinate transformations and provides a flexible scaffold to explore scalar field dynamics across cosmological epochs. One of the essential features of this Lagrangian is its invariance under coordinate transformations which ensures the consistency with the general principle of covariance. The Lagrangian given in above equation is invariant under coordinate transformation i.e. $x^\mu \longrightarrow x'^\mu$, since, ϕ and $V(\phi)$ are independent of the choice of coordinates. The corresponding energy-momentum tensor derived from this Lagrangian is given by:

$$T^{\mu\nu} = \frac{\partial \mathcal{L}_X}{\partial(\partial_\mu\phi)}\partial^\nu\phi - g^{\mu\nu}\mathcal{L}_X. \tag{5.3}$$

which follows the standard prescription for deriving stress-energy tensors from scalar field Lagrangians. From this energy-momentum tensor, the energy density and pressure can be derived using:

$$\rho_\phi = \frac{\partial \mathcal{L}_X}{\partial \dot{\phi}} - \mathcal{L}_X \tag{5.4a}$$

and

$$p_\phi = \mathcal{L}_X. \tag{5.4b}$$

Using the above Eq.(5.4a) and Eq.(5.1) we can obtain the generalized expressions for the energy density as:

$$\rho_\phi = (2\alpha^3 - \alpha)X^{\alpha^2} + V(\phi)(1-2X)^{\beta/2}\left[1 + \frac{2\beta X}{(1-2X)}\right]. \tag{5.5a}$$

For further simplification, we have expanded the last term $(1-2X)^{\beta/2}$ using Taylor's expansion by considering $X << 1$ which futher helps in constraining the values of $\dot{\phi}^2$ as $0 < \dot{\phi}^2 << 1$, so the above expression of energy density can be rewritten as:

$$\rho_\phi \approx (2\alpha^3 - \alpha)X^{\alpha^2} + V(\phi) + \beta X V(\phi)\left(\frac{1+2X(1-\beta)}{1-2X}\right), \tag{5.5b}$$

or, equivalently, in decomposed form as:

$$\rho_\phi \approx \rho_X + \rho_V + \rho_{XV}, \tag{5.5c}$$

where the components are defined as:

$$\rho_X = (2\alpha^3 - \alpha)X^{\alpha^2}, \tag{5.6a}$$

$$\rho_V = V(\phi), \tag{5.6b}$$

$$\rho_{XV} = \beta X V(\phi)\left(\frac{1+2X(1-\beta)}{1-2X}\right). \tag{5.6c}$$

Thus, the energy density is decomposed into three components: the kinetic term ρ_X, potential term ρ_V and mixed term ρ_{XV} which could be due to the non-linear coupling introduced by the parameter β. The pressure derived from the Lagrangian is similarly given by:

$$p_\phi \approx \alpha(X)^{\alpha^2} - V(\phi)\,(1-2X)^{\beta/2}\,. \tag{5.7}$$

Applying the same approximation to the $(1-2X)^{\beta/2}$ term as done previously for Eq. (5.5b), the pressure can also be rewritten in terms of its components as:

$$p_\phi = p_X + p_V + p_{XV} = \alpha X^{\alpha^2} - V(\phi) + X\beta V(\phi). \tag{5.8}$$

So, here again, we can represent pressure in component form as shown below:

$$p_X = \alpha X^{\alpha^2}, \tag{5.9a}$$

$$p_V = -V(\phi), \tag{5.9b}$$

$$p_{XV} = \beta X V(\phi). \tag{5.9c}$$

This decomposition allows for clearer interpretation of the contributions to pressure, similar to energy density, thus facilitating detailed analysis of scalar field dynamics under varying conditions of α and β. In Eq.(5.5) and Eq.(5.8) by using the different values of α and β as mentioned in Eq.(5.2) we can obtain the energy densities and pressure of all the three kinds of scalar fields individually. Now using the spatially flat FRLW model Eq.(1.6), the generalized form for the two Friedmann equations can be obtained as:

$$H^2 = \frac{8\pi G}{3}\rho_\phi \equiv \frac{8\pi G}{3}\left(\rho_X + \rho_V + \rho_{XV}\right) \tag{5.10}$$

and

$$\frac{\ddot{a}}{a} = -\frac{4\pi G}{3}\left((\rho_X + 3p_X) + (\rho_V + 3p_V) + (\rho_{XV} + 3p_{XV})\right) \tag{5.11}$$

and thus EoS in the generalized form becomes:

$$1 + w_\phi = \frac{2\alpha^3\left(\frac{\dot{\phi}^2}{2}\right)^{\alpha^2} + V(\phi)\beta\dot{\phi}^2\left(\frac{(1-\dot{\phi}^2\beta/2)}{(1-\dot{\phi}^2)}\right)}{\rho_\phi} \tag{5.12}$$

or

$$w_\phi = \frac{\alpha(X)^{\alpha^2} - V(\phi)\left(1-2X\right)^{\beta/2}}{(2\alpha^3-\alpha)X^{\alpha^2} + V(\phi)(1-2X)^{\beta/2}\left[1+\frac{2\beta X}{(1-2X)}\right]}. \tag{5.13}$$

So, now next step is to find the equation of motion in the generalized form which we can calculate by solving the conservation equation which reads as:

$$\dot{\rho_\phi} + 3H(1+w_\phi)\rho_\phi = 0 \tag{5.14}$$

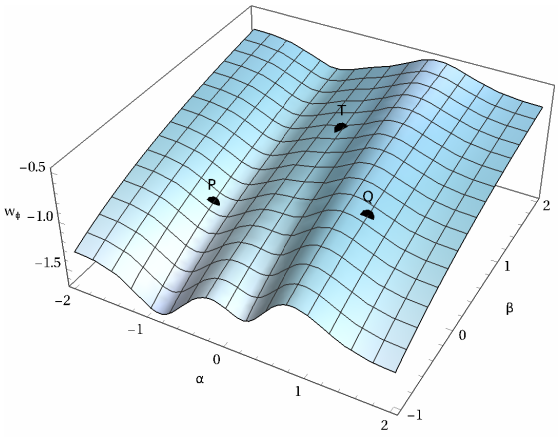

FIGURE 5.1: The plot of Eq.(5.13) shows the points representing the Phantom (P), Quintessence (Q), and Tachyon (T) scalar fields within the framework of the generalized Lagrangian. Here for $\alpha = -1$ and $\beta = 0$ we get $w_\phi = -1.22$, for $\alpha = 1$ and $\beta = 0$ we get $w_\phi = -0.818$ and for $\alpha = 0$ and $\beta = 1$ we get $w_\phi = -0.8$ and for a constant potential $V(\phi) \approx 1$ along with the condition $\dot{\phi}^2 << V(\phi)$.

Therefore using Eqs.(5.5b), (5.8) and (5.12) the equation of motion in this generalized framework is found to be:

$$\begin{aligned}\ddot{\phi}\dot{\phi}\left[\alpha^2(2\alpha^3-\alpha)\left(\frac{\dot{\phi}^2}{2}\right)^{\alpha^2-1}+\frac{V(\phi)(1-\dot{\phi}^2)^{(\beta/2)}\beta}{(1-\dot{\phi}^2)}\left(1+\frac{(2-\beta)\dot{\phi}^2}{1-\dot{\phi}^2}\right)\right]\\ +3H\left[2\alpha^3\left(\frac{\dot{\phi}^2}{2}\right)^{\alpha^2}+\frac{\beta\dot{\phi}^2V(\phi)(1-\dot{\phi}^2)^{(\beta/2)}}{(1-\dot{\phi}^2)}\right]\\ +\frac{dV}{d\phi}\left[\dot{\phi}(1-\dot{\phi}^2)^{(\beta/2)}\left(1+\frac{\beta\dot{\phi}^2}{1-\dot{\phi}^2}\right)\right]=0\end{aligned} \tag{5.15}$$

indeed we can reduce this equation to a standard equation of motion for all the three kinds of scalar fields by substituting the respective values of our parameters α and β. Let's see them one by one:

Case-1: $\alpha = 1, \beta = 0$: Eq.(5.15) reduces to:

$$\ddot{\phi} + 3H\dot{\phi} + V'(\phi) = 0 \tag{5.16}$$

which is the evolution equation of quintessence as mentioned in Eq. (1.51).

Case-2: $\alpha = -1, \beta = 0$: For this case Eq.(5.15) reduces to:

$$\ddot{\phi} + 3H\dot{\phi} - V'(\phi) = 0 \tag{5.17}$$

which represents the evolution equation for the case of phantom scalar field as mentioned in Eq.(1.55).

Case-3: $\alpha = 0, \beta = 1$: For this case Eq.(5.15) reduces to the following form:

$$\frac{\ddot{\phi}}{(1-\dot{\phi}^2)} + 3H\dot{\phi} + \frac{1}{V}\frac{dV}{d\phi} = 0 \tag{5.18}$$

and this above-mentioned equation is the evolution equation for the case of tachyon scalar field as mentioned in Eq.(1.59e). Now let's discuss about the EoS for all three components individually in next section.

5.3.1 EoS and density parameters in Component form:

In this section individual components of EoS are discussed. Here we have three different components of EoS for various values of parameters:

A. Kinetic term: EoS of the kinetic component of the scalar field is:

$$w_X = \frac{p_X}{\rho_X} = \frac{1}{2\alpha^2 - 1} \tag{5.19}$$

from the above equation, we can see that EoS of a kinetic term is independent of second parameter β and only depends on the choice of parameter α similar to [144, 151].

Case A1. For $\alpha >> 1$ the EoS of kinetic term $w_X \longrightarrow 0$ i.e. the kinetic term could play a role of Dark Matter for the larger values of α.

Case A2. When $\alpha = 0$, the kinetic term becomes -1; however, both the pressure and energy density vanish individually, i.e., $p_X = 0$ and $\rho_X = 0$.

Case A3. When $\alpha = \pm 1$ for this case kinetic term behaves like stiff matter i.e. $w_X = 1$.

The kinetic component of the equation of state (EoS) is independent of the parameter β. In the case where $\alpha \gg 1$, only the kinetic component contributes significantly, behaving like dark matter, with the EoS approaching zero. Another limiting case is when $\alpha = 0$; although the EoS formally becomes -1, but both the energy density and pressure individually vanish.

B. Potential term: EoS of the potential component of the scalar field can be written as:

$$w_V = \frac{p_V}{\rho_V} = -1 \tag{5.20}$$

Here, we can interpret the potential term is playing the role of DE. For the simplest case, if we take $V(\phi) = \frac{\Lambda}{8\pi G}$, as considered in [144], then this potential term, along with the kinetic term in the limit $\alpha > 1$, mimics the ΛCDM model (assuming the contribution from the mixed term to the EoS is negligible). Other functional forms of $V(\phi)$ can also be considered; however, in this paper, we focus only on the case of a constant potential.

C. Mixed term: EoS of the mixed components having a combination of both kinetic and potential parts is given as:

$$w_{XV} = \frac{p_{XV}}{\rho_{XV}} = \frac{V(\phi)(1-2X)}{V(\phi)((1-\beta)2X+1)} = \frac{1-\dot{\phi}^2}{(1-\beta)\dot{\phi}^2+1} \tag{5.21}$$

Individually, for the mixed component, both the pressure and energy density depend on the kinetic and potential energy terms. However, the equation of state (EoS) of the mixed term is independent of the potential $V(\phi)$ and the parameter α. Below, we consider two cases corresponding to different values of β:

Case C1: For $\beta = 0$ the EoS becomes: $w_{XV} = \frac{1-\dot{\phi}^2}{1+\dot{\phi}^2}$

Case C2: For $\beta = 1$ the EoS becomes: $w_{XV} = 1 - \dot{\phi}^2$

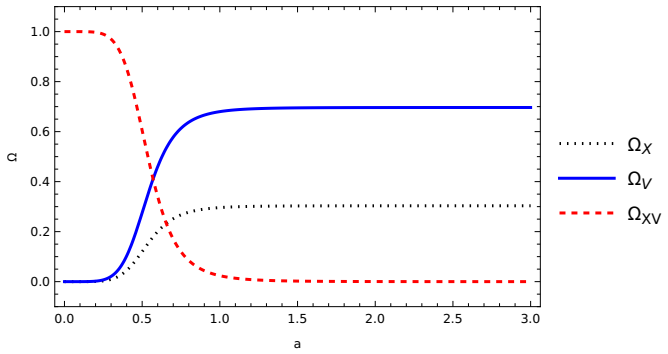

FIGURE 5.2: Evolution of the density parameters corresponding to the kinetic term (Ω_X), potential term (Ω_V), and mixed term (Ω_{XV}).The plot shows that the mixed term dominates initially, while the potential term begins to dominate at $a/a_0 = 1$. Here, $\Omega_X \sim \Omega_m^0 = 0.2962$ (DESI+BBN [5]), $\Omega_V \sim \Omega_{de}^0 = 0.68$, with $\dot{\phi} = 0.9$, $\alpha = 0$, and $\beta = 1$.

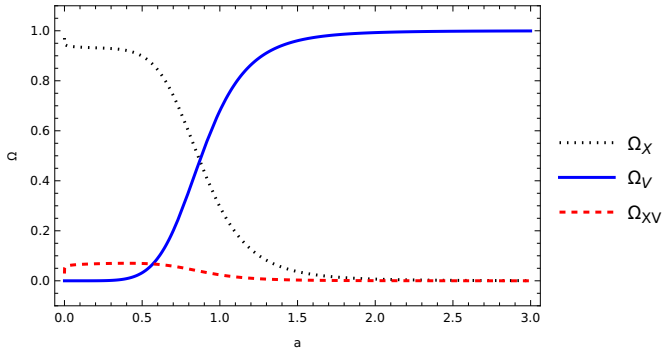

FIGURE 5.3: Evolution of the density parameters for the kinetic term (Ω_X), potential term(Ω_V), and mixed term. The plot shows that the kinetic term dominates initially, while the potential term begins to dominate at $a/a_0 = 1$. Here, $\Omega_X \sim \Omega_m^0 = 0.2962$ (DESI+BBN [5]), $\Omega_V \sim \Omega_{de}^0 = 0.68$, with $\dot{\phi} = 0.9$, $\alpha = 0$, and $\beta = 1$.

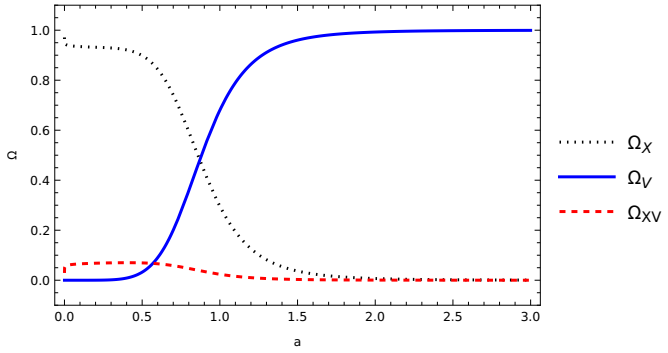

FIGURE 5.4: Evolution of the density parameters corresponding to the kinetic term (Ω_X), potential term (Ω_V), and mixed term (Ω_{XV}). At early times, the kinetic term dominates while at some interval of intermediate times, the potential term again begins dominant over the potential and mixed term. Here, $\Omega_X \sim \Omega_m^0 = 0.2962$ (DESI+BBN [5]) and $\Omega_V \sim \Omega_{de}^0 = 0.68$, with $\alpha = -1$ and $\beta = 0$.

Figs.(5.2), (5.3) and (5.4) show the evolution of the energy density components with respect to the scale factor a/a_0 for different sets of values of α and β. For $\alpha = 1$ and $\alpha = -1$, shown in Figs.(5.3) and (5.4) respectively, although during early times mixed term Ω_{XV} dominates potential term, but still remains small throughout the evolution of the universe and kinetic term dominates at early epochs which may corresponds to a matter-dominated phase. Near $a/a_0 \approx 1$, the potential term starts dominating the universe, possibly indicating a transition to a DE-dominated phase with EoS $w_V \approx -1$. Fig.(5.2) shows the evolution of energy density parameters for $\alpha = 0$ and $\beta = 1$, we can see from the Fig.(5.2) that during early times mixed terms dominates while at late times potential term starts dominating again consistent with the result obtained in Case B which shows EoS of potential component is always -1 similar to cosmological constant.

For the case where $\beta = 1$ and $\alpha = 0$, as shown in Fig.(5.2), the mixed term Ω_{XV} plays a

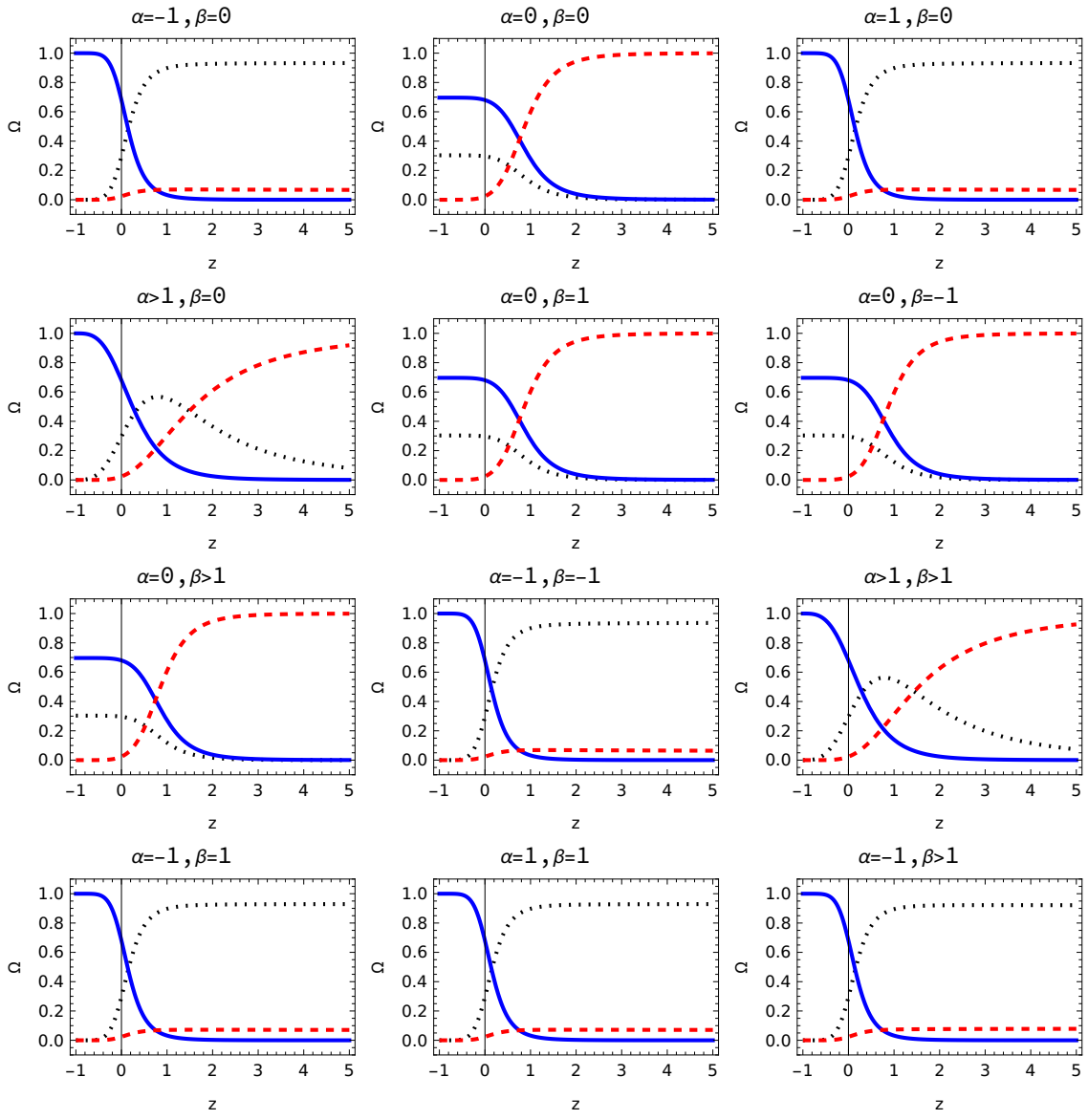

FIGURE 5.5: Evolution of the energy density components Ω_V (blue solid line), Ω_{XV} (red dashed line), and Ω_X (black dotted line) as functions of redshift z for different combinations of the model parameters α and β. Each subplot corresponds to a specific choice of (α, β), demonstrating the contributions of kinetic and potential terms to the total energy density.

significant role, particularly in the early universe as $a/a_0 \longrightarrow 1$, Ω_{XV} starts decreasing, which could indicate an energy transfer between the three components. As $a/a_0 \geq 1$, this mixed term decreases and subsequently, the potential term starts to dominate. At late times, the potential term remains dominant and could behave as DE and could drive the accelerated expansion of the universe.

Plots shown in Figs.(5.5), (5.6) and (5.7) collectively shows the evolution of all three energy density components with respect to the redshift z. There are three broad cases:

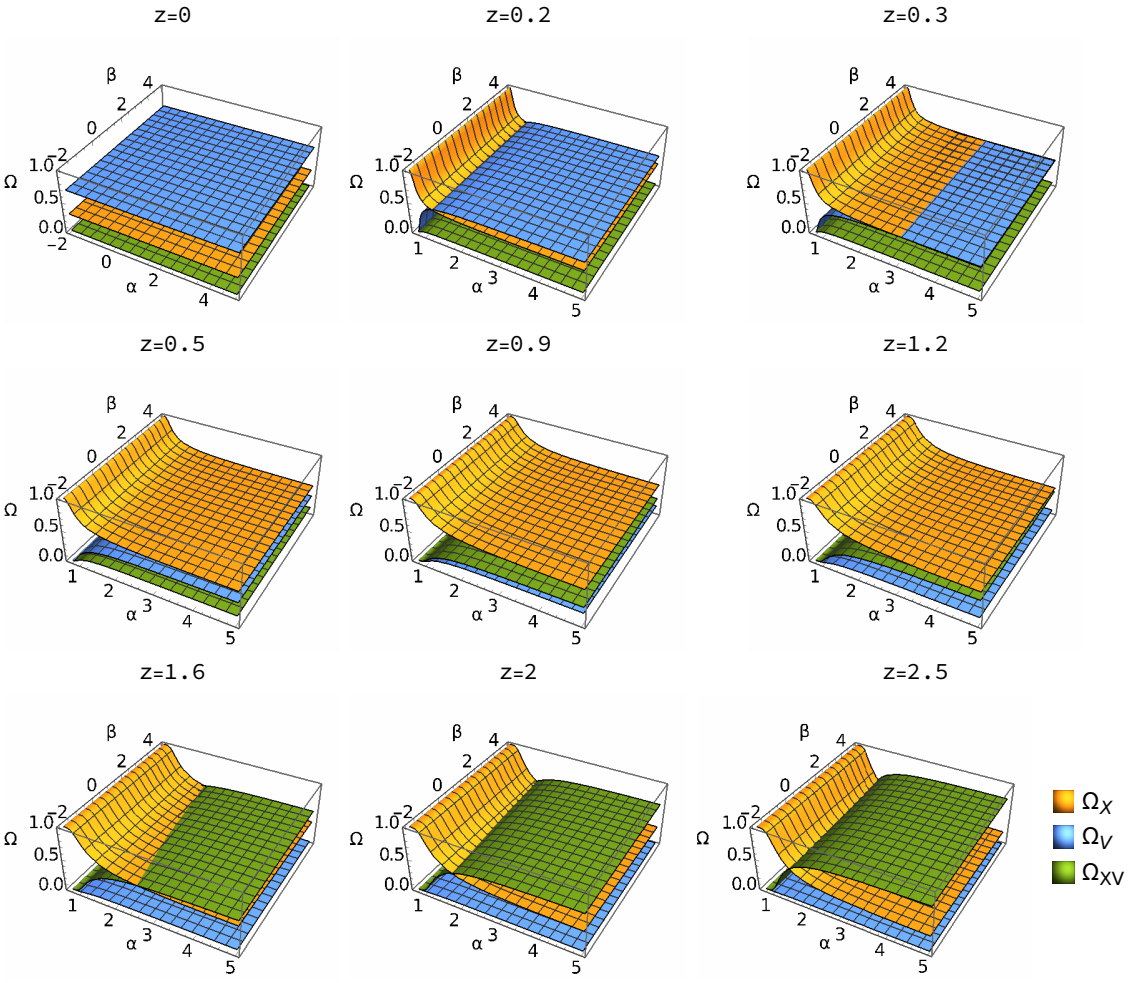

FIGURE 5.6: These 3D plots show the evolution of the energy density parameters Ω_X (orange), Ω_V (blue), and Ω_{XV} (green) plotted as functions of the model parameters α and β at various redshifts: $z = 0, 0.2, 0.5, 0.7, 1, 1.2$. These plots demonstrate how the relative contributions of the kinetic term, potential term, and the mixed term evolve with cosmic time, highlighting the dynamic behavior of the model across different epochs.

$\alpha = \pm 1$, $\alpha = 0$ and $\alpha > 1$ $\forall \beta$. Let's first discuss about the case when $\alpha = \pm 1$; in this case when the redshift $z > 1$, kinetic term is the dominating one while potential term $\Omega_V \approx 0$, as seen in Case A3, Ω_X behaves as stiff matter with EoS $w_X \approx 1$ but, as $z \longrightarrow 0.9$ (as seen in Figs. (5.5), (5.6) and (5.7)) Ω_V starts increasing while Ω_X decreases and as $z \longrightarrow 0.3$, Ω_V starts dominating other two components similar to the one seen in Case B where EoS for potential component is $w_V \approx -1$. At present value of z i.e. $z = 0$, this potential term dominates the universe with values nearly $\Omega_V \approx 0.68 \equiv \Omega_{de}$ and $\Omega_X \approx 0.3 \equiv \Omega_m$ while the mixed term is approximately zero and as we more further with $z < 0$ Ω_V starts increasing more while Ω_X and Ω_{XV} approaches nearly zero.

Now, for the cases with $\alpha = 0$, as shown in Figure (5.7) that when $z > 1$, Ω_{XV} is

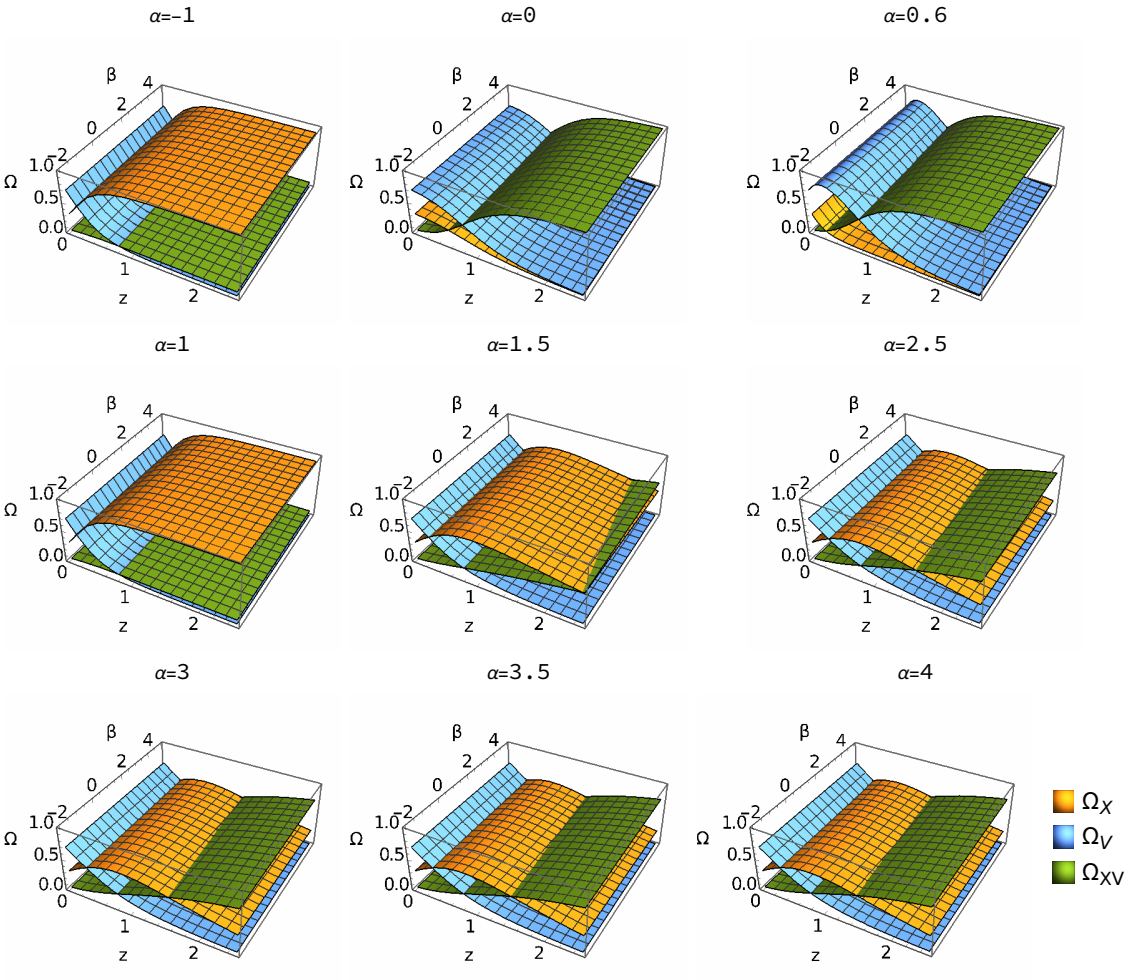

FIGURE 5.7: These 3D plots show the evolution of the energy density parameters Ω_X (orange), Ω_V (blue), and Ω_{XV} (green) as functions of redshift z and the model parameter β, for different fixed values of $\alpha = -1, 0, 0.5, 1, 1.5, 2.5$. These plots illustrate how the contributions from the kinetic, potential and mixed components vary over cosmic time depending on the choice of α, revealing the sensitivity of the model's dynamics to this parameter.

dominating over other two components and from Fig.(5.6) we can see that near $z \approx 2$ density parameters Ω_X and Ω_V starts dominating Ω_{XV} (all balancing each other). Near $z \approx 0.7$, as shown in Figs.(5.5) and (5.7) we can observe a transition between Ω_{XV} and Ω_V while near $z \approx 0.5$, Ω_X surpasses Ω_{XV} while still Ω_V remains the dominant. Near $z \leq 0$ as seen in Fig.(5.5) Ω_V is dominating the evolution behaving as DE with EoS $w_V \approx -1$ while during intermediate times Ω_X behaves as matter with EoS $w_X \approx 0$ for this particular case when $\alpha = 0$.

Another scenario is when $\alpha > 1$, here in this case for $z \geq 2$ as seen in Fig.(5.5), Ω_{XV} is the dominating component as compared to Ω_X and Ω_V but, as $z \longrightarrow 1.48$, we can see a transition between Ω_X and Ω_X after which Ω_X starts dominating the evolution

and dominates until $z \longrightarrow 0.3$ and Ω_V starts dominating Ω_X and Ω_{XV} which can be seen in Figs.(5.5), (5.6) and (5.7) and at present epoch $z = 0$, again Ω_V dominates kinetic and mixed components while Ω_X dominating Ω_{XV} following which again we can say potential term behaves as DE with $w_V \approx -1$ and Ω_X behaves as matter with EoS $w_X \approx 0$ for this case with $\alpha > 1$(as shown in case A1). Together, these figures highlight the dynamical interplay between kinetic, potential and mixed terms, governed by α and β and demonstrate the model's capability to naturally interpolate between matter-dominated and DE-dominated phases of cosmic evolution.

5.4 $Om(z)$ Diagnostics:

To assess the observational viability of the generalized Lagrangian model, Let's perform a preliminary analysis by constraining the model parameters α and β using the evolution of the Hubble parameter as given in Eq. (5.10). For simplification, Let's consider a constant scalar potential $V(\phi) = V_0$ and assume the equation of state parameter for the scalar field takes the form $w_\phi = w_0 + \epsilon$, as introduced in Eq. (5.24).

In order to connect the model with observations, we need fit the parameter space to recent cosmological data. Specifically, using the combined constraints from the DE Spectroscopic Instrument and Big Bang Nucleosynthesis (DESI+BBN) [5], which provide $\Omega_m^0 \approx 0.2962$ and $\Omega_{de}^0 \approx 0.68$, along with the Planck 2018 results [13], which yield a Hubble constant of $H_0 \approx 67.4\,\mathrm{km\,s^{-1}\,Mpc^{-1}}$.

In the limit $\alpha > 1$ and $\beta = 0$, the model reduces effectively to the standard ΛCDM scenario. Under these conditions, the scalar field equation of state approaches $w_\phi \approx -1$, and the potential is approximately given by

$$V_0 \sim \frac{3H_0^2}{8\pi G} \times \Omega_{de}^0 \approx 0.68 \times \frac{3H_0^2}{8\pi G}.$$

This correspondence supports the model's consistency with current DE density estimates when it behaves like a cosmological constant.

For $\beta = 1$, which corresponds to the tachyon field configuration, the requirement $\phi^2 < 1$ ensures that the field does not become superluminal and that the equation of state remains in the range $w_\phi > -1$. This is consistent with observational bounds on

quintessence models, particularly those derived from Type Ia supernovae data, which suggest $w_0 > -1.1$ [2, 3].

Alternatively, the model also accommodates phantom-like behavior for the parameter choice $\alpha = -1$ and $\beta = 0$, where $w_\phi < -1$. Such scenarios are supported by some interpretations of combined Cosmic Microwave Background (CMB) and Baryon Acoustic Oscillation (BAO) data [38, 39]. However, to remain within observationally acceptable limits, the deviation from $w = -1$ must be small, typically requiring $|\epsilon| < 0.1$.

These indicative constraints demonstrate the flexibility of the generalized Lagrangian framework in reproducing key cosmological behaviors such as those corresponding to ΛCDM, quintessence, and phantom DE by suitable choices of the model parameters α and β.

In modern cosmology, one of the essential goals is to distinguish between different models of DE, particularly those that go beyond the standard ΛCDM paradigm. To achieve this, researchers often rely on diagnostic tools that are independent of the assumptions about the underlying nature of DE. One such powerful and widely used tool is the *Om(z)* diagnostic.

The $Om(z)$ diagnostic was introduced as a way to evaluate the behavior of the Hubble parameter $H(z)$ without needing to differentiate it or assume a specific form for the DE equation of state. It is defined using the normalized Hubble parameter $E(z) = H(z)/H_0$, where H_0 is the current value of the Hubble constant. The Om(z) function is given by:

$$Om(z) = \frac{E(z)^2 - 1}{(1+z)^3 - 1}. \tag{5.22}$$

This expression has a particularly important feature: in the standard ΛCDM model, where the universe contains only matter and a cosmological constant, $Om(z)$ remains constant for all redshifts. That is,

$$Om(z) = \Omega_m^0, \tag{5.23}$$

where Ω_m^0 is the present-day matter density parameter. Any deviation from a constant value of $Om(z)$ across redshifts indicates a departure from the ΛCDM model and can signal the presence of dynamic DE or modifications to general relativity.

In models where the DE component evolves with time, $Om(z)$ becomes redshift-dependent. For example:

- If $Om(z)$ increases with redshift, it may indicate a *phantom-like* behavior (i.e., $w < -1$).
- If $Om(z)$ decreases with redshift, it may suggest *quintessence-like* behavior (i.e., $w > -1$).

What makes the $Om(z)$ diagnostic particularly useful is its reliance only on the expansion history, which can be directly reconstructed from observations such as supernovae data, Baryon Acoustic Oscillations (BAO), and Cosmic Chronometers. This avoids complications arising from integrating or differentiating noisy observational data.

In the context of our generalized Lagrangian model, we use the $Om(z)$ diagnostic as an independent test to verify whether the behavior of our scalar field model mimics ΛCDM, deviates towards quintessence, or enters the phantom regime. By comparing the theoretical predictions of $Om(z)$ from our model with observational reconstructions, we can further constrain the parameters α and β and assess the cosmological viability of the model. In order to perform the $Om(z)$ diagnosis let's parameterize the EoS using CPL [155, 156] as shown below:

$$w_\phi = w_0 + \epsilon \tag{5.24}$$

where, w_0 repesents the EoS parameter of standard ΛCDM while ϵ represents the slight deviation from ΛCDM and has the following values for Quintessence and Tachyon scalar field $\epsilon > 0$, for Phantom $\epsilon < 0$, and for Cosmological constant $\epsilon = 0$ and $w_0 = -1$. Using Eq. (5.24) and Eq. (5.12), the general form of the EoS can be rewritten as:

$$w_\phi = \frac{\epsilon\left(2\alpha^3 - \frac{\beta\dot{\phi}^2}{1-\dot{\phi}^2}\right)}{\left(2\alpha^3 - 2\epsilon + (1-2\epsilon)\frac{\beta\dot{\phi}^2}{(1-\dot{\phi}^2)}\right)} - 1 \tag{5.25}$$

Now, for flat universe the $Om(z)$ diagnostic can be written as [156]:

$$O_m(x) = \frac{h^2(x) - 1}{x^3 - 1} \tag{5.26}$$

here $h(x) = \frac{H(x)}{H_0}$. Using Eq.(5.10) the $Om(z)$ diagnostic for flat universe becomes:

$$OM(z) = \Omega_m^0 + (1 - \Omega_m^0) \left(\frac{(1+z)^{3(1+w_\phi)} - 1}{(1+z)^3 - 1} \right) \tag{5.27}$$

From Eq.(5.27) one can find that $OM(z) = \Omega_m^0$ for ΛCDM model, which can also be

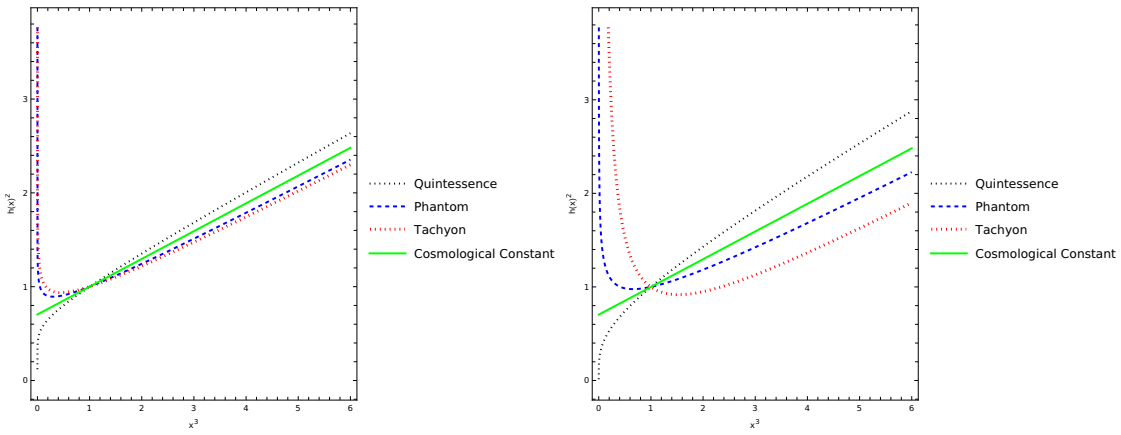

FIGURE 5.8: These plots show the variation of Hubble parameter squared v/s cube of cosmological Redshift parameter $x = 1 + z$. Plot on the left the values of parameter (ϵ) for Quintessence (black-dotted) and Tachyon(red-dotted) is taken to be $\epsilon = 0.1$, $\epsilon = -0.1$ for Phantom (blue-dashed) and $\epsilon = 0$ for Cosmological constant(green-solid) and the graph on the right is for Quintessence and Tachyon with $\epsilon = 0.2$, Phantom with $\epsilon = -0.2$ and Cosmological constant with $\epsilon = 0$ here w_0 is taken to be -1.

seen in the plots shown in Fig.(5.9) that ΛCDM follows a straight path having Ω_m^0 as slope, we can also see that at $x = z + 1 = 1 \implies$ at $z = 0$ all the three curves meet at a single point $h(x) = H(x)/H_0$. $Om(z)$ shows consistent results and differentiates all the three classes of scalar field from ΛCDM.

Plots shown in Fig.(5.8) depict the variation of Hubble parameter squared $H^2(z)$ versus cube of redshift parameter $x^3 = (1+z)^3$ for our proposed generalized form of Lagrangian having different DE models in a single frame. The cosmological (constant green solid line) serves as a baseline where phantom scalar field (blue dashed line) exhibits faster expansion consistent with its repulsive nature while quintessence (black dotted line) diverges slightly slower at higher redshifts $x^3 < 1$ highlighting how this generalized Lagrangian can show smooth transitions between different DE models through a single framework.

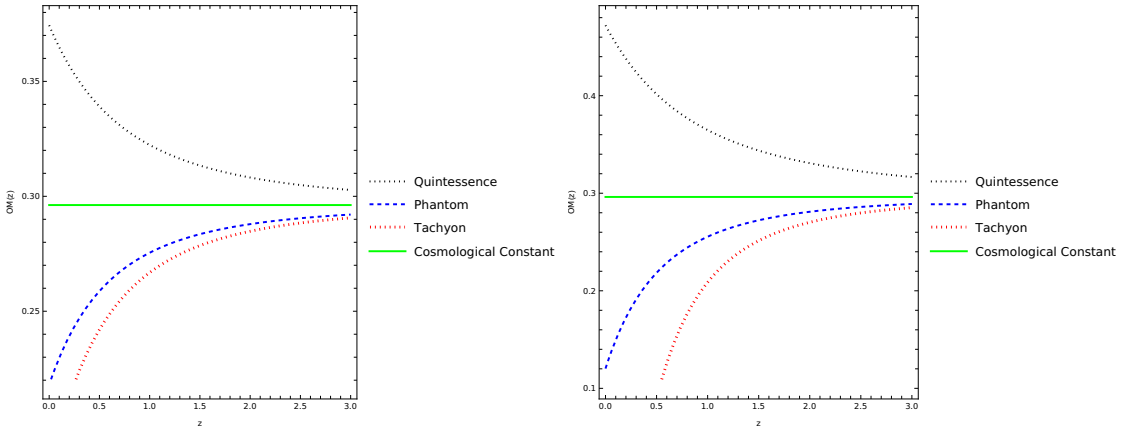

FIGURE 5.9: The plot shows the $Om(z)$ diagnostic of our generalized model, differentiating dynamic DE models from ΛCDM. Plot on the left the values of parameter (ϵ) for Quintessence (black-dotted) and Tachyon(red-dotted) is taken to be $\epsilon = 0.1$, $\epsilon = -0.1$ for Phantom (blue-dashed) and $\epsilon = 0$ for Cosmological constant(green-solid) and the graph on the right is for Quintessence and Tachyon with $\epsilon = 0.2$, Phantom with $\epsilon = -0.2$ and Cosmological constant with $\epsilon = 0$ here w_0 is taken to be -1.

Plots in Fig.(5.9) show that cosmological constant remains static around $\Omega_m^0 \sim 0.2962$ confirming the constant nature of cosmological constant while quintessence, phantom and tachyon shows variation in $Om(z)$ parameter with respect to redshift reflecting their accelerated expansion rate demonstrating time varying EoS. There finding emphasizes the utility of $Om(z)$ diagnostics in distinguishing between DE models and demonstrates just by changing the parameters α and β generalized model can easily transition between quintessence, phantom and tachyon.

Fig: (5.10) shows how the behavior of generalized scalar field model is affected by

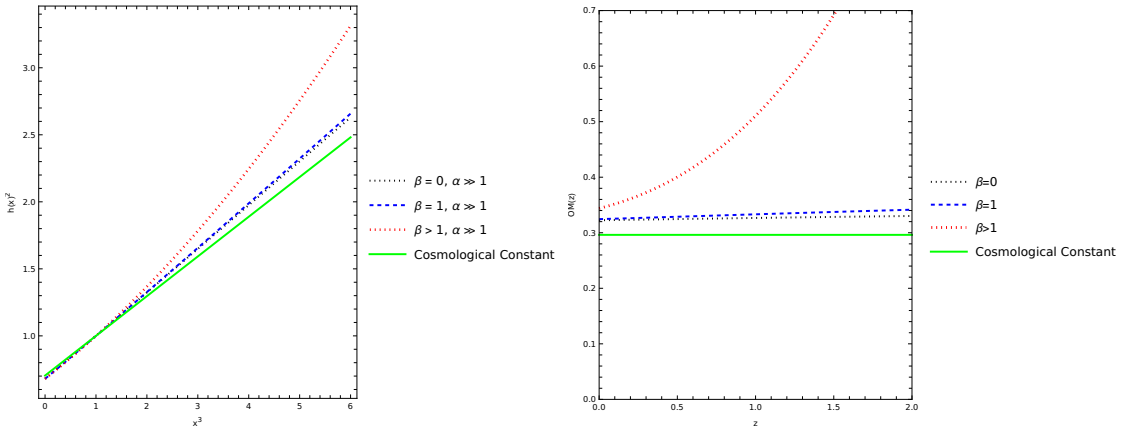

FIGURE 5.10: The plot shows the $Om(z)$ diagnostic of our generalized model, differentiating dynamic DE models from ΛCDM. Plot on the left shows the variation of $H^2(x)$ vs x^3 for $\alpha >> 1$ and for the three cases of parameter β. While plot of the right shows the $Om(z)$ diagnostics for the same cases with $\alpha >> 1$

the choice of parameter β with $\alpha >> 1$. Specifically, for $\beta \sim 0$ and $\alpha >> 1$ case we can say, generalized model mimics cosmological constant behavior and as β increases, curves start deviating away from cosmological constant. The plot on the right side shows the $Om(z)$ diagnostics and as $\beta = 0$ and $\beta = 1$ case aligns with cosmological constant.

5.5 Fifth Interaction via Coupling in Dark Sector:

In the standard cosmological framework, DE and DM are typically treated as independent components that influence the expansion of the universe only through gravity. However, this assumption may be an oversimplification of the true nature of the dark sector. From both theoretical and observational perspectives, there could be a possibility that DE, especially when modeled as a dynamical scalar field, could possibly interact with DM. This interaction can manifest as an additional, non-gravitational force—commonly referred to as the *fifth interaction*.

The concept of a fifth interaction arises naturally in various extensions of general relativity and high-energy physics, including scalar-tensor theories, extra-dimensional models, and string-inspired frameworks. When a scalar field couples to the matter content of the universe, it mediates a force distinct from the four known fundamental interactions: gravitational, electromagnetic, strong, and weak. This additional interaction can modify the cosmic expansion and structure formation, potentially offering new insights into the late-time accelerated expansion of the universe or even providing a more unified understanding of DE and dark matter.

In the context of our generalized Lagrangian framework previously shown to encompass quintessence-, phantom-, and tachyon-like behaviors within a single scalar field model—it is both natural and theoretically motivated to consider a direct coupling within the components of the scalar field itself. Rather than introducing an external matter component, so in this section we will explore the possibility of an internal interaction between the kinetic and potential contributions of the field. To model this, Let's introduce a phenomenological coupling term of the form:

$$Q = 3H\gamma(\rho_X + \rho_V),$$

where Q represents the interaction term, H is the Hubble parameter, γ is a dimensionless coupling constant characterizing the strength of the interaction, and ρ_X and ρ_V are the energy densities corresponding to the kinetic and potential parts of the generalized scalar field, respectively.

This interaction enables a dynamical exchange of energy within the scalar field framework, modifying the background evolution of the universe. Depending on the sign of γ, energy can flow from the kinetic component to the potential component, or vice versa. Such a mechanism may help address cosmological challenges, such as the "coincidence problem," by allowing the effective equation of state to evolve in a way that adjusts the balance between the components dynamically.

Furthermore, the presence of a fifth interaction can lead to observable effects in the cosmic expansion history and structure formation. These include deviations from the standard Hubble evolution, changes in the growth rate of density perturbations, and time-dependent behavior of the effective DE equation of state.

In this chapter, we extend our previously developed non-interacting scalar field model by incorporating this internal coupling with the aim to study its consequences on the cosmological background and assess its viability through suitable diagnostics and observational constraints. As discussed in Chapter 3, introducing a coupling term in the continuity equation leads to local non-conservation of energy, although the total energy-momentum remains conserved globally. Motivated by this, Let's now proceed by assuming a coupling of the form:

$$Q = 3H\gamma(\rho_X + \rho_V),$$

and analyze its impact on the cosmological dynamics within our generalized scalar field framework:

$$\dot{\rho_X} + 3H\rho_X(1 + w_X) = Q_1 \tag{5.28a}$$

$$\dot{\rho_V} + 3H\rho_V(1 + w_V) = -Q_2 \tag{5.28b}$$

$$\dot{\rho_{XV}} + 3H\rho_{XV}(1 + w_{XV}) = Q_2 - Q_1 \tag{5.28c}$$

which is conserved globally as:

$$\dot{\rho_\phi} + 3H\rho_\phi(1 + w_\phi) = Q_1 - Q_2 + Q_2 - Q_1 = 0 \tag{5.29}$$

Here, the coupling under consideration is :

$$Q = 3H\gamma(\rho_X + \rho_V) \tag{5.30}$$

where, we have

$$Q_1 = 3H\gamma\rho_X \tag{5.31a}$$

and

$$Q_2 = 3H\gamma\rho_V \tag{5.31b}$$

Where, $Q = Q_1 + Q_2$ is the phenomenological coupling parameter under consideration. Now, as we did before our next task is to calculate the scaling solutions.

- Scaling solution of kinetic term i.e. Eq. (5.28a):

$$\frac{\dot{\rho}_X}{\rho_X} = -3(1 + w_X - \gamma)\frac{\dot{a}}{a}$$

  which on solving comes out to be:

$$\rho_X = \rho_X^0 \left(\frac{a}{a_0}\right)^{(-3(1+w_X-\gamma))} = \rho_X^0 \, (1+z)^{(-3(1+w_X-\gamma))} \tag{5.32}$$

- Scaling solution of potential term i.e. Eq. (5.28b):

$$\frac{\dot{\rho}_V}{\rho_V} = -3(1 + w_V + \gamma)\frac{\dot{a}}{a}$$

  which on solving comes out to be:

$$\rho_V = \rho_V^0 \left(\frac{a}{a_0}\right)^{(-3(1+w_X+\gamma))} = \rho_V^0 \, (1+z)^{(-3(1+w_X+\gamma))} \tag{5.33}$$

- Scaling solution of mixed term i.e. Eq. (5.28c):

$$\dot{\rho}_{XV} + 3H(1+w_{XV})\rho_{XV} = 3H\gamma \left(\rho_V^0 \left(\frac{a}{a_0}\right)^{(-3(1+w_X+\gamma))} - \rho_X^0 \left(\frac{a}{a_0}\right)^{(-3(1+w_X-\gamma))}\right)$$

which we can easily solve using linear differential equation and the solution is:

$$\rho_{XV} = \rho^0_{XV}\left(\frac{a}{a_0}\right)^{-3(1+w_{XV})} + \frac{\gamma\rho^0_V}{(w_V - w_{XV} + \gamma)}\left[\left(\frac{a}{a_0}\right)^{-3(1+w_{XV})} - \left(\frac{a}{a_0}\right)^{-3(1+w_V+\gamma)}\right] + \frac{\gamma\rho^0_X}{(w_V - w_{XV} - \gamma)}\left[\left(\frac{a}{a_0}\right)^{-3(1+w_{XV}-\gamma)} - \left(\frac{a}{a_0}\right)^{-3(1+w_{XV})}\right] \tag{5.34}$$

In terms of energy density parameter the above equations can be rewritten as:

$$\Omega_X = \Omega^0_X\,(1+z)^{3(1+w_X-\gamma)} \tag{5.35a}$$

$$\Omega_V = \Omega^0_V\,(1+z)^{3(1+w_X+\gamma)} \tag{5.35b}$$

$$\Omega_{XV} = \Omega^0_{XV}\,(1+z)^{3(1+w_{XV})} + \frac{\gamma\Omega^0_V}{(w_V - w_{XV} + \gamma)}\left[(1+z)^{3(1+w_{XV})} - (1+z)^{3(1+w_V+\gamma)}\right] + \frac{\gamma\Omega^0_X}{(w_X - w_{XV} - \gamma)}\left[(1+z)^{3(1+w_{XV}-\gamma)} - (1+z)^{3(1+w_{XV})}\right] \tag{5.35c}$$

5.6 Fifth Interaction from Energy-Momentum Transfer

In this section, we are going to derive the expression for the fifth interaction acting on each component of the generalized scalar field system due to energy-momentum exchange which we assumed is due to the mixed term. The interaction between sub-components of the scalar field leads to non-conservation of individual energy-momentum tensors, while the total energy-momentum remains conserved.

So, here as we have considered in last section; the three interacting components of the scalar field: ϕ_X, ϕ_V, and ϕ_{XV}, each described by a perfect fluid energy-momentum tensor:

$$T^{\mu\nu}_{(i)} = (\rho_i + p_i)U^\mu U^\nu + p_i g^{\mu\nu}, \quad i = X, V. \tag{5.36}$$

The energy-momentum transfer between components is encoded via the covariant conservation equations as:

$$\nabla_\mu T^{\mu\nu}_{(X)} = Q^\nu_1, \tag{5.37}$$

$$\nabla_\mu T^{\mu\nu}_{(V)} = Q^\nu_2, \tag{5.38}$$

$$\nabla_\mu T^{\mu\nu}_{(XV)} = (Q_2 - Q_1)^\nu, \tag{5.39}$$

such that the total conservation condition is satisfied:

$$\nabla_\mu T^{\mu\nu}_{\phi} = \nabla_\mu \left(T^{\mu\nu}_{(X)} + T^{\mu\nu}_{(V)} + T^{\mu\nu}_{(XV)} \right) = 0. \tag{5.40}$$

As we have defined earlier the interaction terms as:

$$Q_1 = 3H\gamma\rho_X, \tag{5.41}$$

$$Q_2 = 3H\gamma\rho_V, \tag{5.42}$$

$$Q = Q_1 + Q_2 = 3H\gamma(\rho_X + \rho_V). \tag{5.43}$$

In order to derive the fifth interaction acting on each component, the covariant derivative of the energy-momentum tensor is found to be:

$$\begin{aligned}
\nabla_\mu T^{\mu\nu}_i =& \nabla_\mu[(\rho_i + p_i)U^\mu U^\nu + p_i g^{\mu\nu}] \\
\equiv& U^\nu[(\rho_i + p_i)\nabla_\mu U^\mu + U^\mu \nabla_\mu(\rho_i + p_i)] + (\rho_i + p_i)U^\mu \nabla_\mu U^\nu + \nabla^\nu p_i \\
\equiv& U^\nu[(\rho_i + p_i)\nabla_\mu U^\mu + U^\mu \nabla_\mu(\rho_i + p_i)] + (\rho_i + p_i)a^\nu + \nabla^\nu p_i
\end{aligned} \tag{5.44}$$

where $U^\nu \nabla_\nu U^\mu = a^\mu$ is the four-acceleration. In relativistic fluid dynamics, the covariant conservation of the energy-momentum tensor,$\nabla_\mu T^{\mu\nu} = Q^\nu$, contains both temporal and spatial components. In order to isolate the spatial acceleration due to pressure gradients or interaction forces, we are required to project this equation orthogonally to the fluid

4-velocity U^μ, which can be achieved using the projection tensor[1]:

$$h^{\mu\nu} = g^{\mu\nu} + U^\mu U^\nu \tag{5.45}$$

which satisfies $h^{\mu\nu}U_\nu = 0$ and acts as a metric on the 3-space orthogonal to U^μ. Now, by applying $h^\mu{}_\nu$ to the conservation equation Eq.(5.44), we can remove the energy-flow terms and yields an expression for the 4-acceleration:

$$h^\mu{}_\nu \nabla_\sigma T^{\sigma\nu}_{(i)} = Q^\mu_i \tag{5.46}$$

where $a^\mu = U^\nu \nabla_\nu U^\mu$ is the fluid's 4-acceleration and $Q^\mu_\perp = h^\mu{}_\nu Q^\nu$ is the spatial interaction force, often referred to as the unknown fifth interaction between dark sector and after projection this energy exchange leads to deviations from geodesic motion. Lets discuss in more details; so the projected divergence using Eq.(5.44) and Eq.(5.45) yields:

$$h^\mu{}_\nu \nabla_\sigma T^{\sigma\nu}_{(i)} = h^\mu{}_\nu \left[U^\nu((\rho_i + p_i)\nabla_\mu U^\mu + U^\mu \nabla_\mu(\rho_i + p_i)) + (\rho_i + p_i)a^\nu + \nabla^\nu p_i\right] \tag{5.47}$$

As mentioned earlier the projection operator $h^{\mu\nu}$ is orthogonal to the four-velocity U^μ of a fluid element. By definition, this orthogonality implies $h^{\mu\nu}U_\nu = 0$, ensuring that any quantity projected using $h^{\mu\nu}$ lies entirely within the spatial hypersurface orthogonal to U^μ, i.e., the local rest frame of the fluid. Using this condition, the equation governing the conservation of energy-momentum for a specific component of the cosmic fluid (in our case X and V, indexed by i) can be projected onto the spatial hypersurface to give:

$$(\rho_i + p_i)a^\mu + h^{\mu\nu}\nabla_\nu p_i = Q^\mu_i \tag{5.48}$$

where:

- ρ_i and p_i are the energy density and pressure of the component $i = X, V$ with XV acting as some interaction between kinetic and potential term.
- $a^\mu = U^\nu \nabla_\nu U^\mu$ is the four-acceleration of the fluid element.

[1]The use of projection tensors is standard in relativistic hydrodynamics and cosmological scalar field dynamics. It has been employed in several works on interacting DE and fifth force scenarios [157–159]. A detailed application to interacting scalar field-fluid models was presented in [107], where the fifth interaction is derived from a variational principle involving coupling to a scalar field. These frameworks all rely critically on the projection tensor to properly separate energy conservation (timelike) and momentum dynamics (spacelike) in curved spacetime.

- Q_i^μ represents the interaction four-vector describing the exchange of energy and momentum with other components.
- and $h^{\mu\nu}\nabla_\nu p_i$ denotes the projected pressure gradient orthogonal to the flow.

Rearranging this equation, we isolate the four-acceleration to determine the effective fifth interaction per unit mass experienced by the component due to the mixed term:

$$f_i^\mu \equiv a^\mu = \frac{1}{\rho_i + p_i}\left(Q_i^\mu - h^{\mu\nu}\nabla_\nu p_i\right) \tag{5.49}$$

This expression reveals that the fifth interaction emerges from both the non-conservation of energy-momentum (encoded in Q_i^μ) and the spatial variation of pressure. The structure of this fifth interaction shows that it is non-gravitational in nature and dependent on the underlying interaction. In the absence of such interactions or pressure gradients, this fifth interaction vanishes, and the fluid element follows geodesic motion as expected in standard general relativity. In the next step, lets proceed to substitute explicit forms for the interaction terms to explore different physical implications and how they influence cosmic evolution through the fifth interaction. So, on substituting the interaction terms we get:

- For the kinetic component of generalized scalar field (say ϕ_X):

$$f_X^\mu \equiv \frac{1}{\rho_X + p_X}\left(3H\gamma\rho_X U^\mu - h^{\mu\nu}\nabla_\nu p_X\right). \tag{5.50}$$

- For the potential component of generalized scalar field (say ϕ_V):

$$f_V^\mu \equiv \frac{1}{\rho_V + p_V}\left(3H\gamma\rho_V U^\mu - h^{\mu\nu}\nabla_\nu p_V\right). \tag{5.51}$$

These expressions could quantify the nature of the fifth interaction acting on each component of the generalized scalar field, arising from both interaction-induced momentum exchange and the spatial variation of pressure. In the above formulation, the interaction terms $Q_X^\mu = 3H\gamma\rho_X U^\mu$ and $Q_V^\mu = 3H\gamma\rho_V U^\mu$ have been substituted into Eq. (5.46) for the kinetic and potential parts of the field, respectively. The resulting fifth interaction f_X^μ and f_V^μ represent the specific acceleration each component experiences due to the coupling.

Physically, the fifth interaction can be interpreted as a non-gravitational, interaction-driven correction to the geodesic motion of the scalar field components. It alters the trajectory of the field fluid in spacetime, and thus has a direct impact on the evolution of the universe's large-scale structure. Notably, this fifth interaction is orthogonal to the four-velocity, as enforced by the projection operator, ensuring that it contributes only to the spatial (non timelike) evolution in the fluid's rest frame.

The relative significance of this interaction varies over cosmic time, depending on which component i.e. kinetic (ϕ_X) or potential (ϕ_V) is dynamically dominant. For instance, may be during early epochs when the kinetic term dominates the f^μ_X could primarily dictate the dynamics. At late times, when the potential energy takes over, f^μ_V could show the more relevant contribution. This transition could have important implications for the effective equation of state of the scalar field, potentially leading to behaviors that mimic DE, dark matter, or maybe even more exotic cosmologies.

By studying these fifth interaction contributions individually, one can gain insights into the role of internal field dynamics in shaping cosmic acceleration, offering a richer framework than models with purely gravitational interactions. The precise nature and fundamental characteristics of this interaction within the dark sector remain among the most intriguing and unresolved problems in modern cosmology. While it is well established that DE and dark matter govern the dynamics of the universe on large scales, the possibility that these two components may interact beyond gravitational coupling opens up new avenues for theoretical and observational investigation. Such interactions could manifest as deviations from geodesic motion (as we have seen in this section), non-conservation of individual energy-momentum tensors or altered growth rates of cosmic structures. Despite various phenomenological models and preliminary constraints, the physical origin, strength, and evolution of this interaction remain largely speculative. A deeper understanding of this interaction not only has the potential to shed light on the fundamental nature of the dark sector but may also provide critical insights into the late-time acceleration of the universe and the resolution of tensions between different cosmological components.

5.7 Conclusion:

In this study, we have developed a novel generalized Lagrangian framework that unifies three distinct scalar field models Quintessence, Tachyon, and Phantom through a parameterized approach using two key constants, α and β. Specifically, the combinations $(\alpha = 1, \beta = 0)$, $(\alpha = -1, \beta = 0)$, and $(\alpha = 0, \beta = 1)$ reproduce the dynamics of Quintessence, Phantom, and Tachyon fields, respectively The proposed Lagrangian, motivated by effective field theories and non-canonical models, contains two parameters, α and β, enabling the scalar field to exhibit the behavior of a three-component fluid model.

A key finding is the Lagrangian's ability to encapsulate these scalar fields as a three-component fluid system, comprising a kinetic term (Ω_X), a potential term (Ω_V), and a mixed term (Ω_{XV}), which we have decomposed by expanding $(1-X^2)^{\beta/2}$ using Taylor's expansion which leads to a constraint $0 < \dot{\phi}^2 << 1$. This decomposition provides a versatile tool for interpreting the interplay between dark energy and dark matter across cosmic evolution where potential component act as dark energy with EoS $w_V \approx -1$ and for $\alpha > 1$ kinetic term behaves as matter with EoS $w_X \approx 0$. We have used preliminary observational constraints using DESI+BBN [5]. The potential term consistently exhibits dark energy-like behavior, while the kinetic term behaves as dark matter for the case only when $\alpha > 1$. Future work will extend this analysis to additional scalar field models, observational constraints and perturbation dynamics.

Our analysis reveals that the potential term consistently exhibits DE-like behavior with an equation of state (EoS) $w_V = -1$, irrespective of α and β, aligning with the cosmological constant in the simplest scenarios. Conversely, the kinetic term demonstrates remarkable flexibility: for large α $(\alpha \gg 1)$, it mimics dark matter with $w_X \to 0$, while at $\alpha = \pm 1$, it transitions to stiff matter with $w_X = 1$.

The $Om(z)$ diagnostic analysis further underscores the model's robustness, effectively distinguishing the evolutionary trajectories of Quintessence, Phantom, and Tachyon from the static ΛCDM baseline. This diagnostic highlights the smooth transitions between these scalar field behaviors, achievable solely through adjustments to α and β,

demonstrating the framework's phenomenological richness. Preliminary constraints using DESI+BBN [5] and Planck data [1, 2, 13] data affirm the model's observational viability, while stability conditions ensure its physical consistency across parameter regimes.

The $O_m(z)$ diagnostic analysis further underscores the model's robustness, effectively distinguishing the evolutionary trajectories of Quintessence, Phantom, and Tachyon from the static ΛCDM baseline. This diagnostic highlights the transitions (at $x^3 \approx 1$ see Fig.(5.8)) between these scalar field behaviors, achievable solely through adjustments to α and β, demonstrating the framework's phenomenological richness. Preliminary constraints using DESI+BBN [5] and Planck data [1, 2, 13] data affirm the model's observational viability.

A notable feature of this model is the emergence of an effective interaction within the dark sector, manifesting as an additional acceleration term in the fluid's dynamical equations. This interaction, derived from projecting the energy-momentum conservation equation orthogonal to the fluid four-velocity, encapsulates the momentum exchange between components without invoking external forces. The resulting interaction term depends on both the energy exchange vector Q^μ and the projected pressure gradients $h^{\mu\nu}\nabla_\nu p$, and its magnitude varies depending on the dominance of the kinetic or potential field components. This interaction modifies the standard geodesic motion, introducing corrections that are purely internal to the field dynamics. Importantly, it becomes a significant driver of cosmic acceleration in epochs where the mixed term is active, enriching the model's capacity to describe transitions between different phases of cosmic expansion.

Although this work does not propose a dynamical unification in the traditional sense, it establishes a cohesive mathematical scaffold that elucidates the shared structural properties of these scalar fields. This reformulation enhances the understanding of their mutual interactions and sets a foundation for deeper exploration of their cosmological implications and fifth interaction in dark sector. Looking ahead, the model can be refined more by incorporating additional scalar field variants, conducting comprehensive observational tests with datasets such as DESI, supernovae Type Ia, cosmic microwave background, large-scale structure surveys and performing detailed perturbation analyses. These efforts will further elucidate the interaction dynamics of the mixed term, the observational signatures of the mixed term's coupling effects and solidify the model's

predictive power potentially offering new insights into the nature of DE and DM in the universe.

Chapter 6

Conclusion

Over the past few decades, the nature of DE and its role in cosmic evolution has emerged as one of the most compelling mysteries in cosmology. Motivated by the remarkable discovery that our universe is not only expanding but accelerating in its expansion, this thesis set out to explore both interacting and non-interacting models of DE within scalar field frameworks. Through a detailed and multi-faceted investigation, we have developed and analyzed models that not only conform to current observations but also provide novel theoretical insights into how the dark sector might behave—particularly around the cosmologically significant epoch known as the inflection point.

In the first major part of this study, we investigated canonical scalar field models, primarily focusing on quintessence, wherein a slowly evolving scalar field rolls down its potential and mimics the negative pressure required to drive cosmic acceleration. By introducing interaction terms between the scalar field and the dark matter component, we studied two specific forms of coupling: one proportional to the Hubble parameter and matter density ($Q = 3H\alpha\rho_m$), and another involving the time derivative of matter density ($Q = 3\beta\dot{\rho}_m$). These forms were not chosen arbitrarily but were inspired by both phenomenological relevance and theoretical consistency. Through analytical derivations and numerical simulations, it was shown that these couplings significantly affect the dynamics of the scalar field near the inflection point, the transitional era where cosmic deceleration gives way to acceleration.

The analysis revealed that the sign and magnitude of the coupling parameters determine the direction of energy flow between DE and dark matter. In cases of negative coupling,

energy is transferred from dark matter to DE, potentially alleviating the coincidence problem by allowing both components to evolve in a correlated manner. Conversely, a positive coupling leads to energy flow in the opposite direction, impacting the effective equation of state and background evolution. Importantly, these models were found to admit stable attractor solutions and remained consistent with present-day observations of density parameters and Hubble evolution.

The second major part of the thesis turned to a non-canonical scalar field model: the tachyon field, which originates from string theory and presents a different dynamical structure due to its Born–Infeld-type action. Here, we explored scenarios without direct coupling to matter, thus allowing a clean investigation of the field's intrinsic dynamics. Using different functional forms of the scale factor including power-law, exponential and hybrid models—we examined the tachyon field's behavior near the inflection point and found it capable of producing stable, accelerating solutions. Phase-space analysis showed that the system admits critical points corresponding to accelerated expansion, and the position and stability of these points depend sensitively on the model parameters. The findings reinforce the tachyon field's role as a viable DE candidate even in the absence of interaction.

Perhaps the most innovative and integrative part of this thesis lies in the formulation of a generalized scalar field model that unifies multiple scalar field theories quintessence, phantom, and tachyon—into a single Lagrangian framework. By introducing two real parameters, α and β, we created a flexible Lagrangian capable of interpolating between different dynamical behaviors. This generalization not only simplifies the comparison between models but also reveals new intermediate behaviors, especially near the inflection point, where the expansion history of the universe undergoes qualitative changes.

One of the most intriguing outcomes of this general framework is the theoretical proposal of a fifth fundamental interaction, mediated through the coupling between DE and dark matter. By carefully analyzing the energy momentum tensor and incorporating a non-zero covariant divergence, we identified terms that naturally give rise to a fifth interaction within the dark sector. This force is neither electromagnetic, gravitational, weak, nor strong—but a consequence of scalar field dynamics in an interacting DE model. The fifth interaction emerges as a dynamical correction to particle motion, altering geodesics and potentially modifying the growth of cosmic structures. These findings hint at the

possibility that the dark sector is governed by its own set of fundamental interactions an idea that, if verified observationally, would mark a paradigm shift in our understanding of nature.

Furthermore, we employed model independent diagnostics such as the $Om(z)$ analysis to distinguish the behavior of our generalized model from the standard ΛCDM cosmology. The results showed deviations that are both physically meaningful and within observational bounds, demonstrating that the proposed models are not only theoretically consistent but also observationally viable. In summary, the key contributions of this thesis can be outlined as follows:

- A detailed analysis of interacting quintessence models was carried out near the cosmic inflection point, offering new insights into how energy exchange between DE and DM affects cosmic dynamics.
- The study of non-interacting tachyonic scalar fields revealed that even in isolation, DE can drive late-time acceleration and admit stable solutions under diverse expansion histories.
- A generalized scalar field Lagrangian was proposed that unifies quintessence, tachyon, and phantom behaviors within a single framework, enhancing our ability to model diverse cosmological phenomena.
- The concept of a fifth fundamental interaction arising from DE-DM interaction was introduced and theoretically justified using the energy-momentum transfer formalism.
- Compatibility of the proposed models with current observational data was demonstrated through diagnostic tools and numerical simulations, reinforcing their potential relevance in explaining the universe's accelerating expansion.

This work not only enriches the theoretical landscape of scalar field cosmology but also opens new directions for research into fundamental interactions in the universe. As observational data from next-generation surveys (such as LSST, Euclid, and future DESI releases) become available, the predictions made in this thesis may be tested with greater precision. It is hoped that the theoretical frameworks and insights developed

here will contribute meaningfully to the continued pursuit of one of the most profound questions in science: What is the true nature of the dark sector in our universe?

Chapter 7

Future Plan

Building my thesis "A Theoretical Analysis of Interacting and Non-Interacting Dark Energy," which explores dark enery (DE) and dark matter (DM) interactions. My future directions of work are for investigating quantum effects of DE focus on integrating quantum gravity frameworks such as the Generalized Uncertainty Principle (GUP), Extended Generalized Uncertainty Principle (EGUP), Causal Set Theory, Loop Quantum Gravity (LQG), and other approaches. In what follows next, we will list out some of these possible paths where we can carry out our future work.

- Investigate how GUP, which introduces a minimal length scale, modifies the dynamics of DE fields (e.g., quintessence or unparticle DE) in interacting DE-DM scenarios.
- Explore the *Extended Generalized Uncertainty Principle (EGUP)*, which includes linear and quadratic momentum terms, to model quantum gravitational effects on DE in higher-dimensional or braneworld scenarios, extending the thesis's tachyon field analysis.
- Study DE dynamics in Causal Set Theory, a quantum gravity approach where spacetime is a discrete, partially ordered set, to explore quantum fluctuations affecting DE-DM interactions.
- Formulate an effective field theory for the DE-DM fifth force and test signatures in modified gravity or equivalence principle experiments.

- Analyze DE dynamics in LQG, where spacetime is quantized into spin networks, to understand how quantum geometry affects interacting DE-DM models and the proposed fifth force.

- Investigate quantum gravitational effects on DE using holographic principles (e.g., AdS/CFT) or string theory, connecting to the thesis's tachyon field and unified dark sector frameworks.

Bibliography

[1] S. Perlmutter et al. Discovery of a supernova explosion at half the age of the universe. *Nature*, 391:51–54, 1998. URL https://www.nature.com/articles/34124.

[2] S. Perlmutter et al. Measurements of Ω and Λ from 42 high-redshift supernovae. *The Astrophysical Journal*, 517(2):565–586, 1999. URL https://ui.adsabs.harvard.edu/abs/1999ApJ...517..565P.

[3] A. G. Riess et al. Observational evidence from supernovae for an accelerating universe and a cosmological constant. *The Astronomical Journal*, 116(3):1009, 1998. URL https://dx.doi.org/10.1086/300499.

[4] F. Zwicky. The redshift of extragalactic nebulae. *Helvetica Physica Acta*, 6:110–127, 1933. URL https://ui.adsabs.harvard.edu/abs/1933AcHPh...6..110Z.

[5] A. G. Adame et al. Desi 2024 vi: cosmological constraints from the measurements of baryon acoustic oscillations. *Journal of Cosmology and Astroparticle Physics*, 2025(2):021, 2025. URL https://ui.adsabs.harvard.edu/abs/2025JCAP...02..021A.

[6] E. Hubble. A relation between distance and radial velocity among extra-galactic nebulae. *Proceedings of the national academy of sciences*, 15(3):168–173, 1929.

[7] J. V. Narlikar. An introduction to cosmology. 2002. URL https://ui.adsabs.harvard.edu/abs/2002itc..book.....N.

[8] L. Amendola and S. Tsujikawa. Dark Energy: Theory and Observations. 2010. URL https://ui.adsabs.harvard.edu/abs/2010deto.book.....A.

[9] D. W. Hogg. Distance measures in cosmology. 2000. URL https://arxiv.org/abs/astro-ph/9905116.

[10] A. V. Filippenko and A. G. Riess. Results from the High-z Supernova Search Team. *Physics Reports*, 307:31–44, 1998. URL https://ui.adsabs.harvard.edu/abs/1998PhR...307...31F.

[11] J. L. Tonry et al. Cosmological Results from High-z Supernovae. *The Astrophysical Journal*, 594(1):1–24, 2003. URL https://ui.adsabs.harvard.edu/abs/2003ApJ...594....1T.

[12] G. Hinshaw et al. Nine-year wilkinson microwave anisotropy probe (wmap) observations: Cosmological parameter results. *The Astrophysical Journal Supplement Series*, 208(2):19, 2013. URL https://ui.adsabs.harvard.edu/abs/2013ApJS..208...19H.

[13] N. Aghanim et al. and Planck Collaboration. Planck 2018 results. vi. cosmological parameters. *Astron. Astrophys*, 641:A6, 2020. URL https://ui.adsabs.harvard.edu/abs/2020A&A...641A...6P.

[14] S. Dodelson and L. Knox. Dark energy and the cosmic microwave background radiation. *Physical Review Letters*, 84(16):3523, 2000. URL https://arxiv.org/pdf/1309.5386.

[15] B. Novosyadlyj et al. Dark energy: observational evidence and theoretical models. *arXiv preprint arXiv:1502.04177*, 2015.

[16] S. Alam et al. The clustering of galaxies in the completed sdss-iii baryon oscillation spectroscopic survey: cosmological analysis of the dr12 galaxy sample. *Monthly Notices of the Royal Astronomical Society*, 470(3):2617–2652, 2017. URL https://academic.oup.com/mnras/article-pdf/470/3/2617/18315003/stx721.pdf.

[17] F. Beutler et al. The 6df galaxy survey: baryon acoustic oscillations and the local hubble constant. *Monthly Notices of the Royal Astronomical Society*, 416(4):3017–3032, 2011. URL https://academic.oup.com/mnras/article-pdf/416/4/3017/2985042/mnras0416-3017.pdf.

[18] D. Wang. The self-consistency of desi analysis and comment on" does desi 2024 confirm Λcdm?". *arXiv preprint arXiv:2404.13833*, 2024. URL https://arxiv.org/pdf/2404.13833.

[19] C. G. Park et al. Using non-desi data to confirm and strengthen the desi 2024 spatially flat w_0w_acdm cosmological parametrization result. *Physical Review D*, 110(12):123533, 2024. URL https://arxiv.org/pdf/2405.00502.

[20] Y. Carloni, O. Luongo, and M. Muccino. Does dark energy really revive using desi 2024 data? *Physical Review D*, 111(2):023512, 2025. URL https://arxiv.org/pdf/2404.12068.

[21] K Lodha et al. Desi 2024: Constraints on physics-focused aspects of dark energy using desi dr1 bao data. *Physical Review D*, 111(2):023532, 2025. URL https://arxiv.org/pdf/2405.13588.

[22] R Calderon et al. Desi 2024: reconstructing dark energy using crossing statistics with desi dr1 bao data. *Journal of Cosmology and Astroparticle Physics*, 2024(10): 048, 2024. URL https://arxiv.org/pdf/2405.04216.

[23] Y. Yang et al. Quintom cosmology and modified gravity after desi 2024. 69(17): 2698–2704, 2024. URL https://arxiv.org/pdf/2404.19437.

[24] A. Einstein. On the cosmological problem of general relativity. 1931.

[25] S. M. Carroll. The cosmological constant. *Living Reviews in Relativity*, 4(1):1, 2001. URL https://ui.adsabs.harvard.edu/abs/2001LRR.....4....1C.

[26] P J. E Peebles and B. Ratra. The cosmological constant and dark energy. *Reviews of modern physics*, 75(2):559, 2003. URL https://link.aps.org/pdf/10.1103/RevModPhys.75.559.

[27] S. Weinberg. The cosmological constant problem. *Reviews of Modern Physics*, 61 (1):1–23, 1989. URL https://ui.adsabs.harvard.edu/abs/1989RvMP...61...1W.

[28] H. E. S. Velten, R. F. Vom Marttens, and W. Zimdahl. Aspects of the cosmological "coincidence problem". *European Physical Journal C*, 74:3160, 2014. URL https://ui.adsabs.harvard.edu/abs/2014EPJC...74.3160V.

[29] J. Martin. Quintessence: A Mini-Review. *Modern Physics Letters A*, 23(17-20): 1252–1265, 2008. URL https://ui.adsabs.harvard.edu/abs/2008MPLA...23.1252M.

[30] N. Roy and N. Banerjee. Quintessence scalar field: A dynamical systems study. *European Physical Journal Plus*, 129(8):162, 2014. URL https://ui.adsabs.harvard.edu/abs/2014EPJP..129..162R.

[31] S. Tsujikawa. Quintessence: a review. *Classical and Quantum Gravity*, 30 (21):214003, 2013. URL https://ui.adsabs.harvard.edu/abs/2013CQGra..30u4003T.

[32] E. V Linder. The dynamics of quintessence, the quintessence of dynamics. *General Relativity and Gravitation*, 40:329–356, 2008. URL https://arxiv.org/pdf/0704.2064.

[33] M Khurshudyan et al. An effective quintessence field with a power-law potential. *Astrophysics and Space Science*, 356:383–391, 2015. URL https://arxiv.org/pdf/1403.3768.

[34] V. Sahni and A. Starobinsky. The Case for a Positive Cosmological Λ-Term. *International Journal of Modern Physics D*, 9(4):373–443, 2000. URL https://ui.adsabs.harvard.edu/abs/2000IJMPD...9..373S.

[35] T. Chiba, T. Okabe, and M. Yamaguchi. Kinetically driven quintessence. *Physical Review D*, 62(2):023511, 2000. URL https://arxiv.org/pdf/astro-ph/9912463.

[36] J. M. Cline, S. Jeon, and G. D. Moore. The phantom menaced: Constraints on low-energy effective ghosts. *Physical Review D*, 70(4):043543, 2004. URL https://arxiv.org/pdf/hep-ph/0311312.

[37] S. M. Carroll, M. Hoffman, and M. Trodden. Can the dark energy equation-of-state parameter w be less than- 1? *Physical Review D*, 68(2):023509, 2003. URL https://arxiv.org/pdf/astro-ph/0301273.

[38] P. Singh, M. Sami, and N. Dadhich. Cosmological dynamics of a phantom field. *Physical Review D*, 68(2):023522, 2003. URL https://arxiv.org/pdf/hep-th/0305110.

[39] M. Sami and A. Toporensky. Phantom field and the fate of the universe. *Modern Physics Letters A*, 19(20):1509–1517, 2004. URL https://arxiv.org/pdf/gr-qc/0312009.

[40] A. Sen. Tachyon condensation on the brane antibrane system. *Journal of High Energy Physics*, 1998(8):012, 1998. URL https://ui.adsabs.harvard.edu/abs/1998JHEP...08..012S.

[41] L. R. Abramo and F. Finelli. Cosmological dynamics of the tachyon with an inverse power-law potential. *Physics Letters B*, 575(3-4):165–171, 2003. URL https://ui.adsabs.harvard.edu/abs/2003PhLB..575..165A.

[42] V Gorini et al. Tachyons, scalar fields, and cosmology. *Physical Review D*, 69(12):123512, 2004. URL https://ui.adsabs.harvard.edu/abs/2004PhRvD..69l3512G.

[43] E. J. Copeland et al. What is needed of a tachyon if it is to be the dark energy? *Physical Review D*, 71:043003, 2005. URL https://link.aps.org/doi/10.1103/PhysRevD.71.043003.

[44] Y. S. Piao et al. . Non-minimally coupled tachyon and inflation. *Physics Letters B*, 570(1-2):1–4, 2003. URL https://ui.adsabs.harvard.edu/abs/2003PhLB..570....1P.

[45] K. Bamba et al. . Dark energy cosmology: the equivalent description via different theoretical models and cosmography tests. *Astrophysics and Space Science*, 342(1):155–228, 2012. URL https://ui.adsabs.harvard.edu/abs/2012Ap&SS.342..155B.

[46] T. Padmanabhan. Accelerated expansion of the universe driven by tachyonic matter. *Physical Review D*, 66(2):021301, 2002. URL https://ui.adsabs.harvard.edu/abs/2002PhRvD..66b1301P.

[47] A. Sen. Rolling Tachyon. *Journal of High Energy Physics*, 2002(4):048, 2002. URL https://ui.adsabs.harvard.edu/abs/2002JHEP...04..048S.

[48] L. Amendola. Coupled quintessence. *Physical Review D*, 62(4):043511, 2000. URL https://ui.adsabs.harvard.edu/abs/2000PhRvD..62d3511A.

[49] W. Zimdahl et al. Interacting quintessence. *Physics Letters B*, 521(3-4):133–138, 2001. URL https://ui.adsabs.harvard.edu/abs/2001PhLB..521..133Z.

[50] M. Szydłowski, T. Stachowiak, and R. Wojtak. Towards testing interacting cosmology by distant supernovae. *Physical Review D*, 73(6):063516, 2006. URL https://ui.adsabs.harvard.edu/abs/2006PhRvD..73f3516S.

[51] L. P. Chimento. Linear and nonlinear interactions in the dark sector. *Physical Review D*, 81(4):043525, feb 2010. doi: 10.1103/PhysRevD.81.043525. URL https://ui.adsabs.harvard.edu/abs/2010PhRvD..81d3525C.

[52] J. H. He, B. Wang, and P. Zhang. Imprint of the interaction between dark sectors in large scale cosmic microwave background anisotropies. *Physical Review D*, 80(6):063530, 2009. URL https://ui.adsabs.harvard.edu/abs/2009PhRvD..80f3530H.

[53] B. Wang, Y. Gong, and E. Abdalla. Transition of the dark energy equation of state in an interacting holographic dark energy model. *Physics Letters B*, 624(3-4):141–146, 2005. URL https://ui.adsabs.harvard.edu/abs/2005PhLB..624..141W.

[54] S. Del Campo, R. Herrera, and D. Pavón. H(z) Diagnostics on the Nature of Dark Energy. *International Journal of Modern Physics D*, 20(4):561–579, 2011. URL https://ui.adsabs.harvard.edu/abs/2011IJMPD..20..561D.

[55] K. R. Mishra et.al. Cosmological implications of an interacting model of dark matter & dark energy. *Physics of the Dark Universe*, 40:101211, 2023. URL https://arxiv.org/pdf/2301.08743.

[56] J. Kang. Reconstructing a non-linear interaction in the dark sector with cosmological observations. 31:100784, 2021. URL https://ui.adsabs.harvard.edu/abs/2021PDU....3100784K.

[57] M. B. Gavela, D. Hernández, L. Lopez Honorez, O. Mena, and S. Rigolin. Dark coupling. , 2009(7):034, 2009. URL https://ui.adsabs.harvard.edu/abs/2009JCAP...07..034G.

[58] S. Bahamonde et al. Dynamical systems applied to cosmology: Dark energy and modified gravity. *Physics Reports*, 775-777:1–122, 2018. URL https://www.sciencedirect.com/science/article/pii/S0370157318302242.

[59] L. Amendola. Scaling solutions in general nonminimal coupling theories. *Physical Review D*, 60(4):043501, 1999. URL https://journals.aps.org/prd/abstract/10.1103/PhysRevD.60.043501.

[60] A. P. Billyard and A. A. Coley. Interactions in scalar field cosmology. *Physical Review D*, 61(8):083503, 2000. URL https://journals.aps.org/prd/abstract/10.1103/PhysRevD.61.083503.

[61] D. J. Holden and D. Wands. Self-similar cosmological solutions with a non-minimally coupled scalar field. *Physical Review D*, 61(4):043506, 2000. URL https://journals.aps.org/prd/abstract/10.1103/PhysRevD.61.043506.

[62] L. Amendola and D. Tocchini-Valentini. Stationary dark energy: The present universe as a global attractor. *Physical Review D*, 64(4):043509, 2001. URL https://journals.aps.org/prd/abstract/10.1103/PhysRevD.64.043509.

[63] D. Tocchini-Valentini and L. Amendola. Stationary dark energy with a baryon-dominated era: Solving the coincidence problem with a linear coupling. *Physical Review D*, 65(6):063508, 2002. URL https://journals.aps.org/prd/abstract/10.1103/PhysRevD.65.063508.

[64] B. Gumjudpai et al. Coupled dark energy: towards a general description of the dynamics. *Journal of Cosmology and Astroparticle Physics*, 2005(06):007, 2005. URL https://iopscience.iop.org/article/10.1088/1475-7516/2005/06/007/meta.

[65] T. Gonzalez, G. Leon, and I. Quiros. Dynamics of quintessence models of dark energy with exponential coupling to dark matter. *Classical and Quantum Gravity*, 23(9):3165, 2006. URL https://iopscience.iop.org/article/10.1088/0264-9381/23/9/025/meta.

[66] C. G. Boehmer et al. Dynamics of dark energy with a coupling to dark matter. *Physical Review D—Particles, Fields, Gravitation, and Cosmology*, 78(2):023505, 2008. URL https://journals.aps.org/prd/abstract/10.1103/PhysRevD.78.023505.

[67] M. Cicoli, F. G. Pedro, and G. Tasinato. Natural quintessence in string theory. *Journal of Cosmology and Astroparticle Physics*, 2012(07):044, 2012. URL https://iopscience.iop.org/article/10.1088/1475-7516/2012/07/044/meta.

[68] K. Tzanni and J. Miritzis. Coupled quintessence with double exponential potentials. *Physical Review D*, 89(10):103540, 2014. URL https://journals.aps.org/prd/abstract/10.1103/PhysRevD.89.103540.

[69] X. Chen and Y. Gong. Fixed points in interacting dark energy models. *Physics Letters B*, 675(1):9–13, 2009. URL https://www.sciencedirect.com/science/article/pii/S037026930900361X.

[70] D. J. Liu and X. Z. Li. Dynamics of quintessence with thermal interactions. *Physics Letters B*, 611(1-2):8–14, 2005. URL https://www.sciencedirect.com/science/article/pii/S037026930500300X.

[71] J. Mimoso, A. Nunes, and D. Pavón. Asymptotic behavior of the warm inflation scenario with viscous pressure. *Physical Review D—Particles, Fields, Gravitation, and Cosmology*, 73(2):023502, 2006. URL https://journals.aps.org/prd/abstract/10.1103/PhysRevD.73.023502.

[72] Y. Zhang et al. Interactions in dark energy models. *arXiv preprint arXiv:1103.0718*, 2011.

[73] C. G. Boehmer et al. Quintessence with quadratic coupling to dark matter. *Physical Review D—Particles, Fields, Gravitation, and Cosmology*, 81(8):083003, 2010. URL https://journals.aps.org/prd/abstract/10.1103/PhysRevD.81.083003.

[74] H. Lopez et al. Higher-order coupled quintessence. *Physical Review D—Particles, Fields, Gravitation, and Cosmology*, 82(12):123525, 2010. URL https://journals.aps.org/prd/abstract/10.1103/PhysRevD.82.123525.

[75] S. C. F. Morris et al. Cosmological effects of coupled dark matter. *Physical Review D—Particles, Fields, Gravitation, and Cosmology*, 88(8):083522, 2013. URL https://journals.aps.org/prd/abstract/10.1103/PhysRevD.88.083522.

[76] M. W. Hossain et al. Variable gravity: A suitable framework for quintessential inflation. *Physical Review D*, 90(2):023512, 2014. URL https://journals.aps.org/prd/abstract/10.1103/PhysRevD.90.023512.

[77] N. Roy and N. Banerjee. Dynamical systems study of chameleon scalar field. *Annals of Physics*, 356:452–466, 2015. URL https://www.sciencedirect.com/science/article/pii/S0003491615001086.

[78] H. Wei. Cosmological evolution of quintessence and phantom with a new type of interaction in dark sector. *Nuclear Physics B*, 845(3):381–392, 2011. URL https://www.sciencedirect.com/science/article/pii/S0550321310006553.

[79] M. Zhang et al. Cosmological evolution of quintessence with a sign-changing interaction in dark sector. *Science China Physics, Mechanics & Astronomy*, 57:1805–1808, 2014. URL https://link.springer.com/article/10.1007/s11433-014-5550-x.

[80] M. Shahalam et al. Dynamics of interacting quintessence. *The European Physical Journal C*, 75:1–9, 2015. URL https://link.springer.com/article/10.1140/epjc/s10052-015-3608-1.

[81] F. F Bernardi and R. G Landim. Coupled quintessence and the impossibility of an interaction: a dynamical analysis study. *The European Physical Journal C*, 77:1–7, 2017. URL https://link.springer.com/article/10.1140/epjc/s10052-017-4858-x.

[82] A. Nunes, J. P. Mimoso, and T. C. Charters. Scaling solutions from interacting fluids. *Physical Review D*, 63(8):083506, 2001. URL https://ui.adsabs.harvard.edu/abs/2001PhRvD..63h3506N.

[83] G. Olivares, F. Atrio-Barandela, and D. Pavón. Dynamics of interacting quintessence models: Observational constraints. *Physical Review D*, 77(6):063513, 2008. URL https://ui.adsabs.harvard.edu/abs/2008PhRvD..77f3513O.

[84] G. Caldera-Cabral et al. Dynamics of interacting dark energy. *Physical Review D*, 79(6):063518, 2009. URL https://ui.adsabs.harvard.edu/abs/2009PhRvD..79f3518C.

[85] M. Quartin et al. Dark interactions and cosmological fine-tuning. *Journal of Cosmology and Astroparticle Physics*, 2008(5):007, 2008. URL https://ui.adsabs.harvard.edu/abs/2008JCAP...05..007Q.

[86] S. Chen, B. Wang, and J. Jing. Dynamics of an interacting dark energy model in Einstein and loop quantum cosmology. *Physical Review D*, 78(12):123503, 2008. URL https://ui.adsabs.harvard.edu/abs/2008PhRvD..78l3503C.

[87] C. Quercellini et al. Late universe dynamics with scale-independent linear couplings in the dark sector. *Physical Review D*, 78(6):063527, 2008. URL https://ui.adsabs.harvard.edu/abs/2008PhRvD..78f3527Q.

[88] S. Li and Y. Ma. Dark energy interacting with dark matter in classical Einstein and loop quantum cosmology. *European Physical Journal C*, 68(1-2):227–239, 2010. URL https://ui.adsabs.harvard.edu/abs/2010EPJC...68..227L.

[89] F. Arévalo et al. Cosmological dynamics with nonlinear interactions. *Classical and Quantum Gravity*, 29(23):235001, 2012. URL https://ui.adsabs.harvard.edu/abs/2012CQGra..29w5001A.

[90] J. Perez et al. The Jungle Universe: coupled cosmological models in a Lotka-Volterra framework. *General Relativity and Gravitation*, 46:1753, 2014. URL https://ui.adsabs.harvard.edu/abs/2014GReGr..46.1753P.

[91] S. Downes, B. Dutta, and K. Sinha. Attractors, universality, and inflation. *Physical Review D—Particles, Fields, Gravitation, and Cosmology*, 86(10):103509, 2012. URL https://journals.aps.org/prd/abstract/10.1103/PhysRevD.86.103509.

[92] C. M. Will. The confrontation between general relativity and experiment. *Living reviews in relativity*, 17:1–117, 2014. URL https://link.springer.com/article/10.12942/lrr-2014-4?affiliation.

[93] R. Bean et al. Constraining interactions in cosmology's dark sector. *Physical Review D—Particles, Fields, Gravitation, and Cosmology*, 78(12):123514, 2008. URL https://journals.aps.org/prd/abstract/10.1103/PhysRevD.78.123514.

[94] W. Yang and L. Xu. Testing coupled dark energy with large scale structure observation. *Journal of Cosmology and Astroparticle Physics*, 2014(8):034–034, 2014. URL https://ui.adsabs.harvard.edu/abs/2014JCAP...08..034Y.

[95] B. Wang et al. Dark matter and dark energy interactions: theoretical challenges, cosmological implications and observational signatures. *Reports on Progress*

in Physics, 79(9):096901, 2016. URL https://ui.adsabs.harvard.edu/abs/2016RPPh...79i6901W.

[96] M. Baldi. Early massive clusters and the bouncing coupled dark energy. *MNRAS*, 420(1):430–440, 2012. URL https://ui.adsabs.harvard.edu/abs/2012MNRAS.420..430B.

[97] D. N. Spergel et al. First-Year Wilkinson Microwave Anisotropy Probe (WMAP) Observations: Determination of Cosmological Parameters. *The Astrophysical Journal Supplement Series*, 148(1):175–194, 2003. URL https://ui.adsabs.harvard.edu/abs/2003ApJS..148..175S.

[98] C Blake and K Glazebrook. Probing Dark Energy Using Baryonic Oscillations in the Galaxy Power Spectrum as a Cosmological Ruler. *The Astrophysical Journal*, 594(2):665–673, 2003. URL https://ui.adsabs.harvard.edu/abs/2003ApJ...594..665B.

[99] H. J. Seo and D. J. Eisenstein. Probing dark energy with baryonic acoustic oscillations from future large galaxy redshift surveys. *The Astrophysical Journal*, 598(2):720–740, 2003. URL https://ui.adsabs.harvard.edu/abs/2003ApJ...598..720S.

[100] D. Huterer and M. S. Turner. Prospects for probing the dark energy via supernova distance measurements. *Physical Review D*, 60(8):081301, 1999. URL https://ui.adsabs.harvard.edu/abs/1999PhRvD..60h1301H.

[101] A. Hebecker and C. Wetterich. Natural quintessence? *Physics Letters B*, 497(3-4):281–288, 2001. URL https://www.sciencedirect.com/science/article/pii/S0370269300013393.

[102] H. K. Jassal J. S. Bagla and T.Padmanabhan. Cosmology with tachyon field as dark energy. *Physical Review D*, 67(6):063504, 2003. URL https://journals.aps.org/prd/abstract/10.1103/PhysRevD.67.063504.

[103] J. M. Aguirregabiria and R. Lazkoz. Tracking solutions in tachyon cosmology. *Physical Review D*, 69(12):123502, 2004. URL https://ui.adsabs.harvard.edu/abs/2004PhRvD..69l3502A.

[104] E. J. Copeland et al. Dynamics of dark energy. *International Journal of Modern Physics D*, 15(11):1753–1935, 2006. URL https://www.worldscientific.com/doi/abs/10.1142/S021827180600942X.

[105] L. A. Ureña-López. Bose-einstein condensation of relativistic scalar field dark matter. *Journal of Cosmology and Astroparticle Physics*, 2009(01):014, 2009. URL https://iopscience.iop.org/article/10.1088/1475-7516/2009/01/014/meta.

[106] M. M. Verma and S. D. Pathak. Shifted cosmological parameter and shifted dust matter in a two-phase tachyonic field universe. *Astrophysics and Space Science,*, 344(2):505–512, 2013. URL https://ui.adsabs.harvard.edu/abs/2013Ap&SS.344..505V.

[107] C. G. Boehmer, N. Tamanini, and M. Wright. Interacting quintessence from a variational approach part i: algebraic couplings. *Physical Review D*, 91(12):123002, 2015. URL https://journals.aps.org/prd/abstract/10.1103/PhysRevD.91.123002.

[108] D Valentino egt al. Can interacting dark energy solve the h 0 tension? *Physical Review D*, 96(4):043503, 2017. URL https://journals.aps.org/prd/abstract/10.1103/PhysRevD.96.043503.

[109] G. Cheng et al. Testing interacting dark matter and dark energy model with cosmological data. *Physical Review D*, 102(4):043517, 2020. URL https://journals.aps.org/prd/abstract/10.1103/PhysRevD.102.043517.

[110] L. F. S et al. Dark energy survey year 3 results: Cosmology from cosmic shear and robustness to modeling uncertainty. *Physical Review D*, 105(2):023515, 2022. URL https://journals.aps.org/prd/abstract/10.1103/PhysRevD.105.023515.

[111] S. D. Storm and R. J. Scherrer. Observational constraints on inflection point quintessence with a cubic potential. *Physics Letters B*, 829:137126, 2022. URL https://ui.adsabs.harvard.edu/abs/2022PhLB..82937126S.

[112] O. Avsajanishvili et al. Observational constraints on dynamical dark energy models. *Universe*, 10(3):122, 2024. URL https://www.mdpi.com/2218-1997/10/3/122.

[113] N. Roy. Dynamical dark energy in the light of desi 2024 data. *Physics of the Dark Universe*, 48:101912, 2025.

[114] W. Zimdahl. Interacting Dark Energy and Cosmological Equations of State. *International Journal of Modern Physics D*, 14(12):2319–2325, 2005. URL https://ui.adsabs.harvard.edu/abs/2005IJMPD..14.2319Z.

[115] A. Kundu, S. D. Pathak, and V. K. Ojha. Interacting tachyonic scalar field. *Communications in Theoretical Physics*, 73(2):025402, 2021. URL https://ui.adsabs.harvard.edu/abs/2021CoTPh..73b5402K.

[116] M. M. Verma and S. D. Pathak. A Tachyonic Scalar Field with Mutually Interacting Components. *International Journal of Theoretical Physics*, 51(8):2370–2379, 2012. URL https://ui.adsabs.harvard.edu/abs/2012IJTP...51.2370V.

[117] M. Shahalam et al. Dynamics of coupled phantom and tachyon fields. *European Physical Journal C*, 77(10):686, 2017. URL https://ui.adsabs.harvard.edu/abs/2017EPJC...77..686S.

[118] G. Garcia-Arroyo, L. A. Ureña-López, and J. A. Vázquez. Interacting scalar fields: Dark matter and early dark energy, 2024. URL https://ui.adsabs.harvard.edu/abs/2024PhRvD.110b3529G.

[119] G. R. Farrar and P. J. E. Peebles. Interacting Dark Matter and Dark Energy. *The Astrophysical Journal*, 604(1):1–11, 2004. URL https://ui.adsabs.harvard.edu/abs/2004ApJ...604....1F.

[120] A. de la Macorra. Interacting dark energy: generic cosmological evolution for two scalar fields. *Journal of Cosmology and Astroparticle Physics*, 2008(1):030, 2008. URL https://ui.adsabs.harvard.edu/abs/2008JCAP...01..030D.

[121] E. Di Valentino et al. Nonminimal dark sector physics and cosmological tensions. *Physical Review D*, 101(6):063502, 2020. URL https://ui.adsabs.harvard.edu/abs/2020PhRvD.101f3502D.

[122] W. Yang et al. Tale of stable interacting dark energy, observational signatures, and the h0 tension. *Journal of Cosmology and Astroparticle Physics*, 2018(09):019, 2018. URL https://iopscience.iop.org/article/10.1088/1475-7516/2018/09/019/meta.

[123] K. Akash, S. D. Pathak, and R. K. Dubey. Dynamical role of scalar fields in k= 0 universe. 1531(1):012086, 2020. URL https://iopscience.iop.org/article/10.1088/1742-6596/1531/1/012086/meta.

[124] R. Allahverdi et al. Gauge-invariant inflaton in the minimal supersymmetric standard model. *Physical review letters*, 97(19):191304, 2006. URL https://ui.adsabs.harvard.edu/abs/2006PhRvL..97s1304A.

[125] A. A. Sen and R. J. Scherrer. Generalizing the generalized Chaplygin gas. *Physical Review D*, 72(6):063511, 2005. URL https://ui.adsabs.harvard.edu/abs/2005PhRvD..72f3511S.

[126] F. C. Carvalho et al. Scalar-Field-Dominated Cosmology with a Transient Acceleration Phase. *Physical review letters*, 97(8):081301, 2006. URL https://ui.adsabs.harvard.edu/abs/2006PhRvL..97h1301C.

[127] S. Panda, M. Sami, and S. Tsujikawa. Prospects of inflation in delicate D-brane cosmology. *Physical Review D*, 76(10):103512, 2007. URL https://ui.adsabs.harvard.edu/abs/2007PhRvD..76j3512P.

[128] K. Enqvist, A. Mazumdar, and P. Stephens. Inflection point inflation within supersymmetry. *Journal of Cosmology and Astroparticle Physics*, 2010(6):020, 2010. URL https://ui.adsabs.harvard.edu/abs/2010JCAP...06..020E.

[129] S. Unnikrishnan and V. Sahni. Resurrecting power law inflation in the light of Planck results. *Journal of Cosmology and Astroparticle Physics*, 2013(10):063, 2013. URL https://ui.adsabs.harvard.edu/abs/2013JCAP...10..063U.

[130] S. Hotchkiss, A. Mazumdar, and S. Nadathur. Inflection point inflation: Wmap constraints and a solution to the fine tuning problem. *Journal of Cosmology and Astroparticle Physics*, 2011(06):002, 2011. URL https://iopscience.iop.org/article/10.1088/1475-7516/2011/06/002/meta.

[131] Y. Bai and D. Stolarski. Dynamical inflection point inflation. *Journal of Cosmology and Astroparticle Physics*, 2021(3):091, 2021. URL https://ui.adsabs.harvard.edu/abs/2021JCAP...03..091B.

[132] A. D. Linde. A new inflationary universe scenario: A possible solution of the horizon, flatness, homogeneity, isotropy and primordial monopole problems. *Physics*

Letters B, 108(6):389–393, 1982. URL https://ui.adsabs.harvard.edu/abs/1982PhLB..108..389L.

[133] A. H. Guth. Inflation and eternal inflation. *Physics Reports*, 333:555–574, 2000. URL https://ui.adsabs.harvard.edu/abs/2000PhR...333..555G.

[134] H. Y. Chang and R. J. Scherrer. Inflection point quintessence. *Physical Review D*, 88(8):083003, 2013. URL https://ui.adsabs.harvard.edu/abs/2013PhRvD..88h3003C.

[135] G. Wolschin. Lectures on Cosmology Accelerated Expansion of the Universe. 800, 2010. URL https://ui.adsabs.harvard.edu/abs/2010LNP...800.....W.

[136] C. P. Burgess. Lectures on cosmic inflation and its potential stringy realizations. *Classical and Quantum Gravity*, 24(21):S795–S852, 2007. URL https://ui.adsabs.harvard.edu/abs/2007CQGra..24S.795B.

[137] S. Yadav et al. Reheating constraints on modified quadratic chaotic inflation. *European Physical Journal Plus*, 139(2):185, 2024. URL https://ui.adsabs.harvard.edu/abs/2024EPJP..139..185Y.

[138] D. Baumann. TASI Lectures on Inflation. *arXiv e-prints*, art. arXiv:0907.5424, 2009. URL https://ui.adsabs.harvard.edu/abs/2009arXiv0907.5424B.

[139] I. Mezo. The lambert w function: its generalizations and applications. 2022. URL https://www.taylorfrancis.com/books/mono/10.1201/9781003168102/lambert-function-istvan-mezo.

[140] G. A. Kalugin. Analytical properties of the lambert w function. 2011.

[141] S.D. Pathak et al. Application of dynamical system analysis in cosmology. pages 37–47, 2025. URL https://www.sciencedirect.com/science/article/pii/B9780443300127000102.

[142] D. K Arrowsmith and C. M. Place. An introduction to dynamical systems. 1990. URL https://books.google.com/books?hl=en&lr=&id=HOU6q6wHCncC&oi=fnd&pg=PP10&dq=an+introduction+to+dynamical+systems&ots=qTMef4CooV&sig=6WxJPWOCCdQwn5-8xOfOARFQmOg.

[143] R. A. Knop et al. New Constraints on Ω_M, Ω_Λ, and w from an Independent Set of 11 High-Redshift Supernovae Observed with the Hubble Space Telescope. *The Astrophysical Journal*, 598(1):102–137, 2003. URL https://ui.adsabs.harvard.edu/abs/2003ApJ...598..102K.

[144] V. Sahni and A. A Sen. A new recipe for λcdm. *The European Physical Journal C*, 77(4):1–8, 2017. URL https://link.springer.com/article/10.1140/epjc/s10052-017-4796-7.

[145] Z. Davari et al. New parametrization for unified dark matter and dark energy. *Physical Review D*, 97(12):123525, 2018. URL https://journals.aps.org/prd/abstract/10.1103/PhysRevD.97.123525.

[146] D. Benisty and E. I. Guendelman. Unified dark energy and dark matter from dynamical spacetime. *Physical Review D*, 98(2):023506, 2018. URL https://journals.aps.org/prd/abstract/10.1103/PhysRevD.98.023506.

[147] P. F. González-Díaz. Unified model for dark energy. *Physics Letters B*, 562(1-2):1–8, 2003. URL https://www.sciencedirect.com/science/article/pii/S0370269303005409.

[148] R. J. Scherrer. Purely kinetic k essence as unified dark matter. *Physical review letters*, 93(1):011301, 2004. URL https://journals.aps.org/prl/abstract/10.1103/PhysRevLett.93.011301.

[149] D. Bertacca et al. Unified dark matter in scalar field cosmologies. *Modern Physics Letters A*, 22(38):2893–2907, 2007. URL https://www.worldscientific.com/doi/abs/10.1142/S0217732307025893.

[150] A. Diez-Tejedor and A. Feinstein. Homogeneous scalar field and the wet dark sides of the universe. *Physical Review D—Particles, Fields, Gravitation, and Cosmology*, 74(2):023530, 2006. URL https://journals.aps.org/prd/abstract/10.1103/PhysRevD.74.023530.

[151] S. S. Mishra and V. Sahni. Unifying dark matter and dark energy with non-canonical scalars. *The European Physical Journal C*, 81(7):1–10, 2021. URL https://link.springer.com/article/10.1140/epjc/s10052-021-09433-w.

[152] A. Sen. Tachyon matter. *Journal of High Energy Physics*, 2002(07):065, 2002. URL https://iopscience.iop.org/article/10.1088/1126-6708/2002/07/065/meta.

[153] A. Sen. Field theory of tachyon matter. *Modern Physics Letters A*, 17(27): 1797–1804, 2002. URL https://www.worldscientific.com/doi/abs/10.1142/S0217732302008071.

[154] M. R. Garousi. Tachyon couplings on non-bps d-branes and dirac–born–infeld action. *Nuclear Physics B*, 584(1-2):284–299, 2000. URL https://www.sciencedirect.com/science/article/pii/S0550321300003618.

[155] E. V. Linder. Exploring the expansion history of the universe. *Physical review letters*, 90(9):091301, 2003. URL https://journals.aps.org/prl/abstract/10.1103/PhysRevLett.90.091301.

[156] V. Sahni et al. Two new diagnostics of dark energy. *Physical Review D—Particles, Fields, Gravitation, and Cosmology*, 78(10):103502, 2008. URL https://journals.aps.org/prd/abstract/10.1103/PhysRevD.78.103502.

[157] T. Koivisto and D. F. Mota. Dark energy anisotropic stress and large scale structure formation. *Physical Review D*, 73:083502, 2006. URL https://journals.aps.org/prd/abstract/10.1103/PhysRevD.73.083502.

[158] J. Gleyzes, D. Langlois, F. Piazza, and F. Vernizzi. Healthy theories beyond horndeski. *Physical Review Letters*, 114(21):211101, 2015. URL https://arxiv.org/abs/1404.6495.

[159] D. Bettoni and S. Liberati. Disformal invariance of second order scalar-tensor theories: Framing the horndeski action. *Physical Review D*, 88(8):084020, 2013. URL https://journals.aps.org/prd/abstract/10.1103/PhysRevD.88.084020.

List of Publications

Research Papers in Peer Reviewed Journal

1. Jaskirat Kaur, S. D. Pathak, Maxim Khlopov, Maxim Krasnov and Manabendra Sharma. *Dynamics of Scalar Fields from a Generalized form of Lagrangian.Nuclear Physics, Section B*, Volume 1018, **3 July 2025**, 117010.

   doi:10.1016/j.nuclphysb.2025.117010

   Journal Details: Nuclear Physics, Section B, Elsevier, Impact Factor: 2.8, Q1.

2. Jaskirat Kaur, S. D. Pathak, Maxim Khlopov and Manabendra Sharma. *Inflection Point Dynamics of Minimally Coupled Tachyonic Scalar Fields. Universe*, Volume 11, **14 April 2025**, 131.

   doi:10.3390/universe11040131

   Journal Details: Universe, MDPI, Impact factor: 2.6, Q1.

3. Jaskirat Kaur, S. D. Pathak, Vikash Kumar Ojha and Maxim Yu Khlopov. *Inflection Point of Coupled Quintessence. Astroparticle Physics*, Volume 157, **1 May 2024**, 102926.

   doi:10.1016/j.astropartphys.2024.102926

   Journal Details: Astroparticle Physics, Elsevier, Impact Factor: 2.9, Q1.

4. Jaskirat Kaur, Devanarayanan Rajeeb Kumar, S. D. Pathak, Maxim Yu Khlopov and Maxim Krasnov. *Canonical scalar field with mutually interacting components.* **2025**

   (Under Review)

Book Chapters:

1. S. D. Pathak, Swapna Sagar Mishra, Jaskirat Kaur, Maxim Khlopov. *Advances in Computational Methods and Modeling for Science and Engineering: Chapter-3 Application of dynamical system analysis in cosmology.* **1 January 2025**, 37-47, ISBN: 978-0-443-30012-7, doi:10.1016/B978-0-44-330012-7.00010-2

Presentations in Conferences/Seminars

- International Conference on Astroparticle Physics, Gravitation and Cosmology (APGC-2025), Oral presentation on "Dynamincs of Quintessence, Phantom and Tachyon Fields in a Generalized Cosmological Framework", on 26-28 June, 2025.
- International Conference on Current Advances in Applied Physics (ICCAAP-2025), Oral presentation on "Inflection Point of Coupled Canonical Scalar Field", on 20-21 February 2025
- 5^{th} International Conference on Recent Advances in Fundamental and Applied Sciences (RAFAS-2024), Oral presentation on "Age of Non-Flat Universe in the Interacting Dark Energy Model" at Lovely Professional University, on April 2024.

Workshops/colloquiums attended

- Introductory Workshop on Astrophysics and Cosmology, Sponsored by IUCAA and Organized by Department of Physics, Integral University Lucknow, from 02-04 May 2024.
- 5^{th} Summer International School on Gravity, Cosmology and Astrophysics (ISGCA-2024), organized by Russian Gravitational society, from 01-08 July 2024.

Talk

- Presented a talk on the topic "Understanding the Mysterious Force Behind the Universe's Expansion", at Introductory Workshop on Astrophysics and Cosmology, on 4^{th} May 2024, at Integral University Lucknow.

Research Visits

- Successfully completed a 35 days research visit at the Inter-University Centre for Astronomy and Astrophysics (IUCAA), Pune, from 18 February-26 March 2025, following selection for the program.